Investigations on Efficient Optical Fiber Communication System with Dispersion and Self Phase Modulation

Thesis submitted in the partial fulfillment of requirement for the award of the degree of

Master of Engineering

in

Electronics and Communication Engineering

Submitted by

Sukhwinder Kaur

Roll. No. 80761025

Under the guidance of

Dr. Hardeep Singh

Assistant Professor, ECED

Thapar University, Patiala.

Electronics and Communication Engineering Department

THAPAR UNIVERSITY

PATIALA-147004, INDIA

JULY-2009

DECLARATION

I hereby declare that the work, which is being presented in the thesis, entitled **"Investigations on Efficient Optical Fiber Communication System with Dispersion and Self Phase Modulation"** in partial fulfillment of the requirements for the award of degree of Master of Engineering in Electronics and Communication Engineering at Electronics and Communication Engineering Department of Thapar University, Patiala, is an authentic record of my own work carried out under the guidance of Dr. Hardeep Singh.

I have not submitted the matter presented in the thesis for the award of any other degree of this or any other university.

Sukhwinder Kaur

(80761025)

This is to certify that the above statement made by the student is correct to the best of my knowledge and belief.

06/07/09

Dr. Hardeep Singh
Assistant Professor
Electronics & Communication Engineering Department,
Thapar University,
Patiala-147004, (Punjab).

Dr. A. K. Chatterjee 7.7.09
Professor & Head
ECED, Thapar University,
Patiala- 147004, (Punjab).

Dr. R. K. Sharma 7/7/09
Dean of Academic Affairs
Thapar University,
Patiala- 147004,(Punjab).

ABSTRACT

Optical fibers are not only used in telecommunication links but also used in the Internet and local area networks (LAN) to achieve high signaling rates. In this dissertation, fiber nonlinearities have been studied and analyze the effect of various parameters on the received power. Optical amplifiers like EDFAs simply amplify the optical signal by several orders of magnitude without being limited by electronic speed. Transmission impairments, which are general not significant in a regenerative system, accumulate along the transmission link when amplifiers are used, so that they can not be simply ignored and this puts a new challenge to transmission design engineers. The nonlinearities in optical fibers fall into two categories. One is stimulated scattering (Raman and Brillouin) and the other is the optical Kerr effect due to changes in the refractive index with optical power. Phase modulation due to intensity dependent refractive index induces various nonlinear effects, namely, self phase modulation (SPM), cross-phase modulation (XPM), and four-wave mixing (FWM).

In the standard single mode fibers, the Polarization Mode Dispersion is the phenomenon that causes the hurdles to reach the high bit-rate-distance product of amplified light wave communication system. The impacts on eye opening, eye closing and output power due to dispersion variation are studied. The impacts of pre compensation, in high data rate transmission systems have been investigated at different bit rates. It is reported that pre compensation produces the adverse effect on the eye opening, eye closing. Due to pre compensation, the significant degradation in the performance of high speed optical transmission system with the increasing bit rate is also reported. At the bit rate of 40 Gb/s and above it is almost impossible to cope with pre compensation without the use of dispersion compensation.

The fiber nonlinear characteristics are the Optical Kerr effect and the stimulated scatterings. The fiber nonlinearities produce the input power limitations on the system as well as maximum transmission distance. To mitigate their effects, the dispersion mappings are used. Pre, post and symmetrical compensation techniques are compared on the basis of bit error rate (BER). The dispersion compensation fiber (DCF) is used in the compensation techniques. It is demonstrated that the hybrid compensation is better to reduce the nonlinear effects than its counter parts.

ACKNOWLEDGEMENT

I would like to express my gratitude to Dr. Hardeep Singh, Assistant Professor, Electronics and Communication Engineering Department, Thapar University, Patiala for his patient guidance and support throughout this thesis work. I am truly very fortunate to have the opportunity to work with him. He has provided me help in technical writing and presentation style and I found this guidance to be extremely valuable.

I am very thankful to the Head of the Department, Dr. A. K. Chatterjee, for his encouragement, support and providing the facilities for the completion of this thesis.

I am also thankful to entire faculty and staff members of Electronics and Communication Engineering Department for their unyielding encouragement.

I am greatly indebted to all my friends, who have graciously applied themselves to the task of helping me with ample morale support and valuable suggestions. Finally, I would like to extend my gratitude to all those persons who directly or indirectly helped me in the process and contributed towards this work.

Sukhwinder Kaur

(80761025)

CONTENTS

LIST OF DIAGRAMS

LIST OF TABLES

CHAPTER 1

INTRODUCTION

1.1 Introduction

In the information age, the demand for networks of higher capacities at lower cost is increasing. Optical communication technology has developed rapidly to achieve larger transmission capacity and longer transmission distance. Focus on development of broadband optical communication systems is incredible since it offers combination of wide bandwidth and low losses unmatched by any other transmission medium but group velocity dispersion [1-3] and fiber nonlinearities due to optical Kerr effects remain inherent limitations of such systems there by degrading the performance. Therefore in order to realize broadband optical communication systems and networks, it is imperative to compensate the pulse spreading due to group velocity dispersion (GVD) and optical Kerr effects [4-5].

With the advent of erbium-doped fiber amplifiers (EDFAs), the attenuation limits on transmission distance have been reduced but since then nonlinearities have become critical issue in the advancement of optical communication systems. The nonlinear interactions of fiber material set an upper limit to the amount of information that can be transmitted. Optical Kerr effects in optical fibers are due to changes in the refractive index with optical power. Particularly for long haul transmission with number of WDM channels, the accumulated nonlinear effects lead to waveform distortion and crosstalk between channels. Power dependence of refractive index is responsible to Kerr effects. Depending on the shape of the input signal, the Kerr nonlinearities manifest itself by different effects such as Self Phase Modulation (SPM) [6-7], Cross Phase Modulation (XPM) [8] and Four Wave Mixing (FWM) [9].

These nonlinear effects are induced by high powers and long distances enabled by erbium-doped fiber amplifiers (EDFA) at high bit rates [10]. These lead to attenuation, distortion and cross channel interference. These constrain the spacing between adjacent wave length channels. These limit the maximum power on any channel and also limit the maximum bit rate.

In the recent past, various dispersion compensation methods have been studied, the impact of GVD on high bit-rate long-distance optical communications have been investigated and limitations of systems due to fiber dispersion and fiber nonlinearities due to optical Kerr effects, have been discussed. However, such studies are very limited as far as the significance of higher order dispersion terms is concerned. In order to bridge the gap in available literature and to further analyze dispersion and higher order effect switch optical Kerr effects, it is important to analyze and investigate the performance of dispersive optical communication systems including higher order dispersion terms. These dispersion and fiber nonlinear effects are further enhanced while realizing ultrahigh dense wavelength division multiplexed systems (DWDM) that are used to exploit optical bandwidth. Other important consideration includes propagation of modulation and noise characteristics of a laser diode with dispersion in the transmission medium. Also, optimization of high data rate long haul optical communication systems using practical methods of dispersion management is need of the hour. This focuses on investigating limitations on multi wavelength optical fibers due to group velocity dispersion (GVD) and nonlinear effects due to optical Kerr effects.

1.2 Historical perspective of fiber optics

People have used light to transmit information for hundreds of years. However, it was not until the 1960s, with the invention of the laser that widespread interest in optical (light) systems for data communications began. The invention of the laser prompted researchers to study the potential of fiber optics for data communications, sensing and other applications. Laser systems could send a much larger amount of data than telephone, microwave and other electrical systems. The first experiment with the laser involved letting the laser beam transmit freely through the air. Researchers also conducted experiments letting the laser beam transmit through different types of waveguides. Glass fibers, gas-filled pipes and tubes with focusing lenses are examples of optical waveguides. Glass fibers soon became the preferred medium for fiber optic research.

The use of light for transmitting information from one place to another place is a very old technique. In 800 BC, the Greeks used fire and smoke signals for sending information

like victory in a war, alerting against enemy, call for help etc. Mostly only one type of signal was conveyed. During the second century BC optical signals were encoded using signaling lamps so that any message could be sent. There was no development in optical communication till the end of the 18th century. The speed of the optical communication link was limited due to the requirement of line of sight transmission paths, the human eye as the receiver and unreliable nature of transmission paths affected by atmospheric effects such as fog and rain. In 1791, Chapped from France developed the semaphore for telecommunication on land. But that was also with limited information transfer [11]. In 1835, Samuel Morse invented the telegraph and the era of electrical communications started throughout the world. The use of wire cables for the transmission of Morse coded signals was implemented in 1844. In 1872, Alexander Graham Bell proposed the photo phone with a diaphragm giving speech transmission over a distance of 200 m. But within four years, Graham Bell had changed the photo phone into telephone using electrical current for transmission of speech signals. In 1878, the first telephone exchange was installed at New Haven. Meanwhile, Hertz discovered radio waves in 1887. Marconi demonstrated radio communication without using wires in 1895. Using modulation techniques, the signals were transmitted over a long distance using radio waves and microwaves as the carrier. During the middle of the twentieth century, it was realized that an increase of several orders of magnitude of bit rate distance product would be possible if optical waves were used as the carrier [1]. In an old optical communication system, the bit rate distance product is only about 1 (bit/s)-km due to enormous transmission loss (105 to 107 dB/km). The information carrying capacity of telegraphy is about hundred times lesser than telephony. Even though the high-speed coaxial systems were evaluated during 1975, they had smaller repeater spacing. Microwaves are used in modern communication systems with the increased bit rate distance product [12].

However, a coherent optical carrier like laser will have more information carrying capacity. So the communication engineers were interested in optical communication using lasers in an effective manner from 1960 onwards. A new era in optical communication started after the invention of laser in 1960 by Maiman. The light waves from the laser, a coherent source of light waves having high intensity, high

monochromatic and high directionality with less divergence, are used as carrier waves capable of carrying large amount of information compared with radio waves and microwaves.

Initially, the very large losses in the optical fibers prevented coaxial cables from being replaced. The loss is the decrease in the amount of light reaching the end of the fiber. Early fibers have losses around 1,000 dB/km making them impractical for communications use. In 1969, several scientists concluded that impurities in the fiber material caused the signal loss in optical fibers. The basic fiber material did not prevent the light signal from reaching the end of the fiber. Researchers believed it was possible to reduce the losses in optical fibers by removing the impurities. By removing the impurities, construction of low-loss optical fibers was possible.

There are two basic types of optical fibers, multimode fibers and single mode fibers. In 1970, Corning Glass Works made a multimode fiber with losses under 20 dB/km.

This same company, in 1972, made a high silica-core multimode optical fiber with 4 dB/km minimum attenuation (loss). Currently, multimode fibers can have losses as low as 0.5 dB/km at wavelengths around 1300 nm. Single mode fibers are available with losses lower than 0.25 dB/km at wavelengths around 1500 nm.

1.3 Literature survey

Scientists have used different techniques of pulse compression based on linear chirp compensation of self phase modulation in dispersion shifted fibers. Cartaxo et. al. Derived expression for relative intensity noise due to dispersion and nonlinearity including fiber loss and showed its impact with first order dispersion term. The optimization procedure was carried out for short span of single mode fiber using parabolic law [13]. Cartledge et. al. combined the use of SPM and joint optimization of the bias and modulation voltages to increase the dispersion limited transmission distance at 10 Gb/s [14]. Tang et. al presented a general treatment of multi span effects of Kerr nonlinearity on Shannon channel capacity for dispersion free nonlinear optical fiber transmissions [15]. Chiang et. al. reported that the phase modulation induced by cross

phase modulation is inversely proportional to the signal base band modulation frequency [8]. Yang et al. derived expression for nonlinear crosstalk due to XPM effect [16]. Sono et. al. described WDM transmission with SPM/XPM suppression through pre chirping and dispersion management [17]. Yu et. al. demonstrated simultaneous demultiplexing and regeneration of 40 Gb/s bit rate bit rate optical time division multiplexed (OTDM) signal based on self phase and cross phase modulation in dispersion shifted fibers [18]. Gobind P. Agrawal the amplified pulse is passed through a fiber, it is initially compressed because of the frequency chirp imposed on it by the amplifier. This feature can be used to compensate for fiber dispersion in optical communication systems.

Numai and Kubota again showed that by repeated unequally spaced channels, the FWM problem can be controlled to great extent [19]. Recently, Radic et. al. investigated efficiency of FWM generation inquest distributed erbium doped fiber sections under general power evolution conditions using new theory. Measured FWM efficiency was found to be in good agreement with newly developed theory [20].

Different compensation methods like Optical Phase Conjugation method [21], Fiber chirped method [17], Bragg-Grating method [22], Filter method, Differential time delay method and dispersion equalizers were studied in the last decade and based on these methods efforts were made to increase the transmission distances and bandwidth of optical communication systems [23]. In the last few years, both dispersion Optical Kerr effects have been studied together creating path ways to techniques called dispersion management techniques. The impact of higher order dispersion terms has also been studied these days by different authors [24-25] .

Masaki Recently showed that there is a significant increase in the transmission speed of optical networks if the impact of higher order terms is clarified [26]. The general expressions that describe pulse broadening due to even and odd higher order dispersion in a single mode fiber were discussed. The intrinsic impulsive response for even order dispersion (beyond the second order) were characterized by symmetrical wave forms with long trailing skirts, whereas the response for odd orders show asymmetrical strongly oscillating waveforms. The transmission limits were also analytically obtained for each higher nth order that induces inter symbol interference.

1.4 Objectives

In this thesis, the research is carried out keeping in view the following main objectives:

1) To investigate efficient optical communication systems for the fiber length 10 km to 60 km
2) To investigate efficient optical communication systems for the fiber dispersion value 8, 10, 12, 14, 15 ps/nm/km.
3) To investigate the bit rate 10 to 40 Gb/s bit rate bit rate in optical communication system.
4) To compare the difference between EDFA (erbium-doped fiber amplifiers) and SOA **(**semiconductor optical amplifier).

1.5 Thesis outline

In chapter 1, the basic introduction, history, literature survey and objectives have been defined. In chapter 2, we have been discussed the basics of fiber optics and in chapter 3, dispersion and nonlinearity in fiber optics have been studied. In chapter 4, we have been investigated the simulation results of pre compensation, post compensation and symmetrical compensation and in chapter 5 we have compared the results of pre compensation with SOA and pre compensation with EDFA. And finally in chapter 6, we have discussed the conclusions and future scope of work.

CHAPTER 2

FIBER OPTIC BASICS

2.1 Introduction

System design has centered on long-haul communications and the subscriber-loop plant. The subscriber-loop plant is the part of a system that connects a subscriber to the nearest switching center. Limited work has also been done on short-distance applications and some military systems.

Initially, central office trunking required multimode optical fibers with moderate to good performance. Fiber performance depends on the amount of loss and signal distortion introduced by the fiber when it is operating at a specific wavelength. Long-haul systems require single mode optical fibers with very high performance. Single mode fibers tend to have lower loss and produce less signal distortion.

In contrast, short-distance and military systems tend to use only multimode technology. Examples of short-distance systems include process control and local area networks (LANs). Short-distance and military systems have many connections. The larger fiber core and higher fiber numerical aperture (NA) of multimode fibers reduce losses at these connections.

In military and subscriber-loop applications, system design and parts selection are related. Designers consider trade-offs in the following areas:

- Fiber properties
- Types of connections
- Optical sources
- Detector types

Designers develop systems to meet stringent working requirements, while trying to maintain economic performance. It is quite difficult to identify a standard system design

approach. This module identifies the types of components chosen by the Navy for shipboard applications [12].

Future system design improvements depend on continued research. Researchers expect fiber optic product improvements to upgrade performance and lower costs for short-distance applications. Future systems center on broadband services that will allow transmission of voice, video and data. Services will include television, data retrieval, video word processing, electronic mail, banking and shopping.

2.2 Transmission of light through optical fibers

The transmission of light along optical fibers depends not only on the nature of light, but also on the structure of the optical fiber. Two methods are used to describe how light is transmitted along the optical fiber. The first method, ray theory, uses the concepts of light reflection and refraction. The second method, mode theory, treats light as electromagnetic waves. These properties affect how light is transmitted through the fiber [27].

2.3 Optical fiber types

Optical fibers are characterized by their structure and by their properties of transmission. Basically, optical fibers are classified into two types. The first type is single mode fibers. The second type is multimode fibers. As each name implies, optical fibers are classified by the number of modes that propagate along the fiber. As previously explained, the structure of the fiber can permit or restrict modes from propagating in a fiber. The basic structural difference is the core size. Single mode fibers are manufactured with the same materials as multimode fibers. Single mode fibers are also manufactured by following the same fabrication process as multimode fibers.

2.3.1 Single mode fibers

The core size of single mode fibers is small. The core size (diameter) is typically around 8 to 10 micrometers. A fiber core of this size allows only the fundamental or lowest order mode to propagate around a 1300 nanometer (nm) wavelength. Single mode fibers

propagate only one mode, because the core size approaches the operational wavelength. The value of the normalized frequency parameter (V) relates core size with mode propagation.

In single mode fibers, V is less than or equal to 2.405. When V is less then 2.405, single mode fibers propagate the fundamental mode down the fiber core, while high-order modes are lost in the cladding. For low V values, most of the power is propagated in the cladding material. Power transmitted by the cladding is easily lost at fiber bends. The value of V should remain near the 2.405 level [22].

Single mode fibers have a lower signal loss and a higher information capacity (bandwidth) than multimode fibers. Single mode fibers are capable of transferring higher amounts of data due to low fiber dispersion. Basically, dispersion is the spreading of light as light propagates along a fiber. Dispersion mechanisms in single mode fibers are discussed in more detail later in this chapter. Signal loss depends on the operational wavelength. In single mode fibers, the wavelength can increase or decrease the losses caused by fiber bending. Single mode fibers operating at wavelengths larger than the cutoff wavelength lose more power at fiber bends. They lose power because light radiates into the cladding, which is lost at fiber bends. In general, single mode fibers are considered to be low-loss fibers, which increase system bandwidth and length.

2.3.2 Multimode fibers

As their name implies, multimode fibers propagate more than one mode. Multimode fibers can propagate over 100 modes. The number of modes propagated depends on the core size and numerical aperture (NA). As the core size and NA increase, the number of modes increases. Typical values of fiber core size and NA are 50 to 100 μm and 0.20 to 0.29, respectively.

A large core size and a higher NA have several advantages. Light is launched into a multimode fiber with more ease. The higher NA and the larger core size make it easier to make fiber connections. During fiber splicing, core-to-core alignment becomes less critical. Another advantage is that multimode fibers permit the use of light-emitting

diodes (LEDs). Single mode fibers typically must use laser diodes. LEDs are cheaper, less complex and last longer. LEDs are preferred for most applications.

Multimode fibers also have some disadvantages. As the number of modes increases, the effect of modal dispersion increases. Modal dispersion (intermodal dispersion) means that modes arrive at the fiber end at slightly different times. This time difference causes the light pulse to spread. Modal dispersion affects system bandwidth. Fiber manufacturers adjust the core diameter, NA and index profile properties of multimode fibers to maximize system bandwidth.

2.4 Properties of optical fiber transmission

The propagation of light depends upon the nature of light and the structure of the optical fiber. In this case, system performance deals with signal loss and bandwidth.

2.4.1 Attenuation

Signal loss and system bandwidth describe the amount of data transmitted over a specified length of fiber. Many optical fiber properties increase signal loss and reduce system bandwidth. The most important properties that affect system performance are fiber attenuation and dispersion.

Attenuation reduces the amount of optical power transmitted by the fiber [3,28]. Attenuation controls the distance an optical signal (pulse) can travel as shown in figure 2.1. Once the power of an optical pulse is reduced to a point where the receiver is unable to detect the pulse, an error occurs. Attenuation is mainly a result of light absorption, scattering and bending losses. Dispersion spreads the optical pulse as it travels along the fiber. This spreading of the signal pulse reduces the system bandwidth or the information-carrying capacity of the fiber. Dispersion limits how fast information is transferred as shown in figure 2.1. An error occurs when the receiver is unable to distinguish between input pulses caused by the spreading of each pulse. The effects of attenuation and dispersion increase as the pulse travels the length of the fiber as shown in figure 2.2.

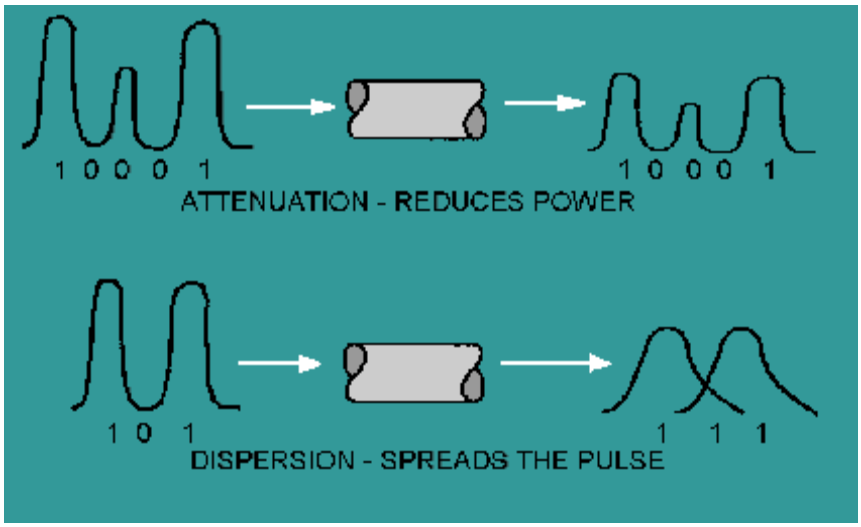

Figure 2.1 Fiber transmission properties.

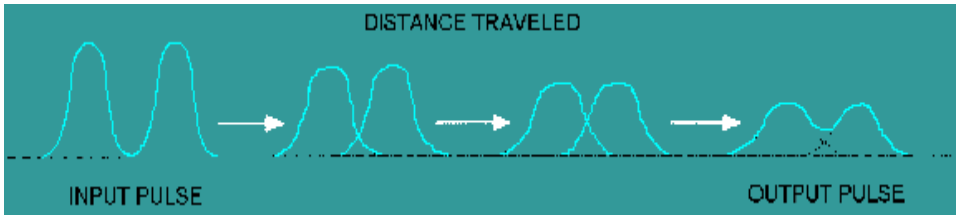

Figure 2.2 Pulse spreading and power loss along an optical fiber.

In addition to fiber attenuation and dispersion, other optical fiber properties affect system performance. Fiber properties, such as modal noise, pulse broadening and polarization can reduce system performance.

2.4.2 Scattering

Basically, scattering losses are caused by the interaction of light with density fluctuations within a fiber. Density changes are produced when optical fibers are manufactured. During manufacturing, regions of higher and lower molecular density areas, relative to the average density of the fiber, are created. Light traveling through the fiber interacts with the density areas as shown in figure 2.3. Light is then partially scattered in all directions.

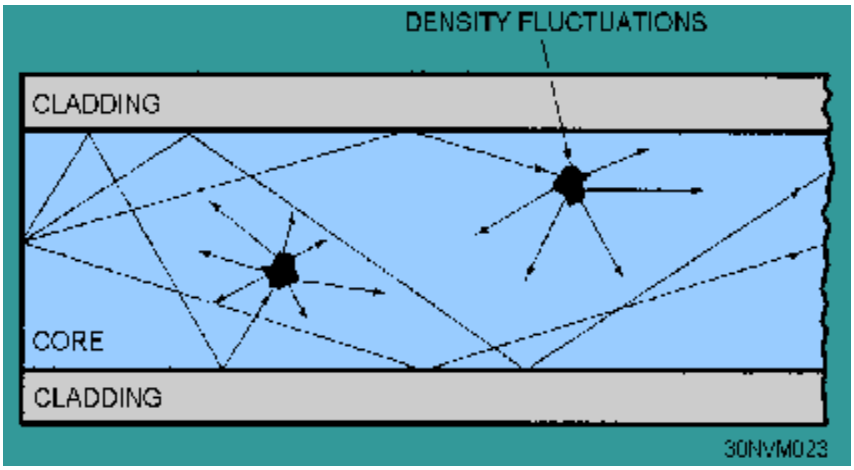

Figure 2.3 Rayleigh scattering.

In commercial fibers operating between 700 nm and 1600 nm wavelength, the main source of loss is called Rayleigh scattering. Rayleigh scattering is the main loss mechanism between the ultraviolet and infrared regions as shown in figure 2.3. Rayleigh scattering occurs when the size of the density fluctuation (fiber defect) is less than one-tenth of the operating wavelength of light. Loss caused by Rayleigh scattering is proportional to the fourth power of the wavelength ($1/\lambda$). As the wavelength increases, the loss caused by Rayleigh scattering decreases.

If the size of the defect is greater than one-tenth of the wavelength of light, the scattering mechanism is called Mie scattering. Mie scattering, caused by these large defects in the fiber core, scatters light out of the fiber core. However, in commercial fibers, the effects of Mie scattering are insignificant. Optical fibers are manufactured with very few large defects.

2.4.3 Bending loss

Bending the fiber also causes attenuation. Bending loss is classified according to the bend radius of curvature: micro bend loss or macro bend loss.

Micro bends are small microscopic bends of the fiber axis that occur mainly when a fiber is cabled. Macro bends are bends having a large radius of curvature relative to the fiber diameter. Micro bend and macro bend losses are very important loss mechanisms. Fiber loss caused by micro bending can still occur even if the fiber is cabled correctly. During installation, if fibers are bent too sharply, macro bend losses will occur.

Micro bend losses are caused by small discontinuities or imperfections in the fiber. Uneven coating applications and improper cabling procedures increase micro bend loss. External forces are also a source of micro bends. An external force deforms the cabled jacket surrounding the fiber but causes only a small bend in the fiber. Micro bends change the path that propagating modes take, as shown in figure 2.4. Micro bend loss increases attenuation because low-order modes become coupled with high-order modes that are naturally lossy.

.

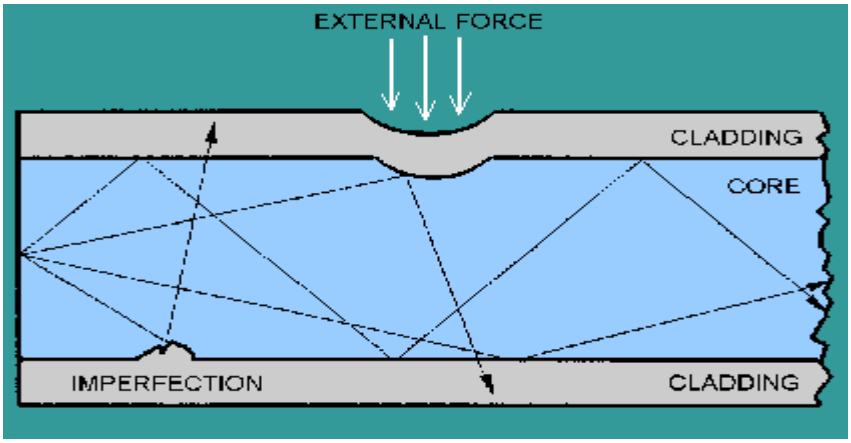

Figure 2.4 Micro bend loss

Macro bend losses are observed when a fiber bends radius of curvature is large compared to the fiber diameter.

These bends become great source of loss when the radius of curvature is less than several centimeters. Light propagating at the inner side of the bend travels a shorter distance than that on the outer side. To maintain the phase of the light wave, the mode phase velocity must increase. When the fiber bend is less than some critical radius, the mode phase

velocity must increase to a speed greater than the speed of light. However, it is impossible to exceed the speed of light. This condition causes some of the light within the fiber to be converted to high-order modes. These high-order modes are then lost or radiated out of the fiber [29].

Fiber sensitivity to bending losses can be reduced. If the refractive index of the core is increased, then fiber sensitivity decreases. Sensitivity also decreases as the diameter of the overall fiber increases. However, increases in the fiber core diameter increase fiber sensitivity. Fibers with larger core size propagate more modes. These additional modes tend to be more loss.

2.5 Dispersion compensation fiber

Dispersion Compensating Fiber (DCF) represents the most widely used in-line dispersion compensation technique in today's transmission systems. The DCFs are characterized by a large negative dispersion and a small core diameter. The large negative dispersion values can be achieved by variation of the fiber profile by doping the fiber cladding (e.g. by fluorine), introducing an increase in the refractive index difference between the core and cladding. The demands on DCFs are a large negative dispersion (-70-300 ps/nm), low insertion losses, low polarization dependent losses (PDL), a low polarization mode dispersion (< 0.05 ps/km), a large effective area (A_{eff}) and a negative dispersion slope. The DCFs can be used for simultaneous compensation of several channels, but due to imperfections in slope compensation, a small amount of residual dispersion remains especially in outer channels [30-31].

CHAPTER 3

DISPERSION AND NONLINEARITIES IN FIBERS

3.1 Introduction

The transmission of optical signals in an optical communication system may be limited by optical effects such as dispersion. Optical signals may be transmitted as pulses of light in an optical fiber. As a pulse spreads, energy is overlapped. This condition is shown in figure 3.1. The spreading of the optical pulse as it travels along the fiber limits the information capacity of the fiber. When light propagating within an optical fiber undergoes chromatic dispersion, the light is delayed within the optical fiber. The delay causes spreading of the light pulses, which may affect the performance of the system. The specific amount of dispersion that an optical signal undergoes varies depending upon the wavelength of the optical signal. The extent to which dispersion varies as a function of light wavelength is often referred to as dispersion slope. Various dispersion management techniques have been used to reduce dispersion and to manage dispersion slope by reducing dispersion at individual channel wavelengths. Dispersion management is particularly important in wavelength division multiplexed (WDM) optical communication systems transmitting multiple channels at multiple wavelengths.

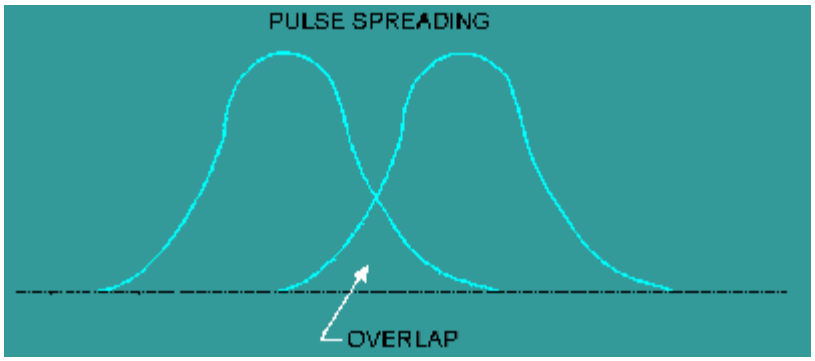

Figure 3.1 Pulse overlap

3.2 Types of dispersion

There are two different types of dispersion in optical fibers. The types are intramodal and intermodal dispersion. Intramodal, or chromatic, dispersion occurs in all types of fibers.

Intermodal or modal dispersion occurs only in multimode fibers. Each type of dispersion mechanism leads to pulse spreading.

3.2.1 Intramodal dispersion

Intramodal, or chromatic, dispersion depends primarily on fiber materials. There are two types of intramodal dispersion. The first type is material dispersion. The second type is waveguide dispersion. Intramodal dispersion occurs because different colors of light travel through different materials and different waveguide structures at different speeds [32-33].

3.2.1.1 Material dispersion

Material dispersion occurs because the spreading of a light pulse is dependent on the wavelengths interaction with the refractive index of the fiber core. Different wavelengths travel at different speeds in the fiber material. Different wavelengths of a light pulse that enter a fiber at one time exit the fiber at different times. Material dispersion is a function of the source spectral width. The spectral width specifies the range of wavelengths that can propagate in the fiber. Material dispersion is less at longer wavelengths.

3.2.1.2 Waveguide dispersion

Waveguide dispersion occurs because the mode propagation constant is a function of the size of the fiber's core relative to the wavelength of operation. Waveguide dispersion also occurs because light propagates differently in the core than in the cladding.

In multimode fibers, waveguide dispersion and material dispersion are basically separate properties. Multimode waveguide dispersion is generally small compared to material dispersion. Waveguide dispersion is usually neglected. However, in single mode fibers, material and waveguide dispersion are interrelated.

The total dispersion present in single mode fibers may be minimized by trading material and waveguide properties depending on the wavelength of operation.

3.2.2 Modal dispersion

Modal dispersion occurs because each mode travels a different distance over the same time span, as shown in figure 3.2. The modes of a light pulse that enter the fiber at one time exit the fiber a different time. This condition causes the light pulse to spread. As the length of the fiber increases, modal dispersion increases.

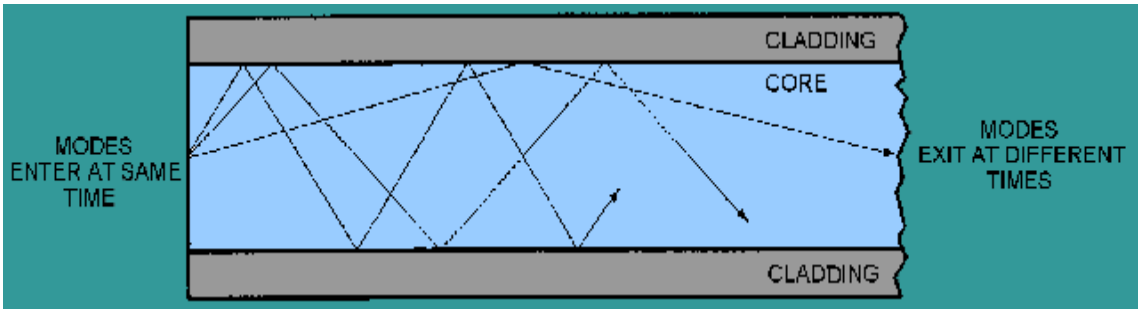

Figure 3.2 Distance traveled by each mode over the same time span.

Modal dispersion is the dominant source of dispersion in multimode fibers. Modal dispersion does not exist in single mode fibers. Single mode fibers propagate only the fundamental mode. Therefore, single mode fibers exhibit the lowest amount of total dispersion. Single mode fibers also exhibit the highest possible bandwidth [3].

3.3 Dispersion compensation techniques

The ideal dispersion compensator must have a quite stringent list of characteristics. Regarding the chromatic dispersion, it has to be well matched to the transport fiber, have a smooth dispersion profile (i.e. no dispersion ripples or group delay ripples), be tunable potentially provide a high channel-to-channel variation in the dispersion. Furthermore, it has to be free of polarization effects [polarization dependent loss (PDL) and polarization mode dispersion (PMD)]. Regarding the wavelength, it has to be broadband, being usable over the whole wavelength range (high spectral efficiency) and should accommodate high signal bandwidths. The ideal compensator must also provide low insertion loss and being capable of handling high optical power. Finally it must be compact, consume no or low power and must be low-cost [34].

Obviously, such a long list of requirements is virtually impossible to fulfill. Trade-offs must be made between the different requirements. Different technologies exist for compensating the chromatic dispersion. Each of them contains inherent trade-offs that render it more suitable for an application and less for another one. The main technologies are dispersion compensating fiber, fiber Bragg gratings, etalon filter and virtually imaged phased array. Furthermore, not truly dispersion compensation devices, electronic dispersion compensation and advanced modulation formats are attractive due to the high dispersion tolerance they provide [35].

3.3.1 Fiber based method

The fiber based method employs the dispersion compensation through a small section of fiber length. Their are various techniques such as dispersion compensation fiber (DCF), reverse dispersion fiber, negative dispersion fiber to compensate the dispersion of the system.

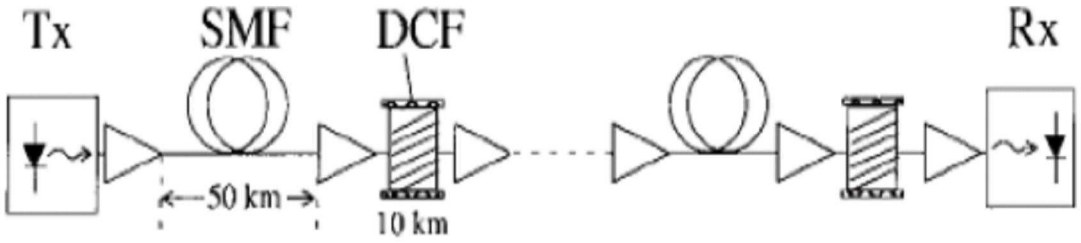

Figure 3.3 Dispersion compensation fibers in optical communication system

Dispersion compensating fiber (DCF) is the predominant technology for dispersion compensation. It consists of an optical fiber that has a special design such as providing a large negative dispersion coefficient while the dispersion of the transport fiber is positive. A proper length of DCF allows the compensation of the chromatic dispersion accumulated over a given length of the transport fiber, although standard modules with predetermined dispersion values (with a typical granularity corresponding to the dispersion of 20 km of SSMF) are commercially available. The main advantage of this technology is the fact that it provides a broadband operation with a smooth dispersion property and good optical characteristics. In the first generation of DCF, only about 60%

of the SSMF dispersion slope was allowed to be compensated. Now, 100% slope-matching for both SSMF and E-LEAF is commercially available. However, dispersion compensation modules based on a first-generation DCF are largely deployed and their associated slope-mismatch is a problem we have to live with. DCF also presents a quite large insertion loss although improvements have been reported recently.

Dispersion compensation modules based on DCF are also bulky and again, size reduction is expected in the future as bend loss reduction could allow a significant improvement in the compactness [36].

The disadvantages of the fiber-based methods are the extra fiber loss in, high non-linearity and the additional cost of the DCF. The maximum dispersion of such DCF is about -100 ps/nm/km, which is limited by the mismatching of the glass properties between the core and the cladding. Therefore, the up gradation of already installed systems is difficult with DCFs, as the dispersion in the 1550 nm region is 17 ps/nm/km. Hence very long lengths of dispersion compensating fiber will be required to compensate for the dispersion of even modest lengths of transmission.

3.3.2 Fiber Bragg grating

The first in-fiber Bragg grating was demonstrated by Hill in 1978 [37]. A fiber Bragg grating (FBG) is a type of distributed Bragg reflector is constructed in a short segment of optical fiber that reflects particular wavelengths of light and transmits all others. This is achieved by adding a periodic variation to the refractive index of the fiber core, which generates a wavelength specific dielectric mirror. A fiber Bragg grating can therefore be used as an inline optical fiber to block certain wavelengths, or as a wavelength-specific reflector.

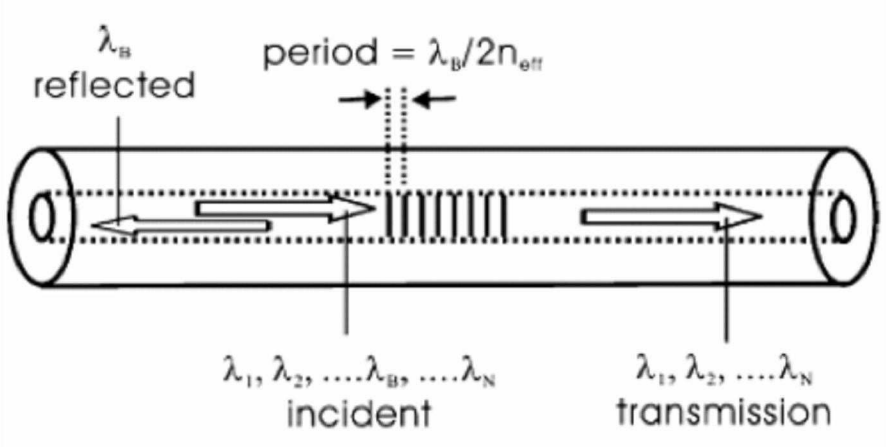

Figure 3.4 Basic structure of fiber Bragg grating

The Bragg wavelength λ_B, of an FBG, which is given by the following relation

$$\lambda_B = 2\, n_{eff} \Lambda \qquad \ldots \ldots \ldots \ldots \ldots \ldots 3.1$$

Here $n_{eff}\Lambda$ the modal refractive index and Λ is represents the index modulation period of the Bragg grating. Assume that the incident light fulfils the Bragg condition given by eq. 3.1. The incident light will be Fresnel reflected at one of the grating plane. Under the Bragg condition, the reflected light is exactly in-phase with reflected lights from other grating planes. Since all of these reflected lights would be constructively interfered at the incident edge of the FBG, the incident light is reflected as shown in figure 3.4. On the other hand, other wavelength components will pass through the FBG. Therefore, the FBG acts as a band-pass filter at the reflection port and a band-rejection filter at the transmission port.

Such interferometric effect can exhibit a very narrow bandwidth characteristic of filters. Fiber Bragg gratings (FBG) have been proposed for compensating the chromatic dispersion several years ago. Such a device reflects light when its wavelength corresponds to the grating period. When the grating is chirped, that is when its period varies linearly along the axis; the different spectral components of the light are reflected at different location along the grating. In such a way, a spectral component traveling faster in the transport fiber can be delayed by the FBG compared to a spectral component

that travels slower. Its a narrowband operation, FWBG can now be operated over the full C-band though a multi-channel operation where the same portion of optical fiber reflects over many wavelength regions instead of only one. The multi-channel operation can be achieved by grating superposition or by a sampling approach. Dispersion compensation of 80 km of SSMF over 51 channels covering the full C-band has been reported with a good slope-matching.

Each reflection region or grating component can be made independent on each other allowing for a large flexibility in the channel-to-channel variation of the optical characteristics. Such a device can provide a tunable dispersion by imposing a thermal gradient on the FBG. Multi-channel tunable dispersion compensation has been obtained in this manner. FBG-based dispersion compensation provides a low loss and small footprint solution. Multi-channel FBGs are channelized devices that can be incompatible with a cascade of a large number of units. Furthermore, overall nonlinearities in the group delay (group delay ripples) also increases with the square root of the number of cascaded units [38].

3.3.3 Optical phase conjugation method

Optical phase conjugation (OPC) is used as e generic term for a multitude of nonlinear optical processes. The common feature is that all these processes are capable of reversing both the direction of propagation and the phase factor for each plane wave component of an arbitrary incoming beam of light. This mean phase conjugator can be considered as a kind of mirror with very unusual reflection properties. Unlike a conventional mirror, where a ray of light bits redirected according to ordinary law of reflection, a phase Conjugator mirror (PCM) retro-reflects all incoming rays back to the original path. When a conventional mirror only the wave vector component normal to the surface of the mirror reflects a ray changes sign the tangential components are unchanged. This means that the propagation direction of the reflected ray depends on the angle between the surface normal and the incident ray. A PCM, on the other hand, changes the sign of the complete wave vector so that the reflected ray is always anti parallel to the incident ray, independent of the orientation of the mirror surface. The concept here is to use a device

in the middle of the link to invert the spectrum. This process changes the short wavelengths to long wave length and the long ones into short once. If the spectrum is inverted in the middle of the link (using standard single mode fiber) the second half of the link acts in the opposite direction. When the pulse arrives it has been rebuilt exactly compensated for by the second half of the fiber. Mid span spectral inversion is bit difficult to implement in all situations because active device have to be put in the middle of the link. This may or may not be practical. A process called "optical phase conjugation" performs this spectral inversion.

3.4 Nonlinearities in fibers

3.4.1 Dispersion mapping

The advent of optical repeaters based on erbium doped fiber amplifiers (EDFAs) has opened the new era of optical transmission technologies, allowing us to use wavelength division multiplexing (WDM) technologies with simple, compact and economical approaches [39]. In fact, the demonstrated capacity for long-haul optical transmission has been growing remarkably and more than a thousand fold increase in capacity has been achieved over the past ten years. The price we have to pay for such success is the combat with the accumulated impact of fiber nonlinearity, interplaying with the chromatic dispersion of the transmission fiber, which grows with transmission distance and, therefore, becomes significant for ultra-long-haul systems. Dispersion management technologies have been invented to overcome such inherent problems in optically amplified transmission systems [40].

The transmission of optical signals in an optical communication system may be limited by optical effects such as chromatic dispersion. Optical signals may be transmitted as pulses of light in an optical fiber. When light propagating within an optical fiber undergoes chromatic dispersion, the light is delayed within the optical fiber. The delay causes spreading of the light pulses, which may affect the performance of the system. The specific amount of dispersion that an optical signal undergoes varies depending upon the wavelength of the optical signal. The extent to which dispersion varies as a function of

light wavelength is often referred to as dispersion slope. Various dispersion management techniques have been used to reduce dispersion and to manage dispersion slope by reducing dispersion at individual channel wavelengths. Dispersion management is particularly important in wavelength division multiplexed (WDM) optical communication systems transmitting multiple channels at multiple wavelengths.

Dispersion can be minimized when the signals are placed symmetrically around the fiber's zero-dispersion wavelength $\lambda_D = 0$, but then FWM will increase and severely degrade system performance. Since higher dispersion will eliminate FWM, therefore, two solutions to suppress FWM include: (1) placing all wavelengths away from and on only one side of $\lambda_D = 0$; and (2) utilizing alternating fiber segments with positive and negative dispersion values in a dispersion managed system in which there is always an absolute dispersion value exists along the link, but the total accumulated dispersion is 0. In both these cases, each WDM channel accumulates a different amount of dispersion because of the spectrally dependent dispersion slope of the fibers. Additionally, each channel experiences SPM/XPM which interacts with the GVD, resulting in further degradation.

To combat dispersion and nonlinearities, each WDM channel can separately be either pre-compensated, post-compensated or dual-compensated (using a combination of pre and post-compensation) in total accumulated dispersion [41].

3.4.2 Origins of nonlinearities

When radiation is incident upon a medium, the oscillating electromagnetic field interacts with electric dipoles in the molecules of the medium and causes them to oscillate. The result is a time-varying local electric polarization in the medium. This oscillating electric field then re-radiates the electromagnetic field and the incident wave is considered to propagate through the medium via a series of such absorption and re-radiation processes. The polarization vector P, induced by an electric field with amplitude vector E can be expressed as a general series expansion of the form [42].

$P = \varepsilon_0 (\chi .E + \chi_2 .E\,E + \chi_3 .EEE + \ldots\ldots\ldots\ldots\ldots 3.2)$

ε_0 is the electric permeability of a vacuum,

χ is the linear susceptibility tensor of the medium and

χ_2 and χ_3 are second and third order susceptibility tensor terms.

If the induced polarization has a purely linear dependence on the applied electric field then the re-radiated electric field will be identical to the incident field. However, when second or higher-order susceptibility terms are nonzero, harmonics begin to appear in the radiated field that was not present in the incident field. For materials that have a symmetrical molecular structure, the polarization induced by an incident electric field is symmetrical, as illustrated in figure 3.5. The susceptibility of these materials contains only odd expansion terms, as opposed to anti-symmetric molecules for which even terms such as may be non-zero.

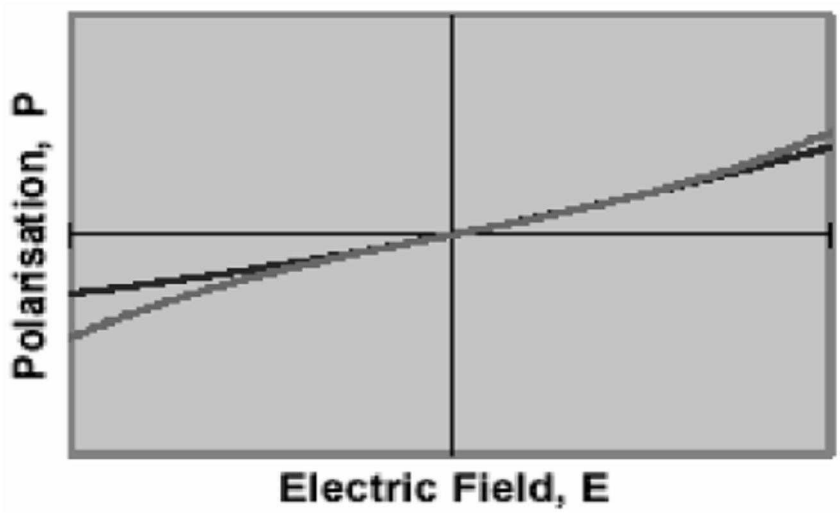

Figure 3.5 Electric polarizations versus electric field for materials with inversion symmetry (broken line) and with asymmetric molecular structure (Solid dark line).

The dominant susceptibility term is the linear term, χ which determines the linear refractive index of the medium, n and the absorption attenuation coefficient α. The orders

of the non-zero expansion terms determine the type of nonlinearity to which the medium is susceptible. In materials, which lack a center of symmetry, such as quartz, KDP and ADP, the second order susceptibility is responsible for second harmonic generation, in which an intense wave at angular frequency $\acute{\omega}_1$ generates another wave at twice this frequency, $2\acute{\omega}_1$. Another effect which is possible in these materials is sum frequency generation; in which two waves at $\acute{\omega}_1$ and $\acute{\omega}_2$ interact to produce waves at $\acute{\omega}_1 + \acute{\omega}_2$, $\acute{\omega}_1 + 2\acute{\omega}_2$, $2\acute{\omega}_1 + \acute{\omega}_2$ [43].

3.4.3 Optical Kerr effect

The optical Kerr effect or AC Kerr effect is the case in which the electric field is due to the light itself. This causes a variation in index of refraction which is proportional to the local irradiance of the light. This refractive index variation is responsible for the nonlinear optical effects of self focusing and self phase modulation. This effect only becomes significant with very intense beams such as those from lasers. In fact, phase modulation due to intensity dependent refractive index induces various nonlinear effects, namely, self phase modulation (SPM), cross phase modulation (XPM) and four wave mixing (FWM).

3.4.3.1 Self phase modulation (SPM)

Phase modulation of an optical signal by itself is known as self phase modulation (SPM). SPM is primarily due to the self modulation of the pulses. Generally, SPM occurs in single-wavelength systems. At high bit rates however, SPM tends to cancel dispersion. However, consideration must be given to receiver saturation and to nonlinear effects such as SPM, which occurs with high signal levels. SPM results in phase shift and a nonlinear pulse spread. As the pulses spread, they tend to overlap and are no longer distinguishable by the receiver. The acceptable norm in system design to counter the SPM effect is to take into account a power penalty that can be assumed equal to the negative effect posed by XPM. By the SPM-impact new spectral components are generated in the optical signal spectrum resulting in a spectral broadening.

3.4.3.2 Cross phase modulation (XPM)

Cross phase modulation (XPM) is a nonlinear effect that limits system performance in wavelength Division Multiplexed (WDM) systems. (XPM) is the phase modulation of a signal caused by an adjacent signal within the same fiber. (XPM) is related to the combination (dispersion/effective area). (XPM) results from the different carrier frequencies of independent channels, including the associated phase shifts on one another. The induced phase shift is due to the walkover effect, whereby two pulses at different bit rates or with different group velocities walk across each other. As a result, the slower pulse sees the walkover and induces a phase shift. The total phase shift depends on the net power of all the channels and on the bit output of the channels. Maximum phase shift is produced when bits belonging to high-powered adjacent channels walk across each other.

3.4.3.3 Four wave mixing (FWM)

FWM can be compared to the intermodulation distortion in standard electrical systems. When three wavelengths (λ_1, λ_2 andλ_3) interact in a nonlinear medium, they give rise to a fourth wavelength (λ_4), which is formed by the scattering of the three incident photons, producing the fourth photon. This effect is known as four wave mixing (FWM) and is a fiber-optic characteristic that affects (WDM) systems. The effects of (FWM) are pronounced with decreased channel spacing of wavelengths and at high signal power levels. High chromatic dispersion also increases (FWM) effects. FWM also causes inter channel crosstalk effects for equally spaced (WDM) channels.

CHAPTER 4

DEPENDENCE OF SELF PHASE MODULATION IMPAIRMENTS ON RESIDUAL DISPERSION IN 10 Gb/s BASED TERRESTRIAL TRANSMISSION USING STANDARD FIBER WITH EDFA

4.1 Introduction

The most effective and practical strategy for upgrading the already-installed transmission systems is using standard single mode fiber (SMF), the periodical insertion of dispersion compensating fiber (DCF) for suppressing the linear distortion induced by group velocity dispersion (GVD). Nonlinear effects are self phase modulation (SPM) and cross phase modulation (XPM). The signal distortion cannot be fully suppressed because the generation of nonlinear phase modulation, in which induces intensity distortion through GVD is distributed during the propagation [44].

The transmission performance is dependent on the position of the DCF and the zero residual dispersion is not the best choice. In the case of full compensation, the dependence on the DCF position shows the pre compensation technique achieves the best results as shown in figure 4.1. Pre or post compensation when the DCF is located before or after the transmission fiber.

If consider the cases of partial compensation the most performing technique turns out to be the post compensation. We also show that pre compensation is not a valid technique when the dual stage strategy is adopted for span amplification. We proposed a practical design rule for SPM-limited transmission systems and show that the presence of multi wavelength nonlinear effects [45-46].

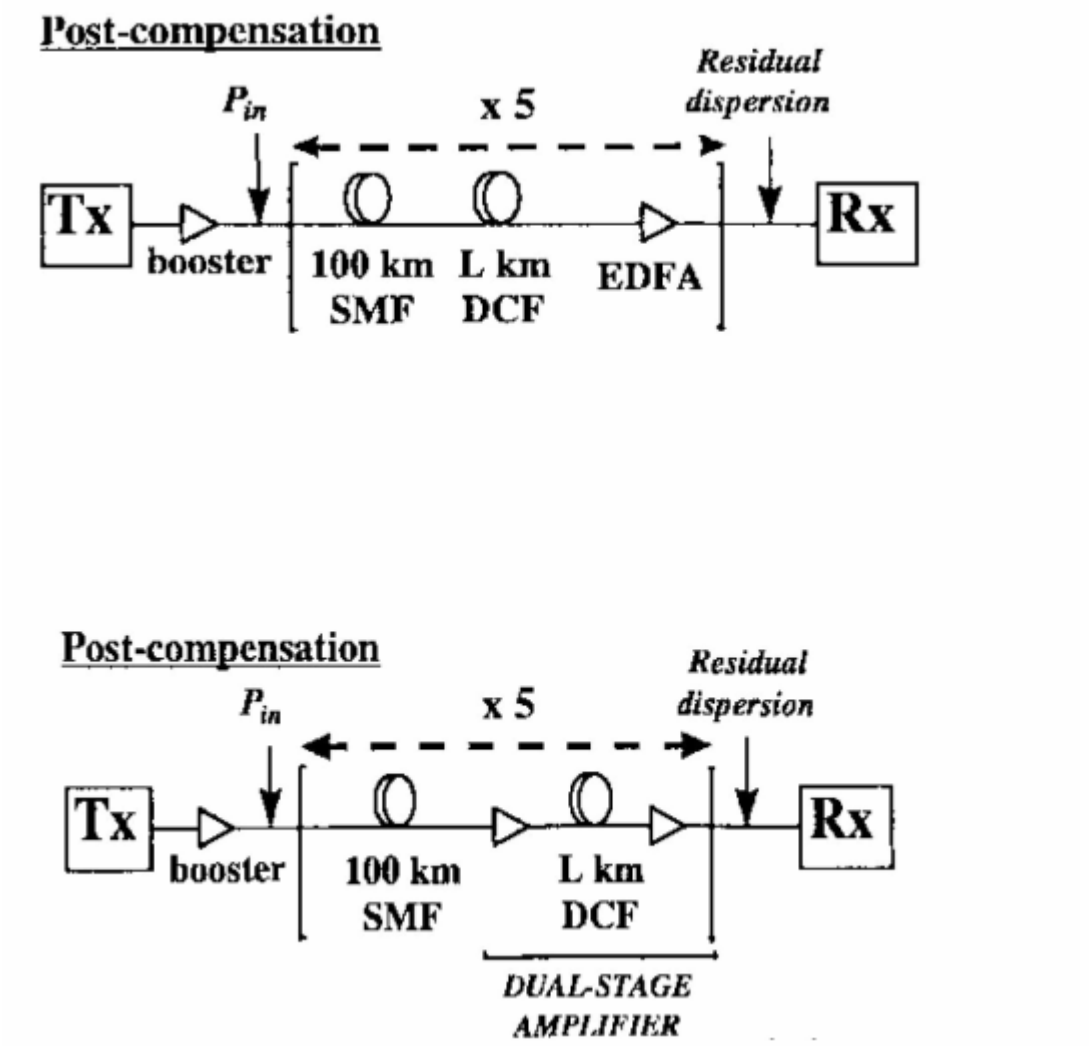

Figure 4.1 Post compensation

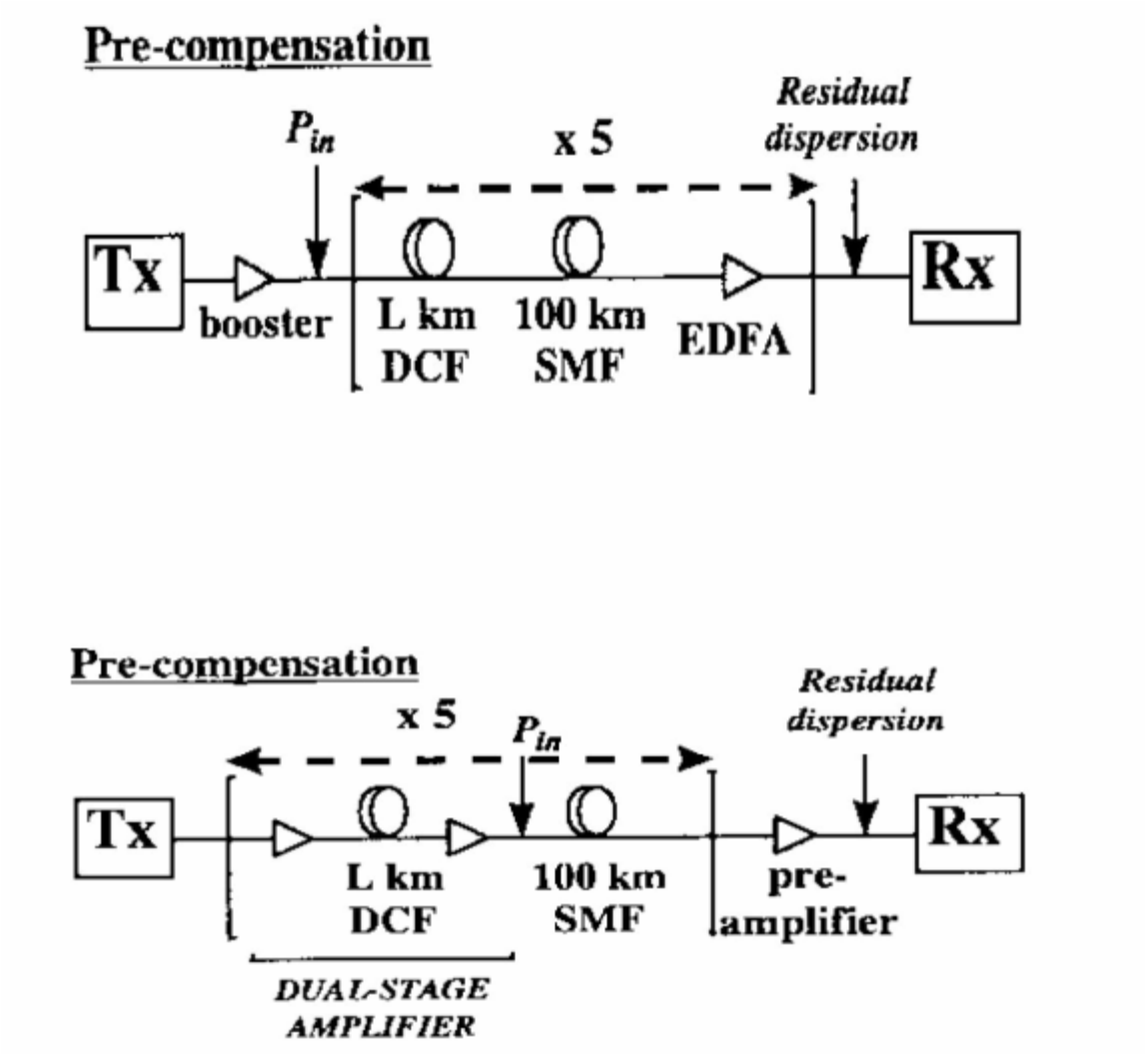

Figure 4.2 Pre compensation

4.2 Simulation setups

The various simulation setups under consideration are shown in following sections, the first section 4.2.1 is the simulation for pre compensation, the second section 4.2.2 is the simulation for post compensation and third section 4.2.3 is the simulation for symmetrical compensation. The results of simulations are reported in last section 4.3.

4.2.1 Simulation for pre compensation

In order to illustrate how pre compensation can be studied, the system is simulated with block diagram shown in figure 4.3. In this case, the transmitter section consists of data source, electrical driver (NRZ), laser source (CW_ Lorentzian) and amplitude modulator ($\sin^2$_MZ) is connected with optical spectrum analyzer which is used to observe the optical spectrum. Three EDFA and two SSMF are connected in alternate to each other such that the output of EDFA is fed to the next SSMF connected to it. The output of last EDFA is given to optical raised cosine filter which is connected to receiver section. In receiver section PIN is connected to an electrical Bessel filter and the final result is shown through electrical scope, Q estimator and bit error rate estimator.

4.2.2 Simulation for post compensation

In order to illustrate how post compensation can be studied, the system is simulated with block diagram shown in figure 4.4. In this case, the transmitter section consists of data source, electrical driver (NRZ), laser source (CW_ Lorentzian) and amplitude modulator ($\sin^2$_MZ). Here four EDFA and four SSMF are connected in alternate to each other such that the output of EDFA is fed to the next SSMF connected to it. The second SSMF is connected with splitter in order to make the whole system as post compensation by changing the value of dispersion which causes SSMF to work as DCF. The output of last EDFA is given to optical raised cosine filter which is connected to receiver section. In

receiver section PIN is connected to an electrical Bessel filter and the final result is shown through electrical scope, Q estimator and bit error rate estimator.

4.2.3 Simulation for symmetrical compensation

In order to illustrate how symmetrical compensation can be studied, the system is simulated with block diagram shown in figure 4.3. In this case, the transmitter section consists of data source, electrical driver (NRZ), laser source (CW_ Lorentzian) and amplitude modulator ($\sin^2$_MZ). Five EDFA and four SSMF are connected in alternate to each other such that the output of EDFA is fed to the next SSMF connected. The output of last EDFA is given to the receiver section. In receiver section PIN is connected to an electrical Bessel filter and the final result is shown through electrical scope, Q estimator and bit error rate estimator.

4.3 Results for simulations

4.3.1.1 Results and discussions regarding simulation of pre compensation based on 10 Gb/s bit rate

The simulation results from different simulation systems are predicted. The results of simulation setup in figures 4.6 to 4.11 shows the electrical spectrum on 10 Gb/s bitrate on different length of 10, 20, 30, 40, 50, 60 km and dispersion values 8, 10, 12, 14, 15, 16 ps/nm/km.

Eye diagrams for different length

The results of eye diagrams are shown in figures 4.12 to 4.17 for different length. Eye opening decreases and eye closure increases with increase the length of SSMF i.e. eye opening penalty increases as the length of single mode fiber increases. The best result is observed with 10 km length of single mode fiber. Figure 4.18 shows the comparison of eye diagrams on 10, 20, 30, 40, 50, 60 km length of single mode fiber.

Eye diagrams for different dispersion

The results of eye diagrams are shown in figures 4.19 to 4.23 for different dispersion Eye opening decreases and eye closure increases with increase the dispersion of SSMF i.e. eye opening penalty increases as the dispersion of single mode fiber increases. The best result is observed with 10 ps/nm/km dispersion of single mode fiber. Figure 4.24 shows the comparison of eye diagrams on 8, 10, 12, 14, 15, ps/nm/km dispersion of single mode fiber.

Optical spectrums

The results of optical spectrum at frequency range [193.362, 193.467 THz] are shown in Figure 4.25 to 4.30.

Result based on Q estimator for different lengths

Figure 4.31 shows the result of Q value on 10, 20, 30, 40, 50, 60 km length of fiber which is 29 dB at 10 Km and 11 dB at 60 Km.

Figure 4.32 shows the result of eye opening on 10, 20, 30, 40, 50, 60 km length of fiber which is 0.00075 at 10 Km and 0.00740 at 60 Km.

Figure 4.33 shows the result of equivalent Q at mean threshold on 10, 20, 30, 40, 50, 60 km length of fiber which is 22.5 dB at 10 Km and 17.2 dB at 60 Km.

Figure 4.34 shows the result of equivalent Q at optimal threshold on 10, 20, 30, 40, 50, 60 km length of fiber which is 22.5 dB at 10 Km and 16.1 dB at 60 Km.

Result based on bit error rate estimator for different lengths

Figure 4.35 shows the result of eye closure on 10, 20, 30, 40, 50, 60 km length of fiber which is 0.4 dB at 10 Km and 1.2 dB at 60 Km.

Figure 4.36 shows the result of Average eye opening on 10, 20, 30, 40, 50, 60 km length of fiber which is 0.0094 at 10 Km, 0.0098 (Highest) at 30 Km and 0.00946 at 60 Km.

Figure 4.37 shows the result of BER at optimal threshold on 10, 20, 30, 40, 50, 60 km length of fiber which is 1e-040 at 10 Km and 1e-13 at 60 Km.

Figure 4.38 shows the result of BER at mean threshold on 10, 20, 30, 40, 50, 60 km length of fiber which is 1e-040 at 10 Km and 1e-13 at 60 Km.

Result based on Q estimator for different dispersion

Figure 4.39 shows the result of equivalent Q at mean threshold on 7, 9, 11, 13, 15 ps/nm/km dispersion of fiber which is 21 dB at 7 ps/nm/km and 17.2 dB at 15 ps/nm/km.

Figure 4.40 shows the result of equivalent Q at optimal threshold on 7, 9, 11, 13, 15 ps/nm/km dispersion of fiber which is 21 dB at 7 ps/nm/km and 17.2 dB at 15 ps/nm/km.

Result based on bit error rate estimator for different dispersion

Figure 4.41 shows the result of BER at mean threshold on 7, 9, 11, 13, 15 ps/nm/km dispersion of fiber which is 1e-040 at 7 ps/nm/km and 1e-008 at 15 ps/nm/km.

Figure 4.42 shows the result of BER at optimal threshold on 7, 9, 11, 13, 15 ps/nm/km dispersion of fiber which is 1e-040 at 7 ps/nm/km and 1e-008 at 15 ps/nm/km.

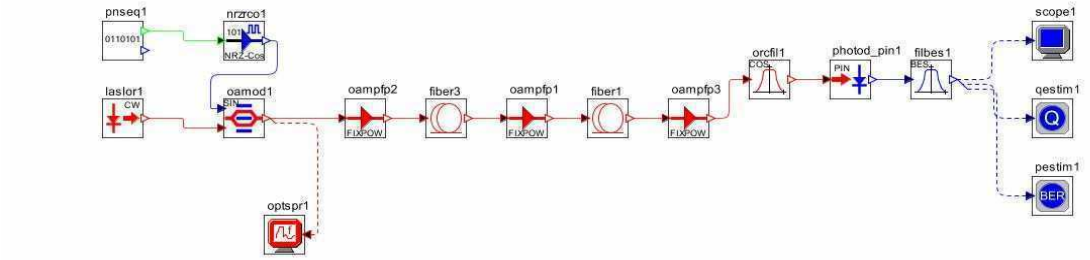

Figure 4.3 Pre compensation

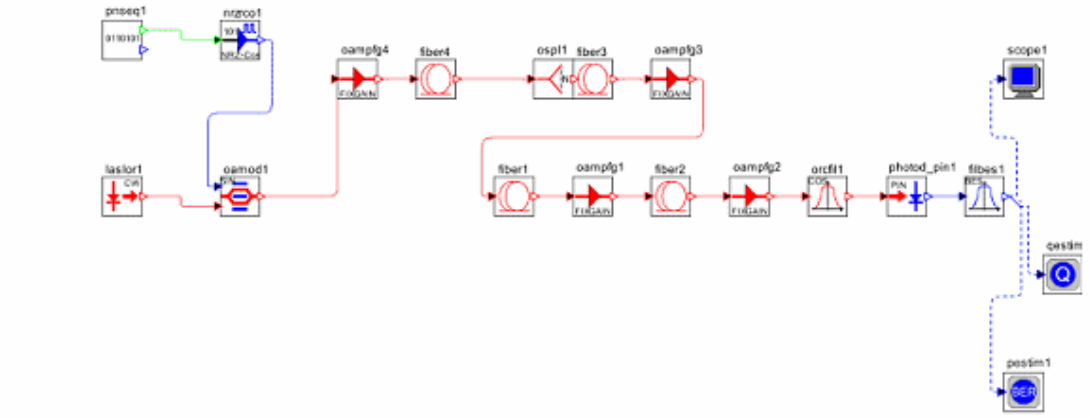

Figure 4.4 Post compensation

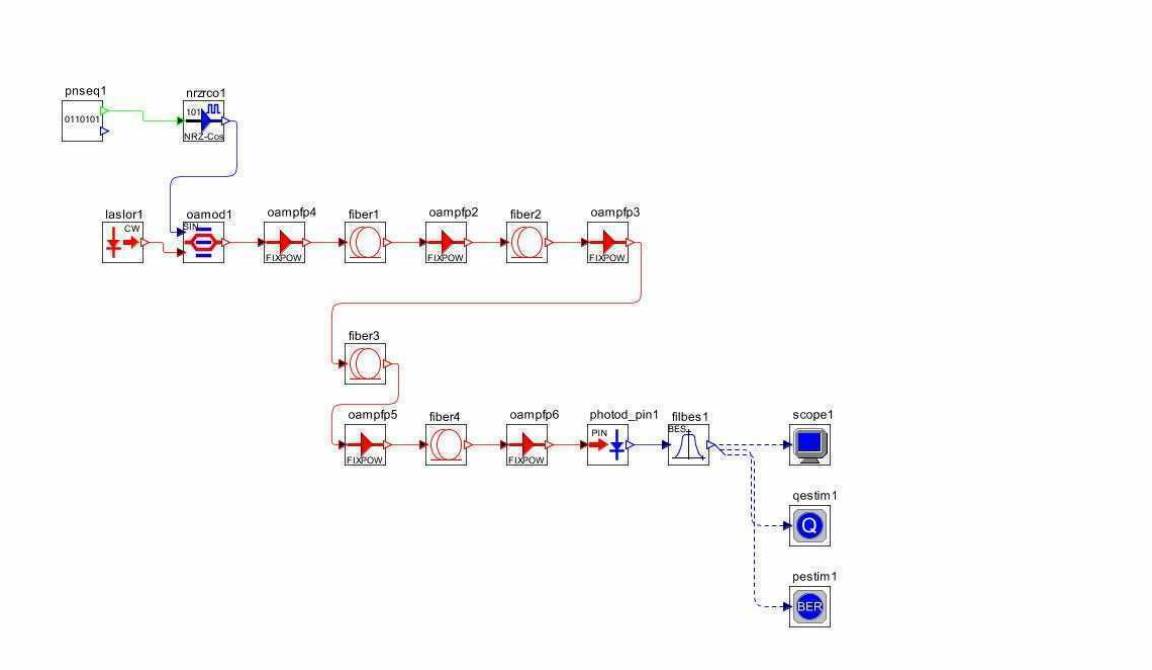

Figure 4.5 Symmetrical compensation

Parameter	Value
Center emission wavelength(nm)	1550
Center emission frequency(GHz)	193.41
CW power(mw)	0.0
CW power(dB)	1.0

Table 4.1 Properties of laser

Parameter	Value
Excess loss(dB)	3.0
% Transmission per applied voltage	20.0
Chirp factor	0.0

Table 4.2 Properties of Amplitude modulation

Parameter	Value
Bit rate	10
Corresponding simulation bit rate	10
Baud rate	10.0
Samples per bit	13
Sequence	Random

Table 4.3 Properties of Data source

Parameter	Value
Low Level	0.0
High Level	5.0
Duty cycle	0.5

Table 4.4 Properties of Modulator driver

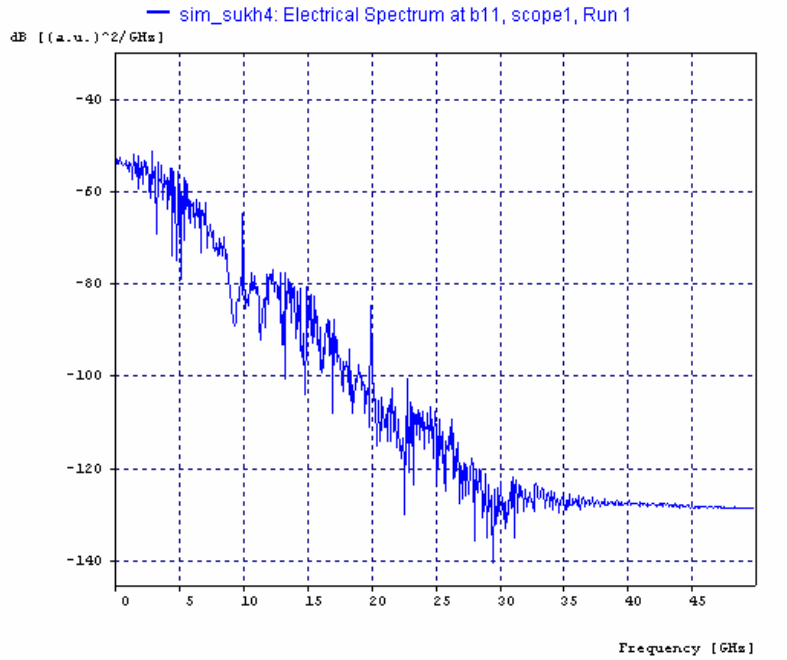

Figure 4.6 Electrical spectrum

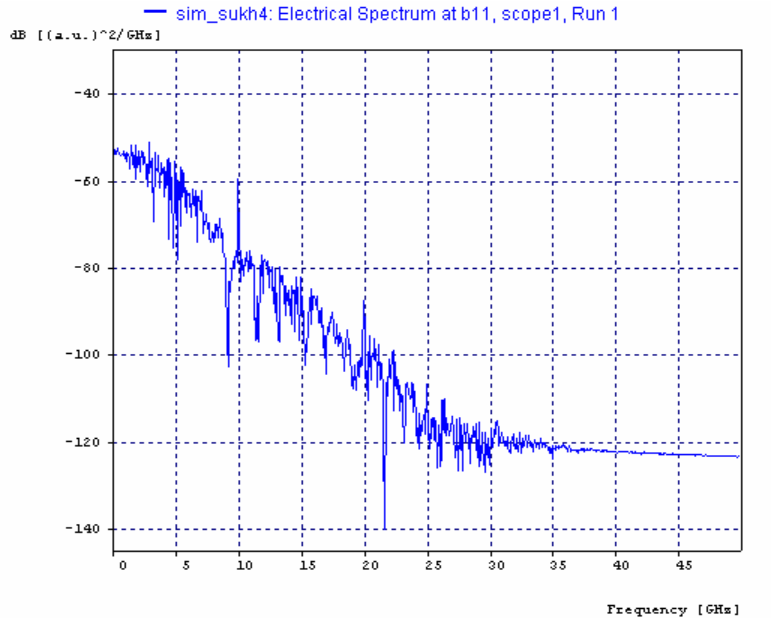

Figure 4.7 Electrical spectrum

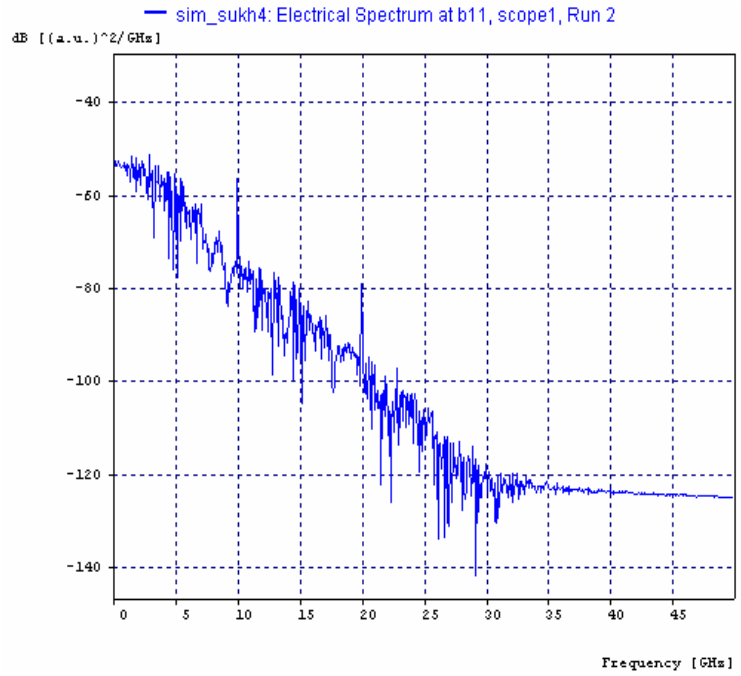

Figure 4.8 Electrical spectrum

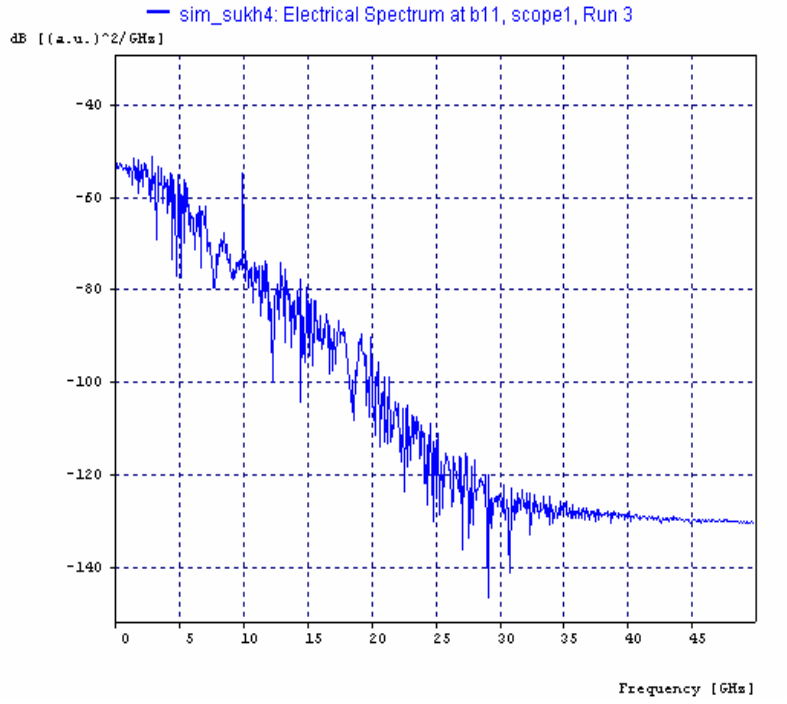

Figure 4.9 Electrical spectrum

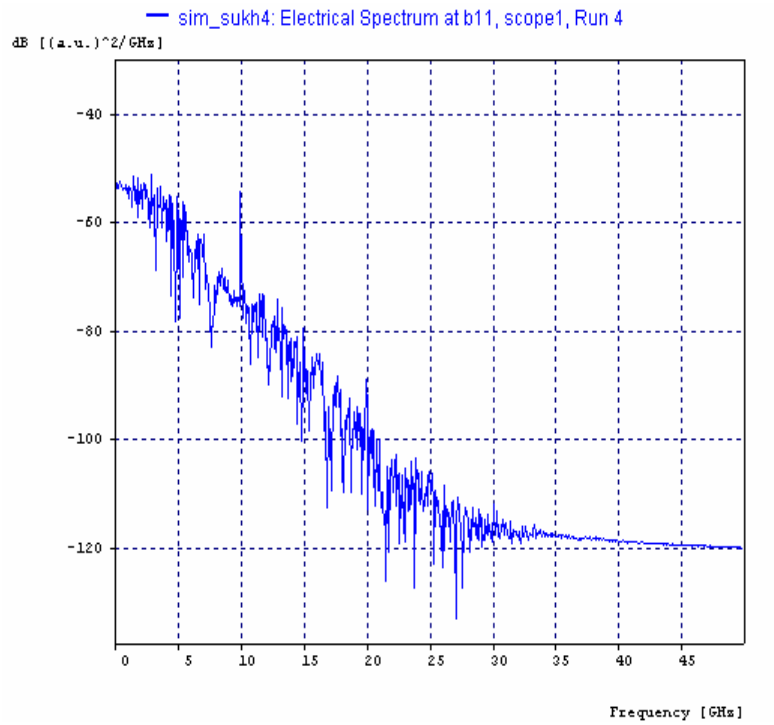

Figure 4.10 Electrical spectrum

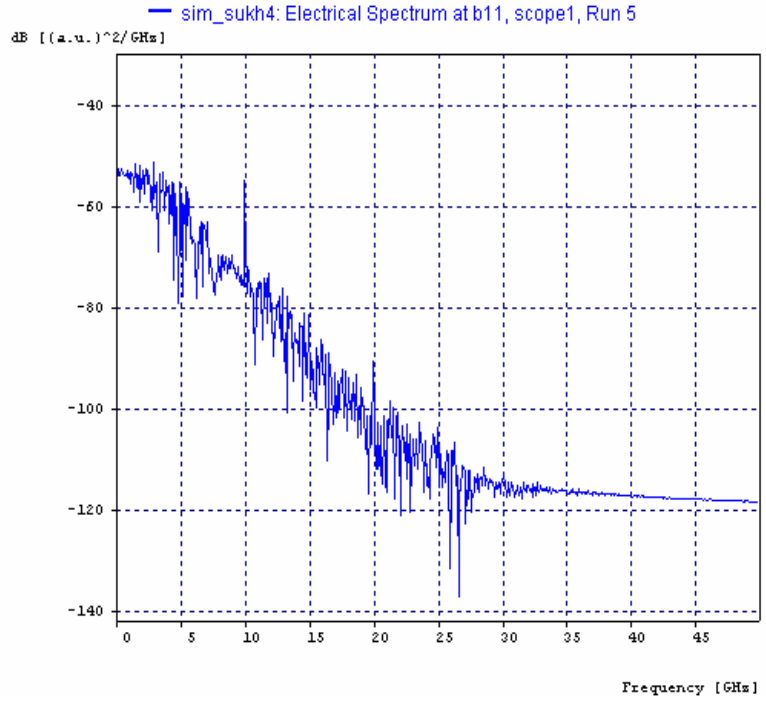

Figure 4.11 Electrical spectrum

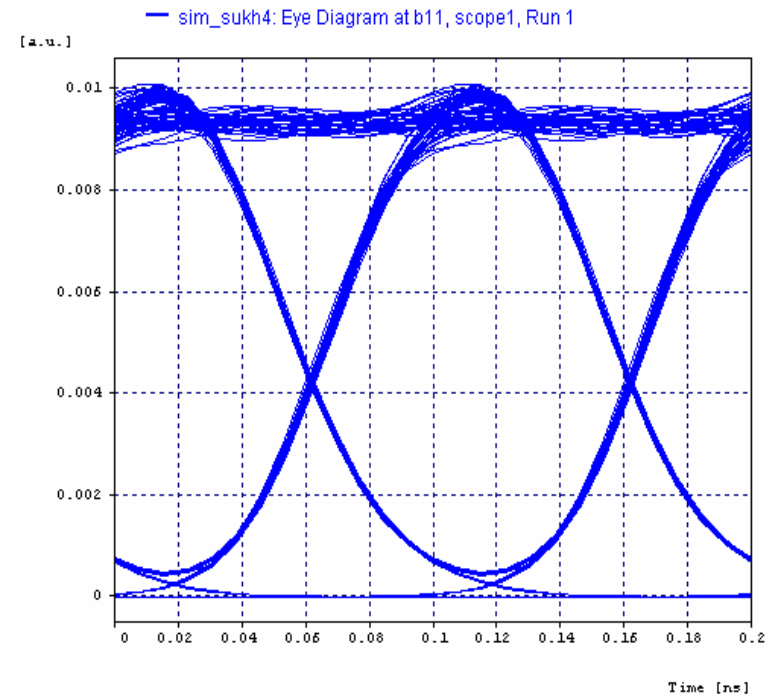

Figure 4.12 Eye diagram at 10 km length

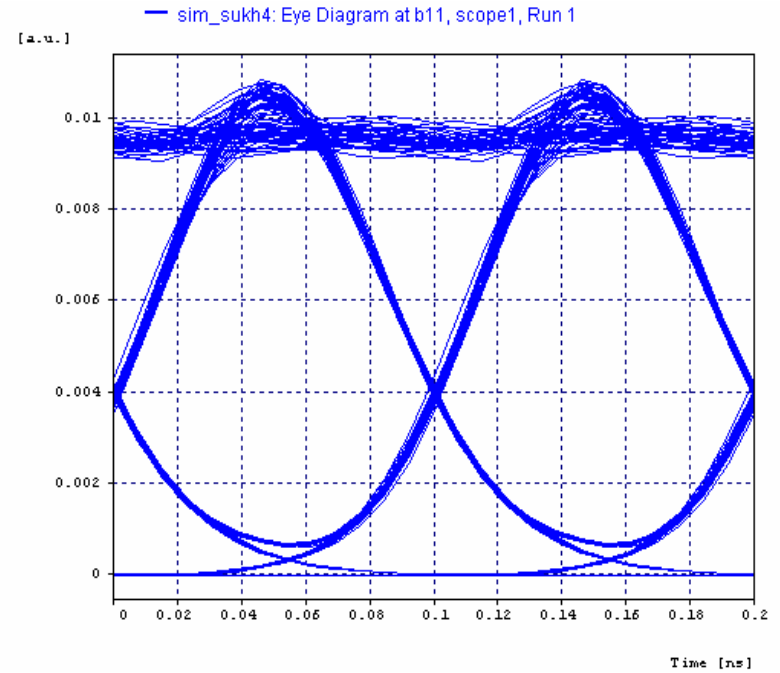

Figure 4.13 Eye diagram at 20 km length

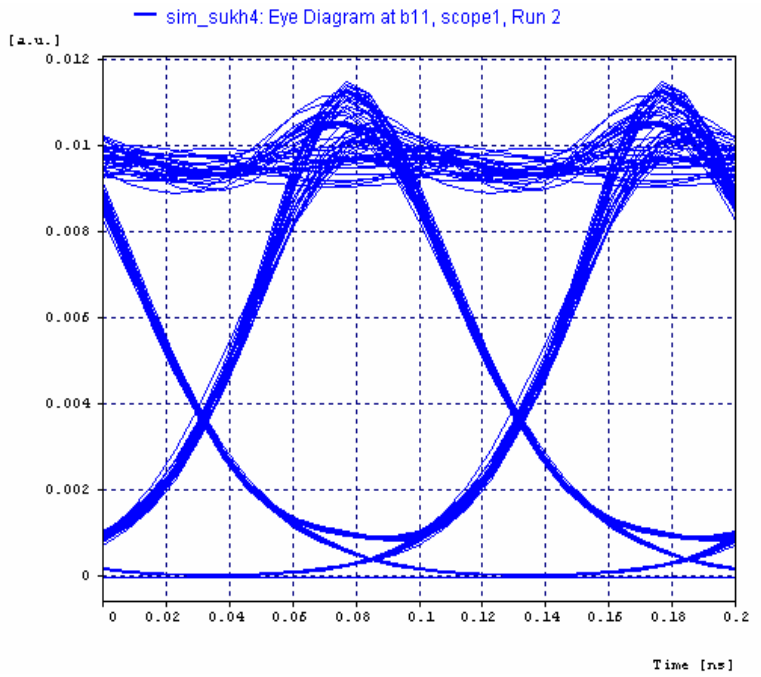

Figure 4.14 Eye diagram at 30 km length

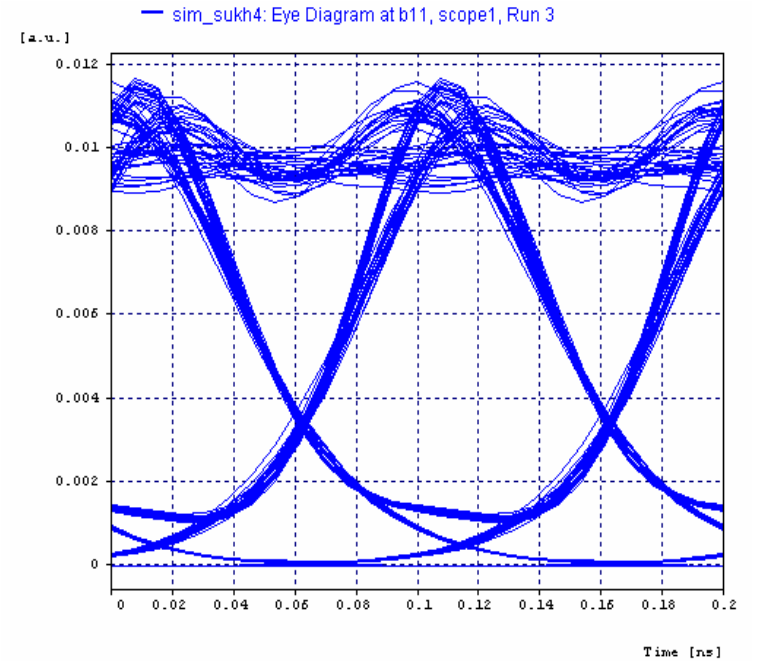

Figure 4.15 Eye diagram at 40 km length

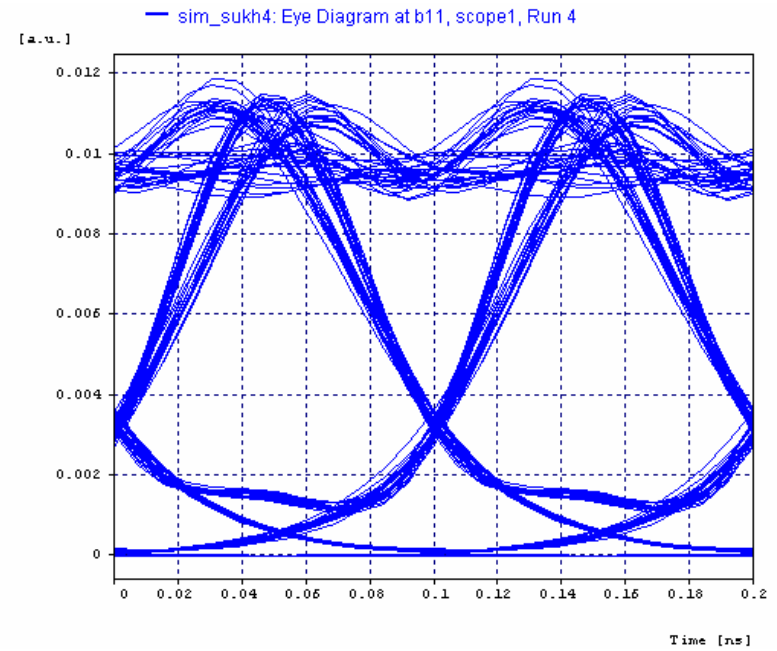

Figure 4.16 Eye diagram at 50 km length

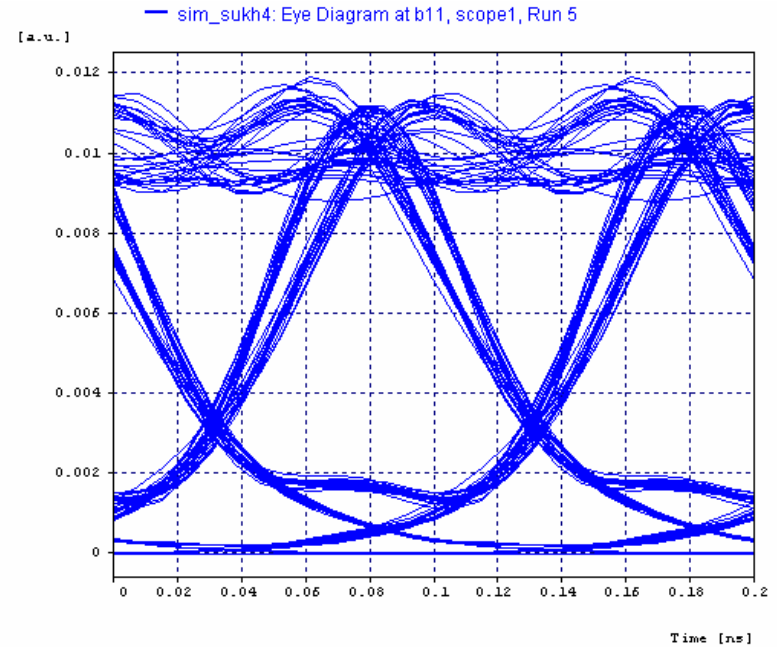

Figure 4.17 Eye diagram at 60 km length

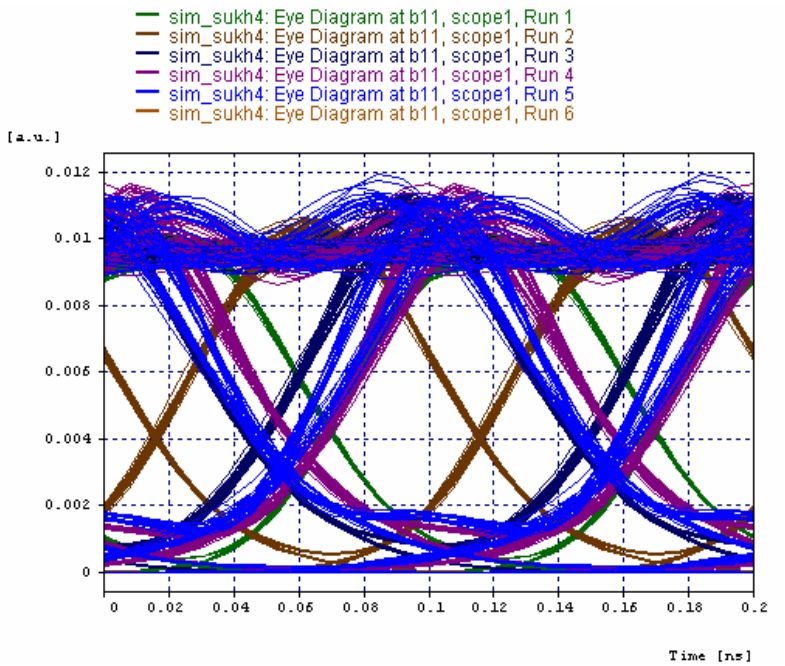

Figure 4.18 Eye diagram at 10, 20, 30, 40, 50, 60 km length

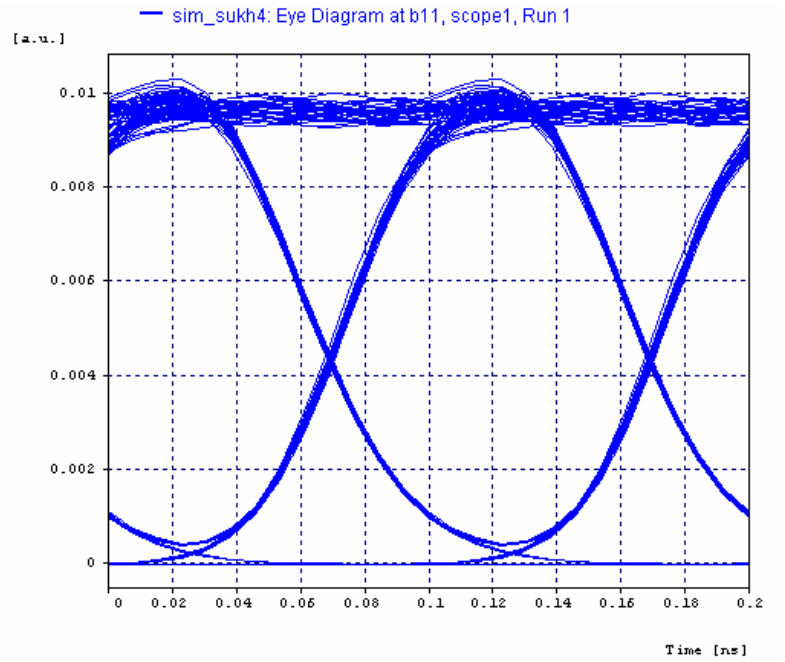

Figure 4.19 Eye diagram at dispersion 8 ps/nm/km

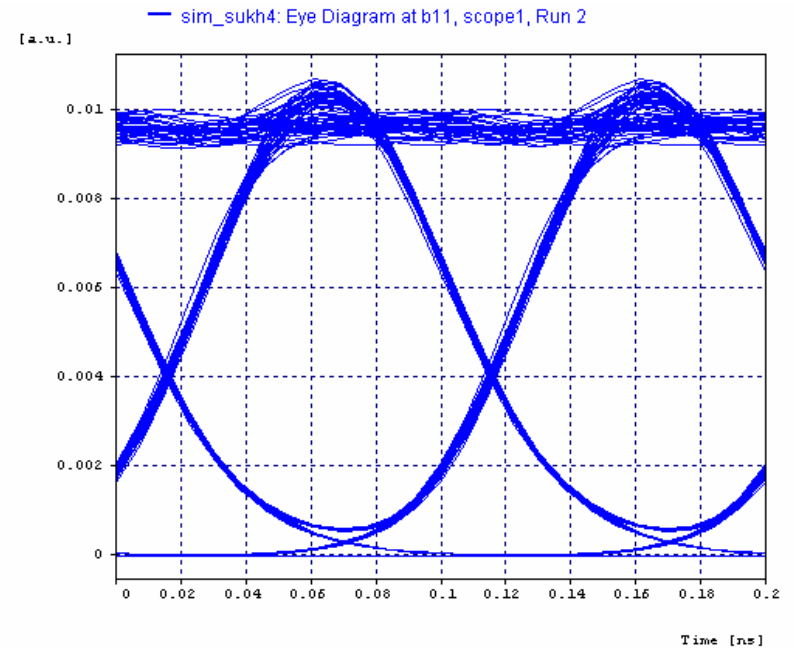

Figure 4.20 Eye diagram at dispersion 10 ps/nm/km

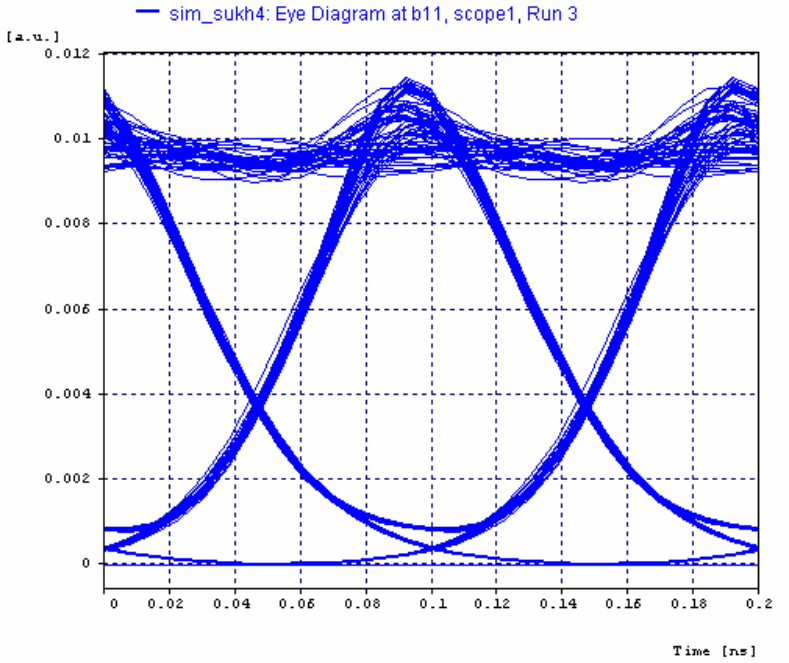

Figure 4.21 Eye diagram at dispersion 12 ps/nm/km

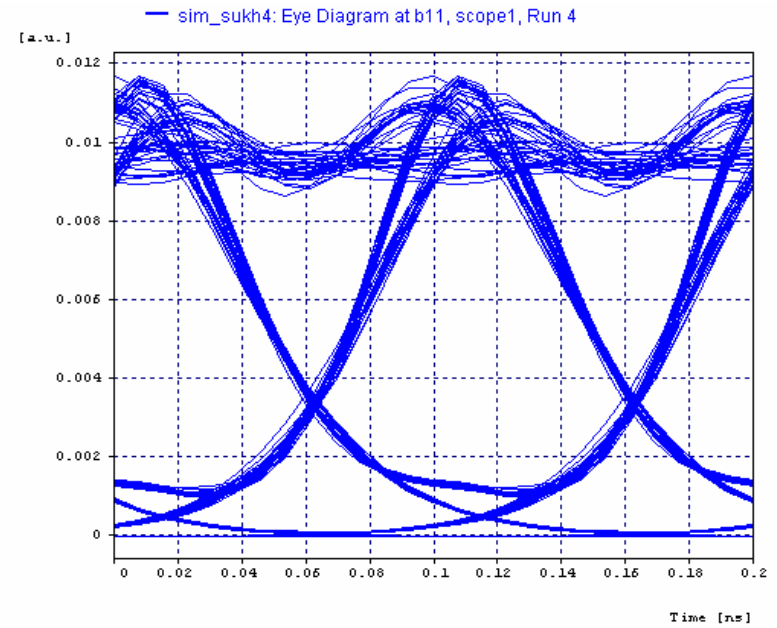

Figure 4.22 Eye diagram at dispersion 14 ps/nm/km

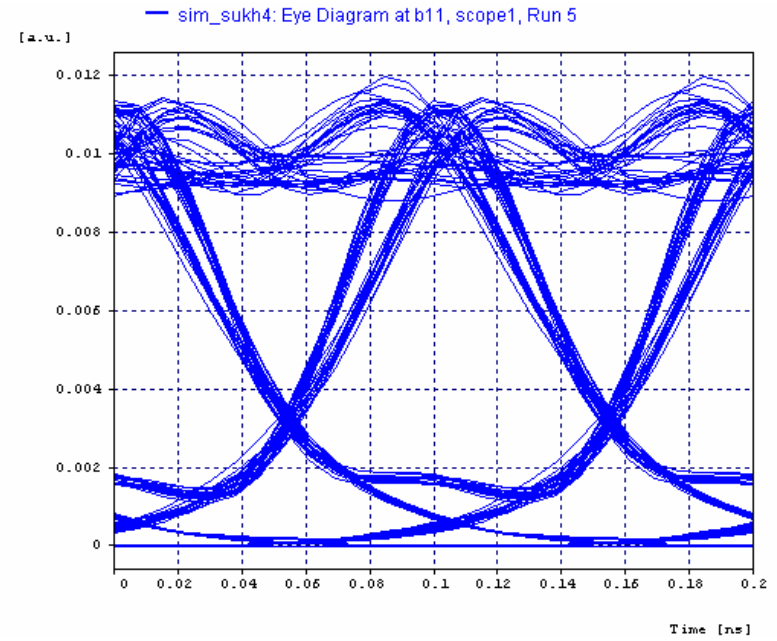

Figure 4.23 Eye diagram at dispersion 15 ps/nm/km

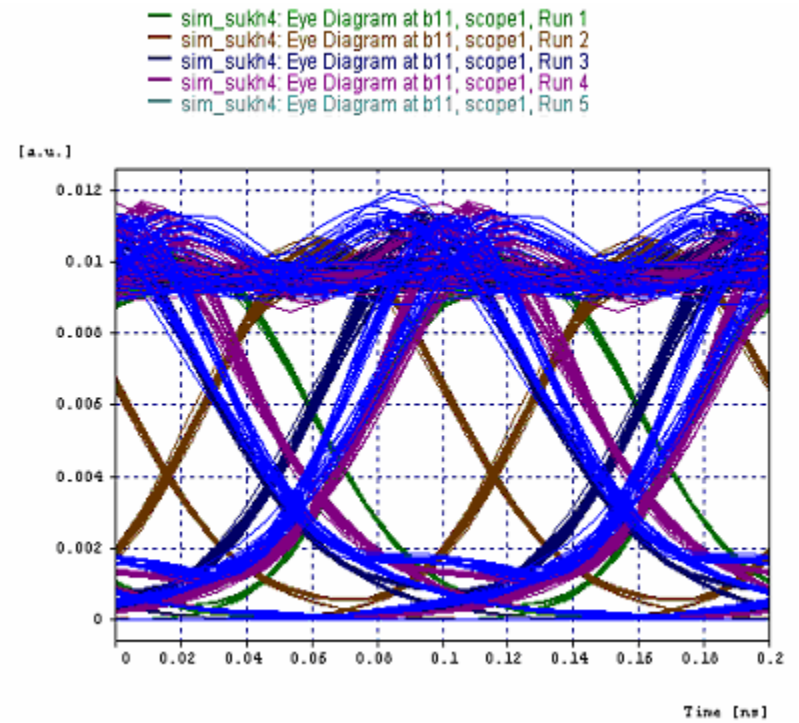

Figure 4.24 Eye diagram at dispersion 8, 10, 12, 14, 15 ps/nm/km

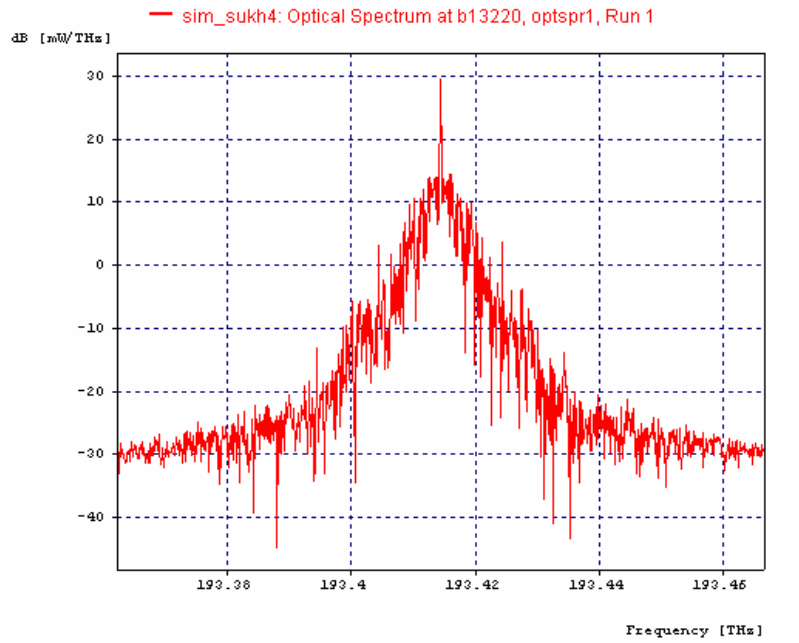

Figure 4.25 Optical spectrum

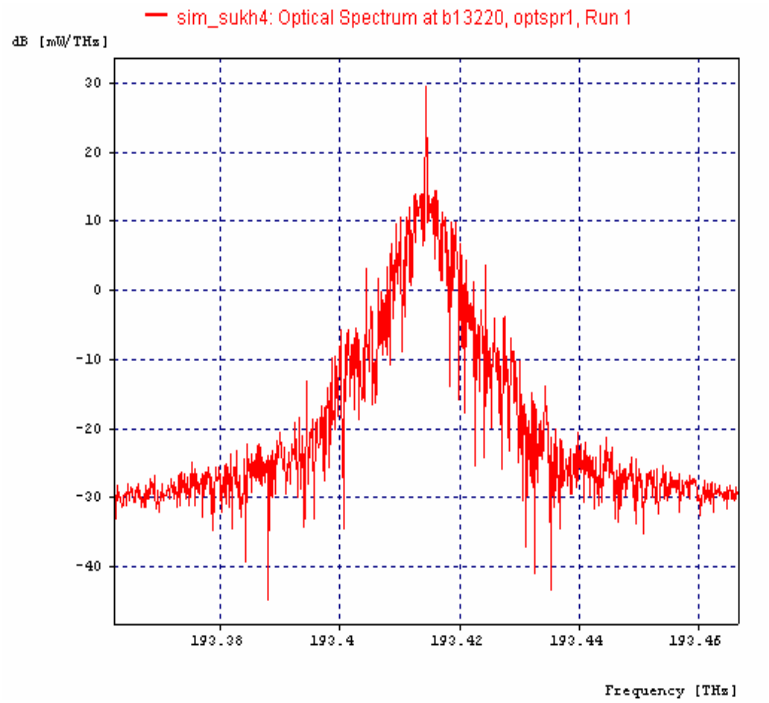

Figure 4.26 Optical spectrum

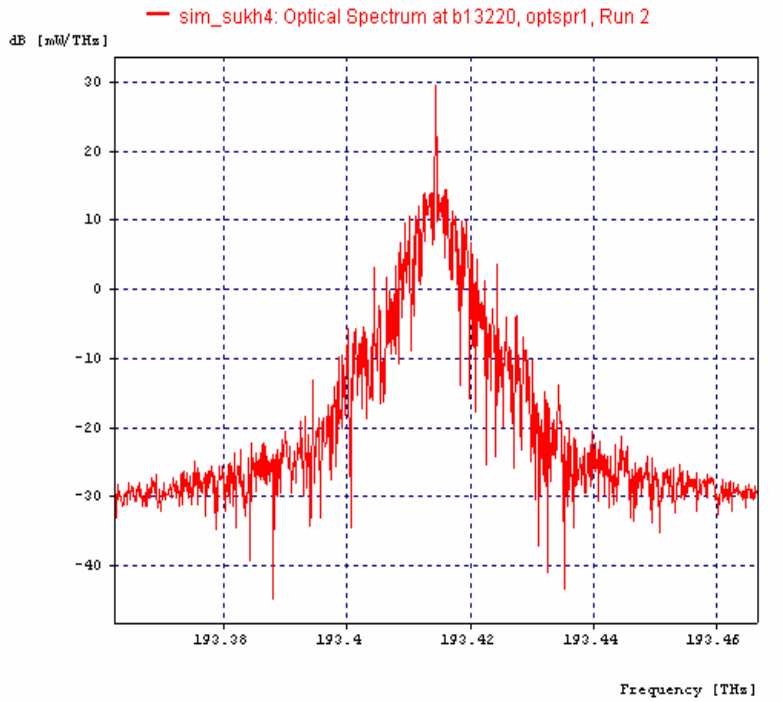

Figure 4.27 Optical spectrum

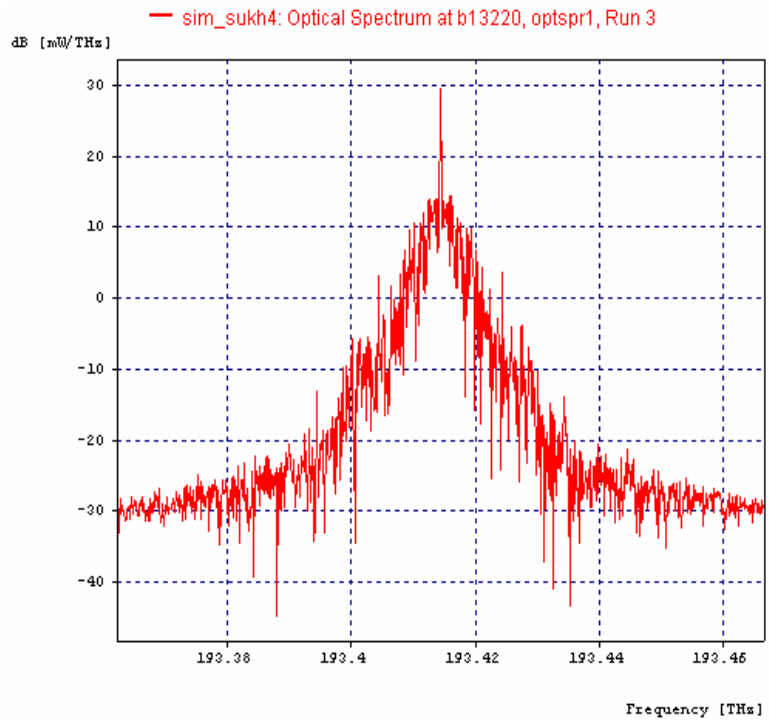

Figure 4.28 Optical spectrum

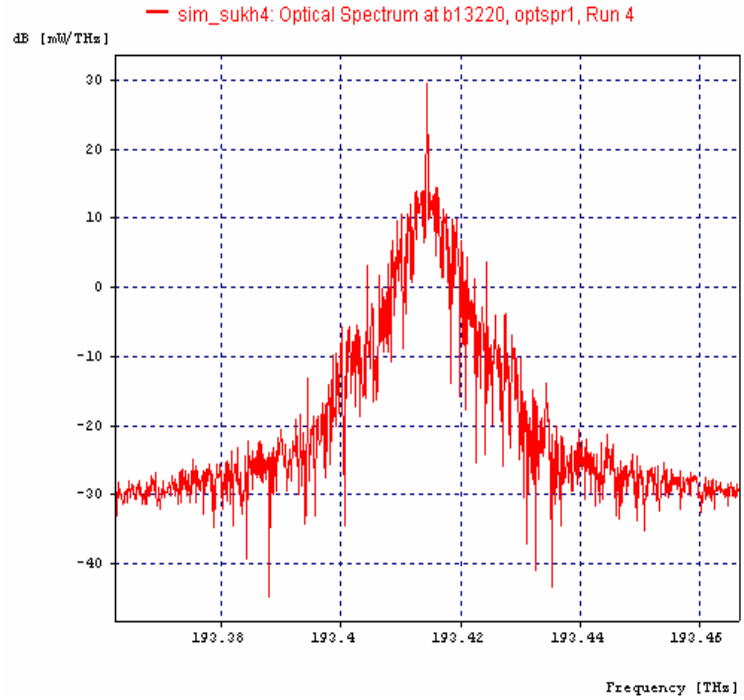

Figure 4.29 Optical spectrum

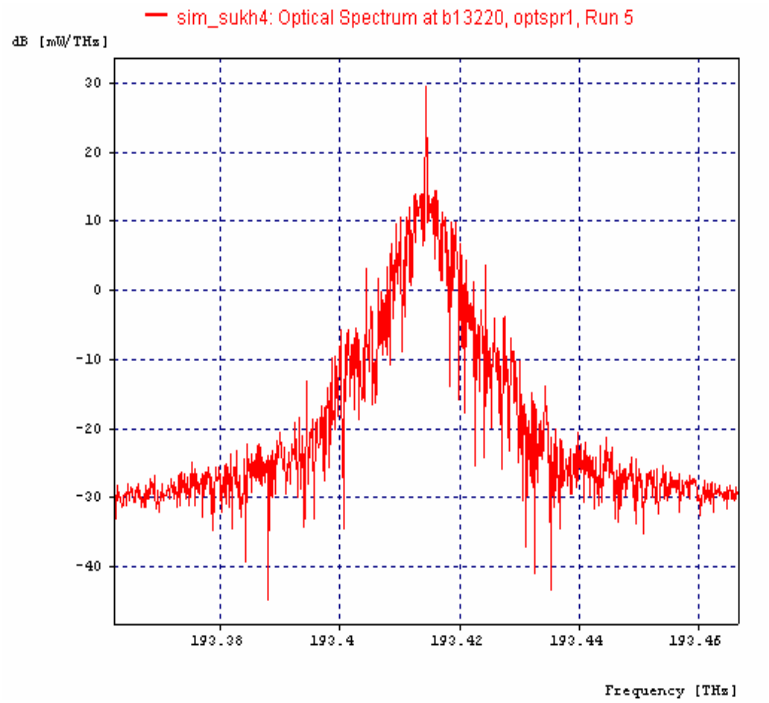

Figure 4.30 Optical spectrum

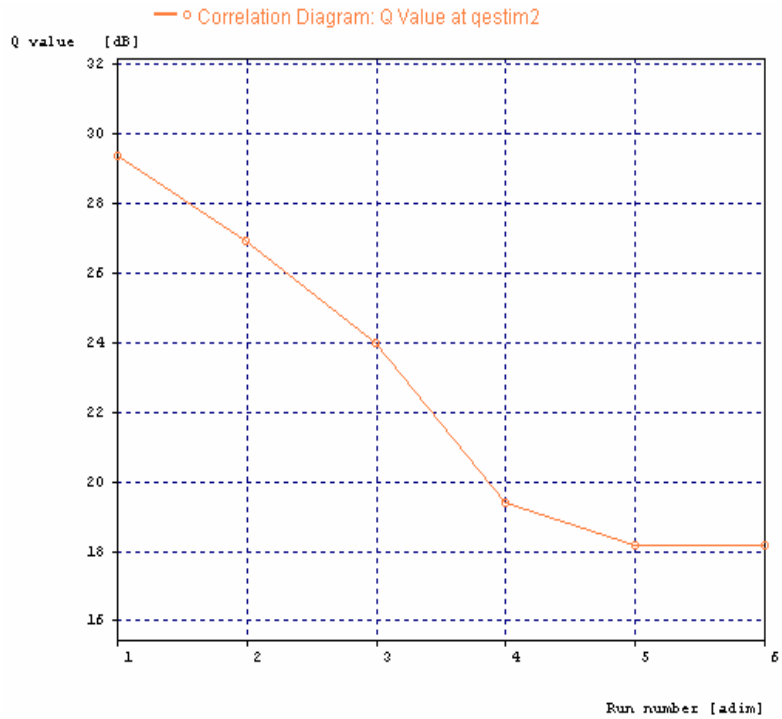

Figure 4.31 Q value

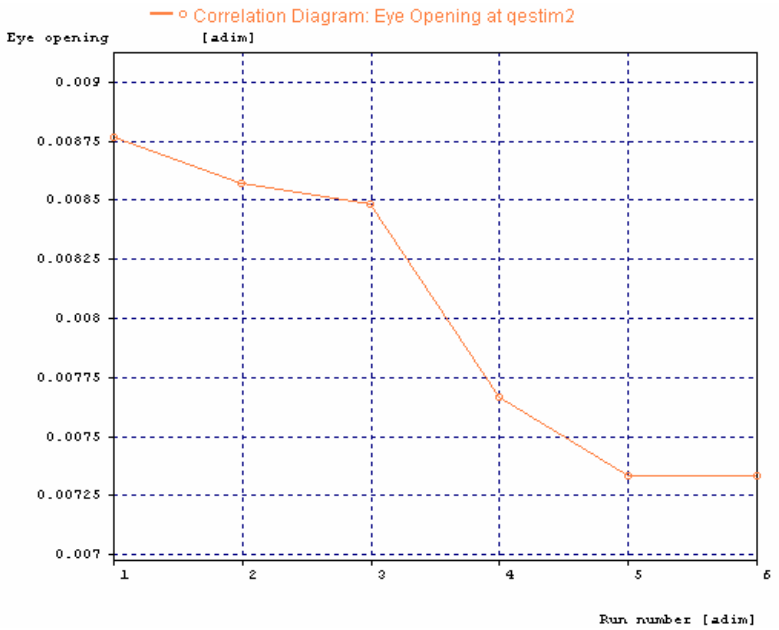

Figure 4.32 Eye opening

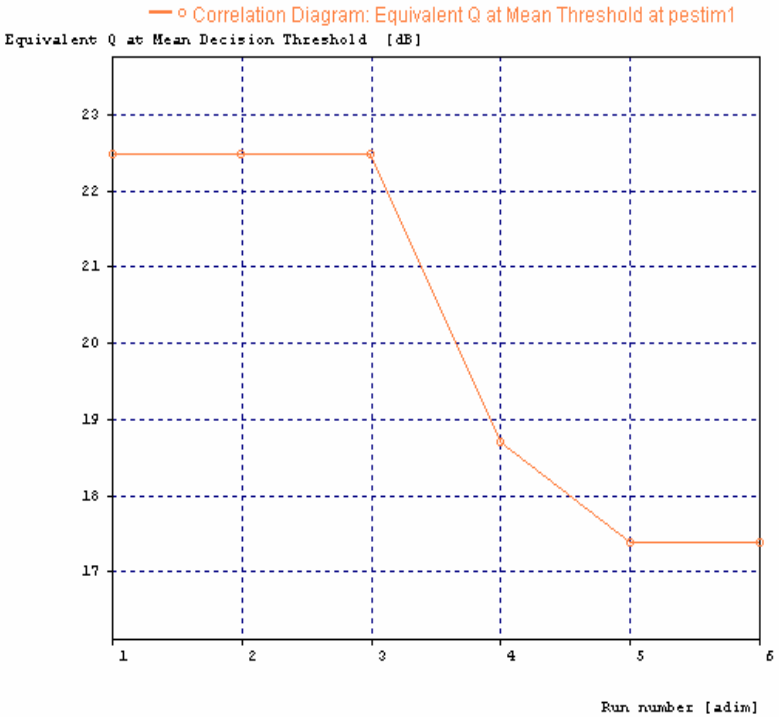

Figure 4.33 Equivalent Q at mean threshold

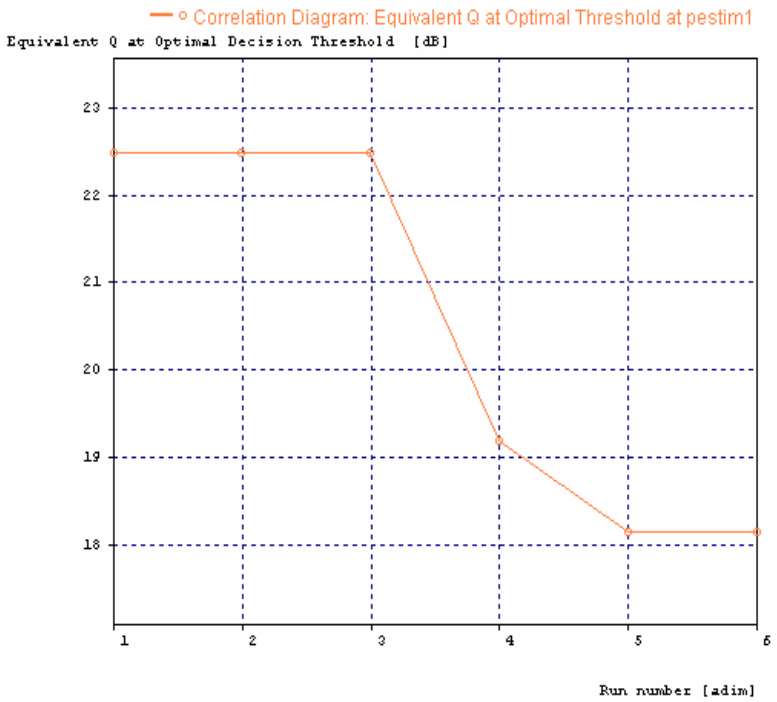

Figure 4.34 Equivalent Q at optimal threshold

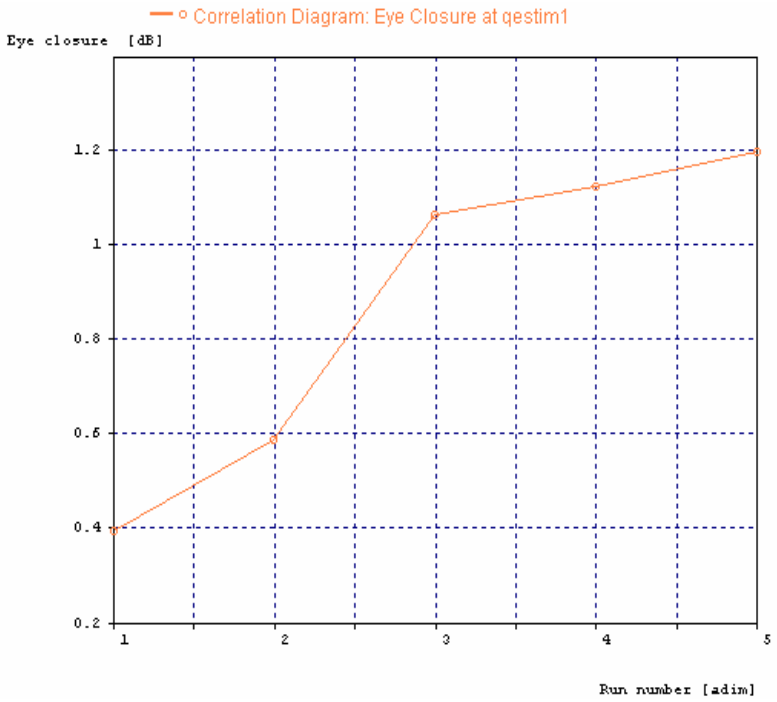

Figure 4.35 Eye closure

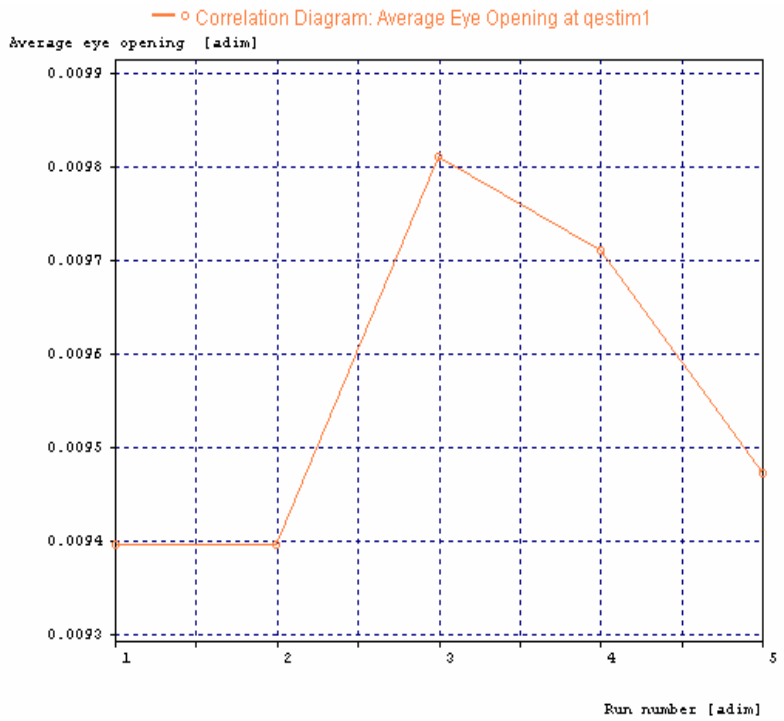

Figure 4.36 Average eye opening

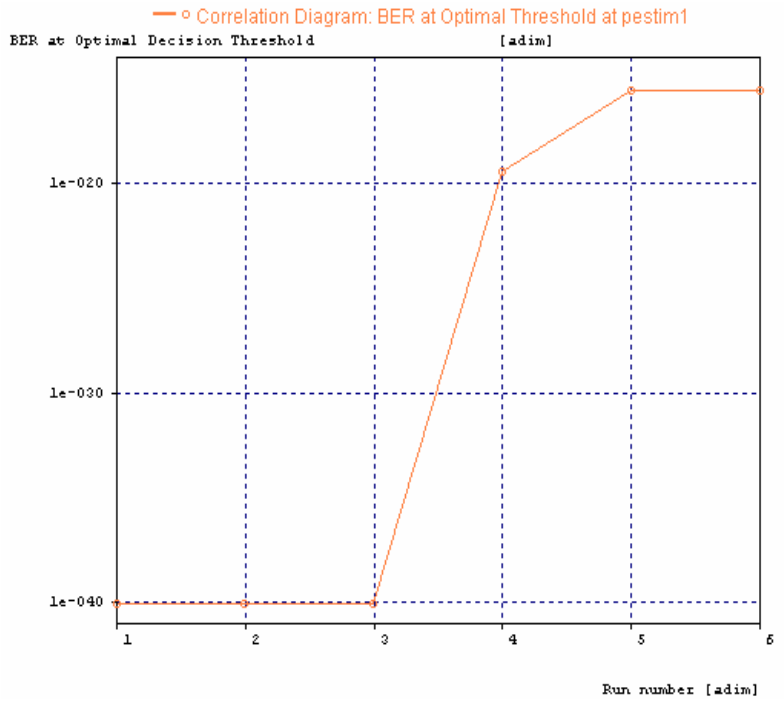

Figure 4.37 BER at optimal threshold

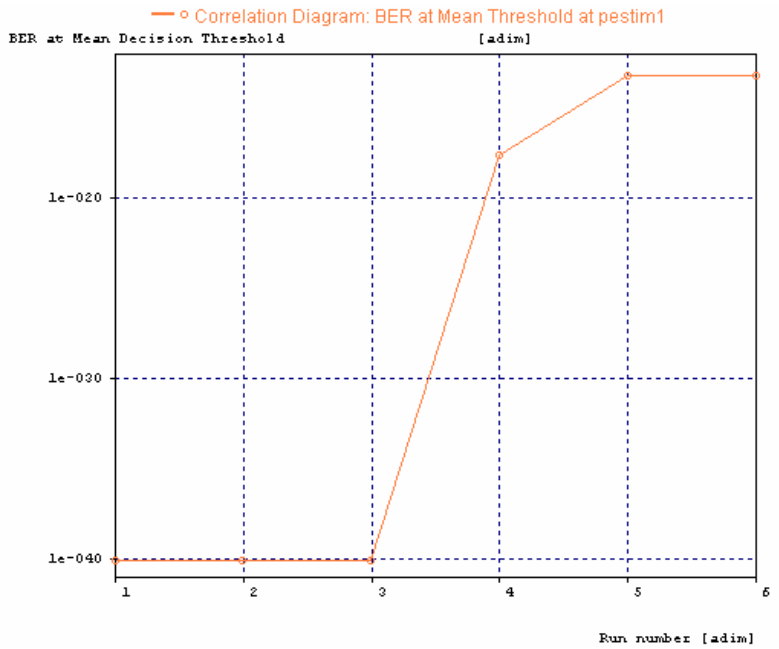

Figure 4.38 BER at mean threshold

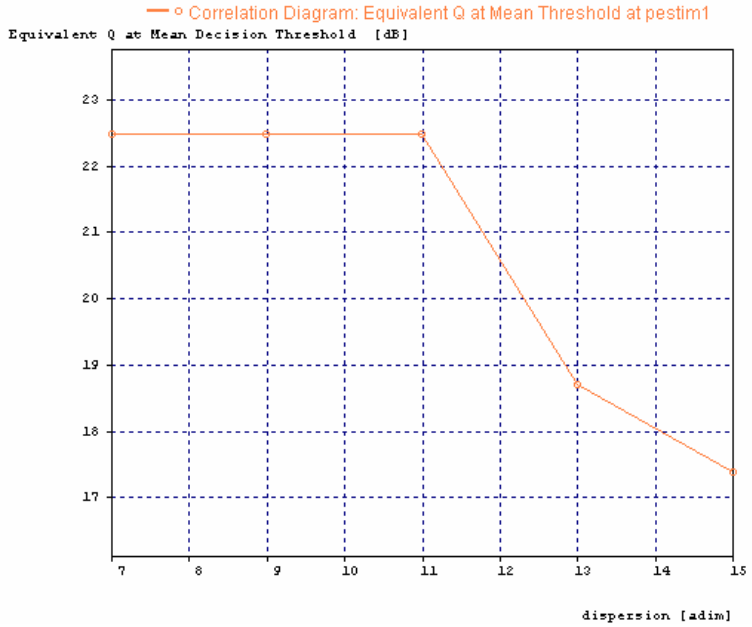

Figure 4.39 Equivalent Q at mean threshold

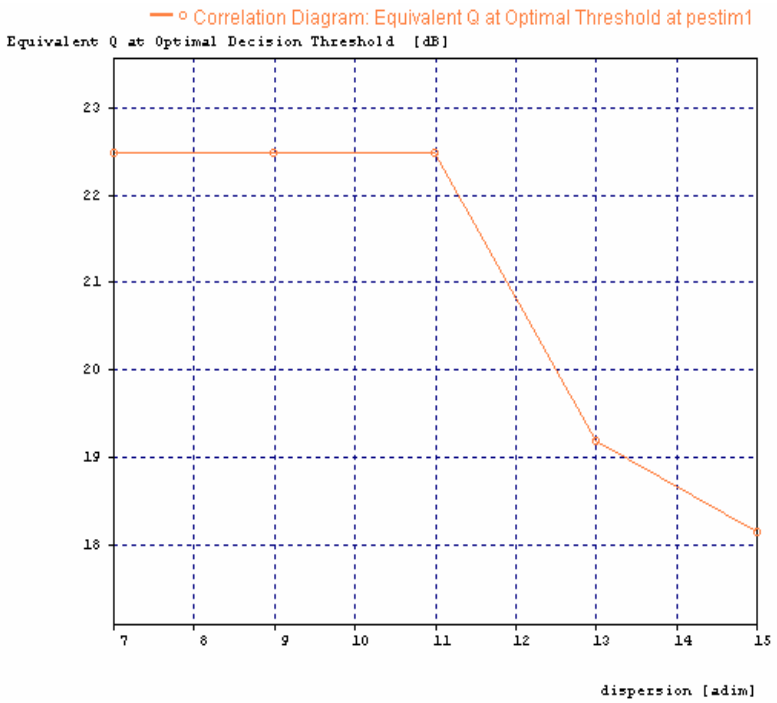

Figure 4.40 Equivalent Q at optimal threshold

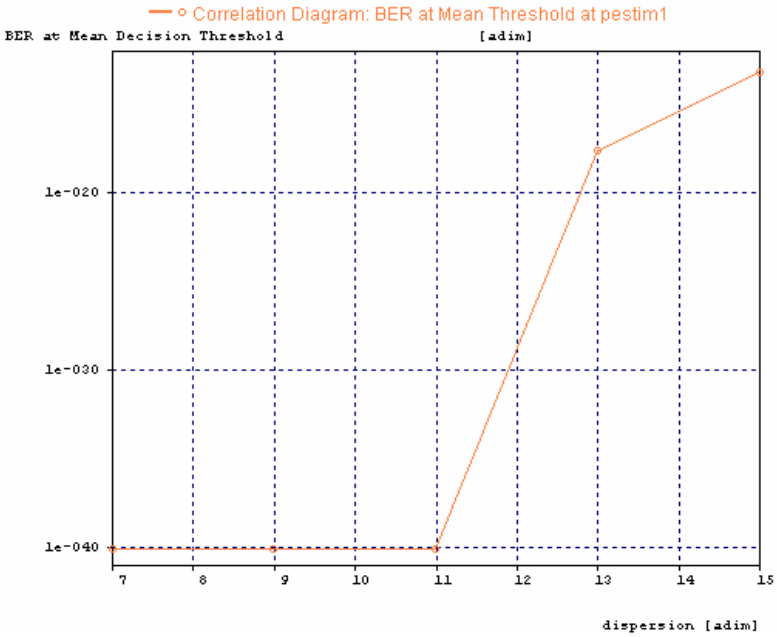

Figure 4.41 BER at mean threshold

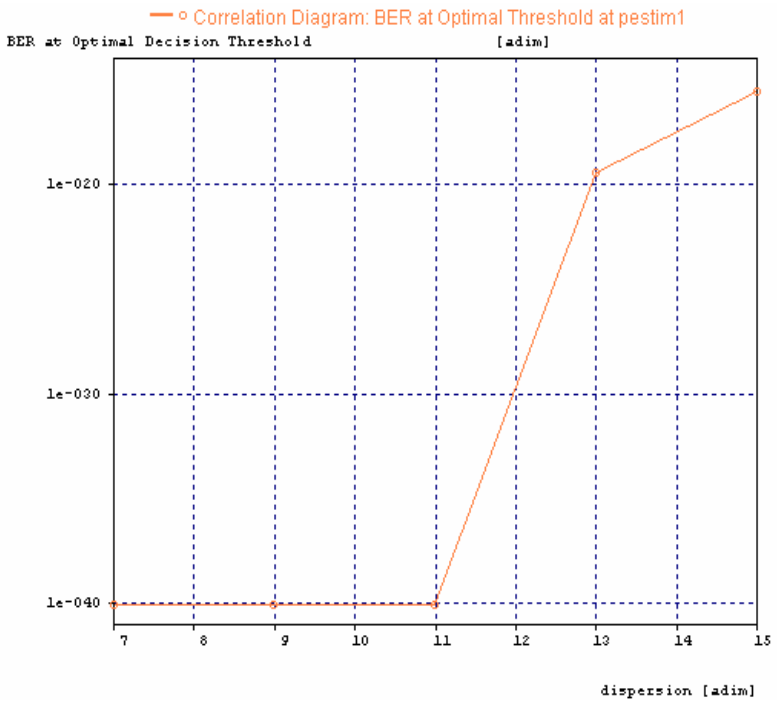

Figure 4.42 BER at optimal threshold

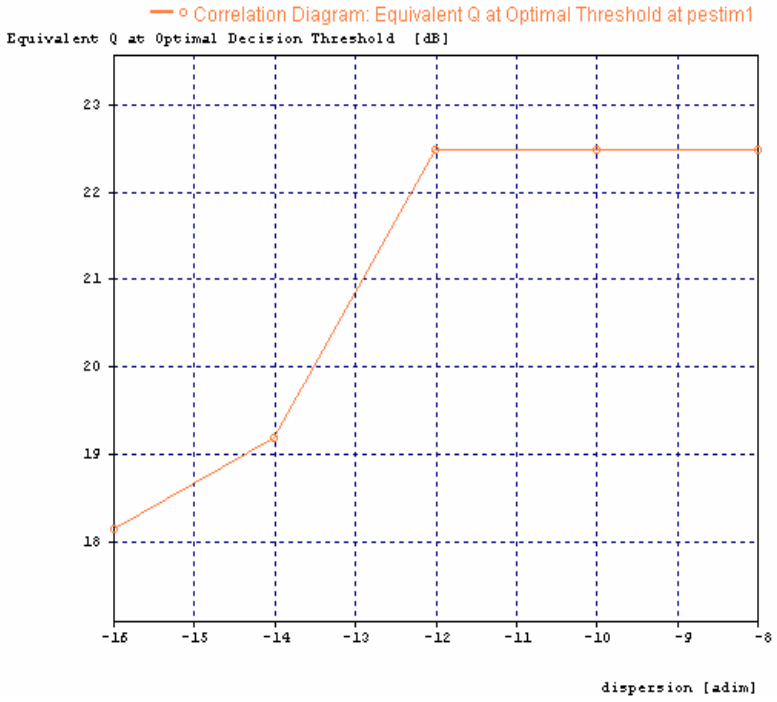

Figure 4.43 Equivalent Q at optimal threshold

4.3.1.2 Results of fiber used as a DCF

The results of fiber used as DCF is shown in figure 4.43 Equivalent Q at optimal threshold which is negative dispersion -8, -10, -12,-14, -16 ps/nm/km and figure 4.44 BER at optimal threshold negative dispersion -8, -10, -12,-14, -16 ps/nm/km.
Figure 4.45 shows the BER at optimal threshold positive and negative dispersion.
Figure 4.46 shows the comparison of eye diagram at negative dispersion -8, -10, -12, -14, -15, -16 ps/nm/km.

4.3.2 Results and discussions regarding simulation of post compensation based on 10 Gb/s bitrate

The simulation results from different simulation systems are predicted. The results of simulation setup are shown in figure 4.47 is electrical spectrum and figure 4.48 is eye diagram.

4.3.3 Results and discussion regarding simulation of symmetrical compensation based on 10 Gb/s bitrate

The simulation results from different simulation systems are predicted. The results of simulation setup in figure 4.49 is electrical spectrum

Eye diagrams for different length

The results of eye diagrams are shown in figures 4.50 to 4.55 for different length. Eye opening decreases and eye closure increases with increase the length of SSMF i.e. eye opening penalty increases as the length of single mode fiber increases. The best result is observed with 10 km length of single mode fiber. Figure 4.56 shows the comparison of eye diagrams on 10, 20, 30, 40, 50, 60 km length of single mode fiber.

Eye diagrams for different dispersion

The results of eye diagrams are shown in figures 4.57 to 4.61 for different dispersion Eye opening decreases and eye closure increases with increase the dispersion of SSMF i.e. eye opening penalty increases as the dispersion of single mode fiber increases. The best result is observed with 10 ps/nm/km dispersion of single mode fiber. Figure 4.62 shows the comparison of eye diagrams on 8, 10, 12, 14, 16, ps/nm/km dispersion of single mode fiber.

Result based on Q and bit error rate estimator

Figure 4.63 shows the result of Q value on 20, 30, 40, 50, 60 km length of fiber which is 19.6 dB at 20 Km and 16.4 dB at 60 Km.

Figure 4.64 shows the result of eye closure on 20, 30, 40, 50, 60 km length of fiber which is 1.05 dB at 20 Km and 1.0 dB at 60 Km.

Figure 4.65 shows the result of BER at optimal threshold on 20, 30, 40, 50, 60 km length of fiber which is 1e-022 at 20 Km and 1e-009 at 60 Km.

Figure 4.66 shows the result of BER at mean threshold on 20, 30, 40, 50, 60 km length of fiber which is 1e-019 at 20 Km and 1e-004 at 60 Km.

Figure 4.67 Average eye opening on 20, 30, 40, 50, 60 km length of fiber which is 0.00848 at 20 Km and 0.00798 at 60 Km.

Figure 4.68 shows the result of equivalent Q at mean threshold on 20, 30, 40, 50, 60 km length of fiber which is 19 dB at 20 Km and 14.9 dB at 60 Km.

Figure 4.69 shows the result of equivalent Q at optimal threshold on 20, 30, 40, 50, 60 km length of fiber which is 19.6 dB at 20 Km and 16.3 dB at 60 Km.

Figure 4.70 shows the result of BER at optimal threshold on 10, 20, 30, 40 Gb/s bit rate dispersion of fiber which is 22.5 dB at 10 Gb/s bit rate and 18.2 dB at 40 Gb/s bit rate.

Figure 4.71 shows the result of BER at mean optimal threshold on 10, 20, 30, 40 Gb/s bit rate dispersion of fiber which is 1e-040 at 10 Gb/s bit rate and 1e-012 at 40 Gb/s bit rate .

Figure 4.72 shows the result of equivalent Q at mean threshold on 10,20, 30, 40, 50 Gb/s bit rate of fiber which is 21.5 dB at 10 Gb/s bit rate and 17.4 dB at 50 Gb/s bit rate

Figure 4.73 shows the result of Q value on 10, 20, 30, 40, 50 Gb/s bit rate of fiber which is 28.8 dB at 10 Gb/s bit rate and 18.1 dB at 50 Gb/s bit rate

Figure 4.74 shows the result of eye closure on 10, 20, 30, 40, 50 Gb/s bit rate of fiber which is 0.34 at 10 Gb/s bit rate and 1.12 at 50 Gb/s bit rate

Figure 4.75 shows the result of average eye opening on 10, 20, 30, 40, 50 Gb/s bit rate of fiber which is 0.009445 at 10 Gb/s bit rate and 0.00951 at 50 Gb/s bit rate

Figure 4.76 shows the result of eye opening on 10, 20, 30, 40, 50 Gb/s bit rate of fiber which is 0.08756 at 10 Gb/s bit rate and 0.00750at 50 Gb/s bit rate.

Figure 4.77 shows the result of equivalent Q at optimal threshold on 10, 20, 30, 40, 50 Gb/s bit rate of fiber which is 22.5 dB at 10 Gb/s bit rate and 18.2 dB at 50 Gb/s.

Figure 4.78 shows the result of BER at mean threshold on 10, 20, 30, 40, 50 Gb/s bit rate dispersion of fiber which is 1e-040 at 10 Gb/s bit rate and 1e-004 at 50 Gb/s bit rate.

Figure 4.79 shows the result of equivalent Q at mean threshold on 10,20, 30, 40, 50 Gb/s bit rate of fiber which is 22.5 dB at 10 Gb/s bit rate and 17.2 dB at 50 Gb/s.

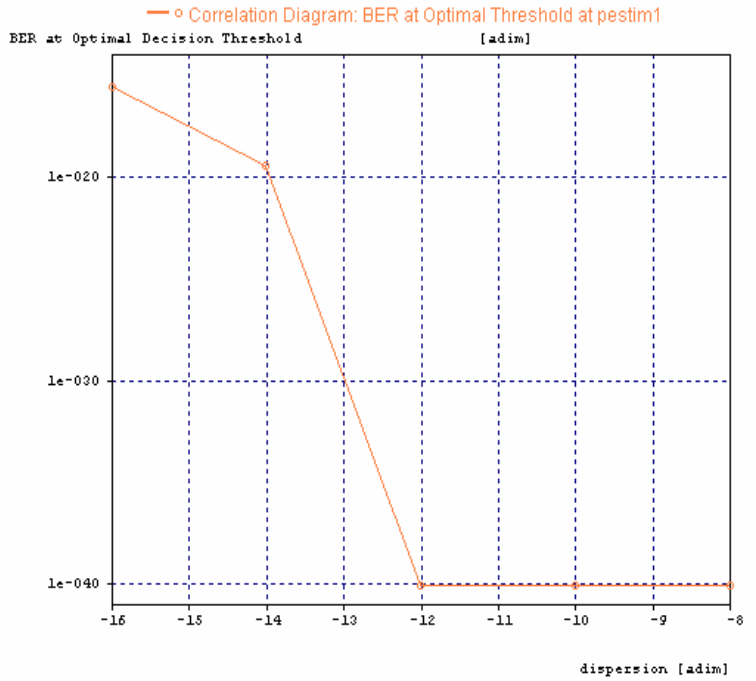

Figure 4.44 BER at optimal threshold

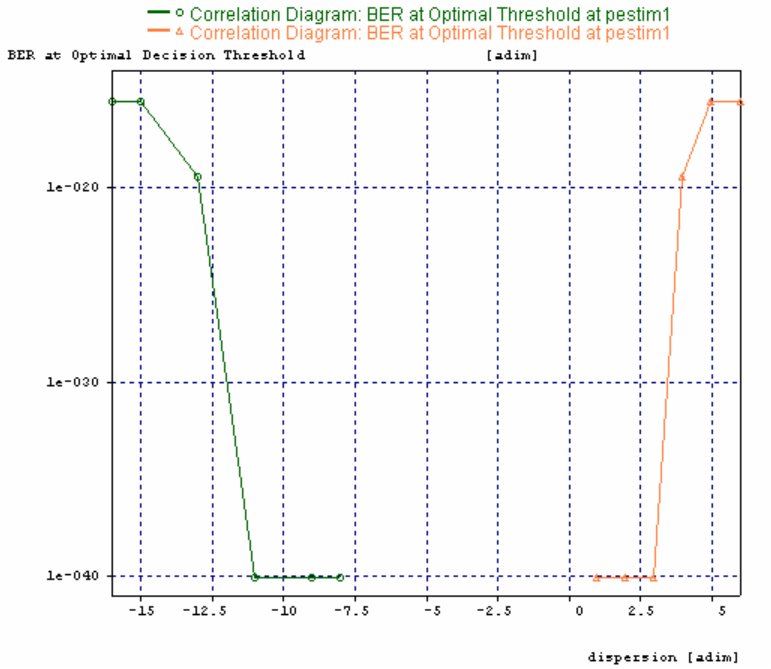

Figure 4.45 BER at optimal threshold positive and negative dispersion

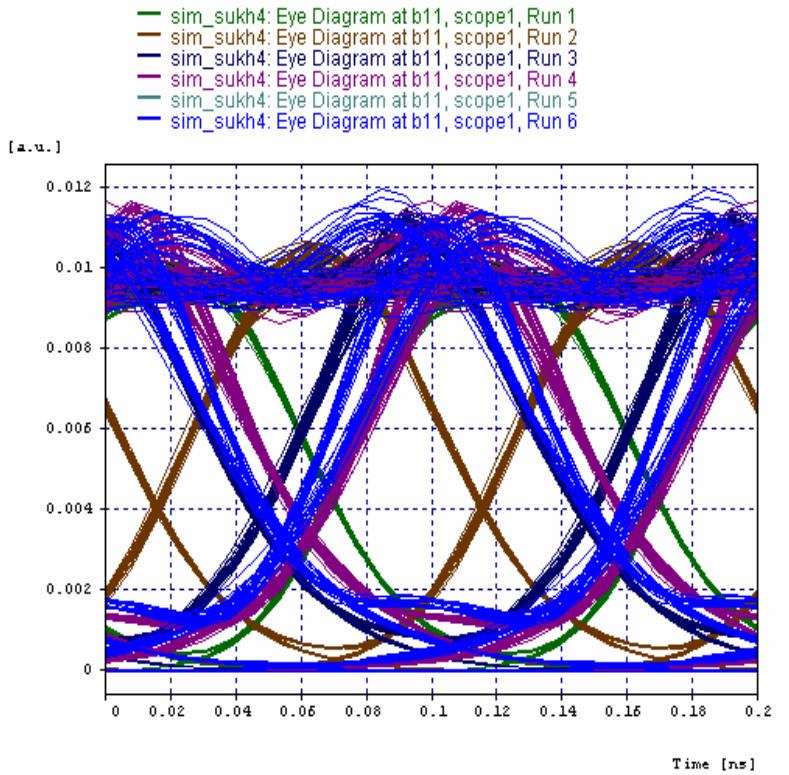

Figure 4.46 Eye diagram at negative dispersion -8, -10, -12, -14, -15, -16 ps/nm/km

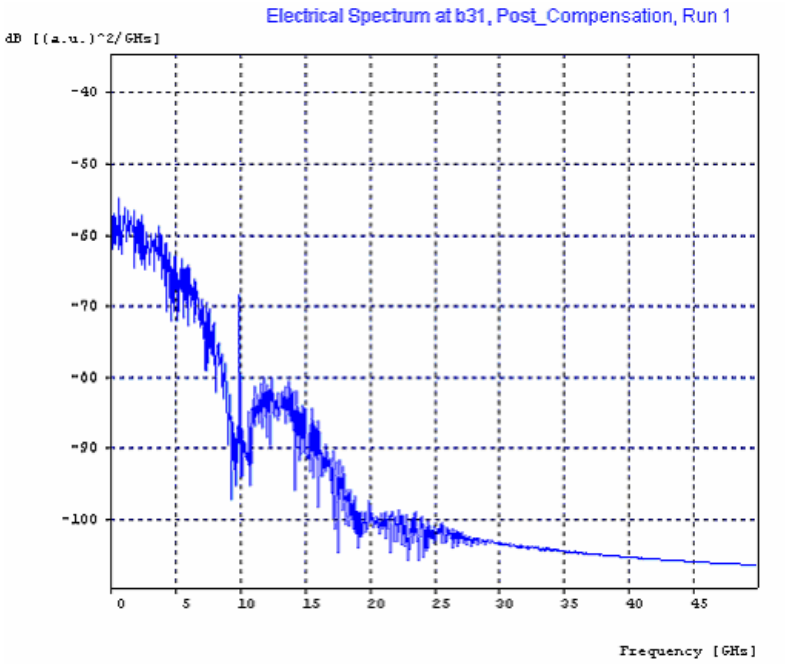

Figure 4.47 Electrical spectrum

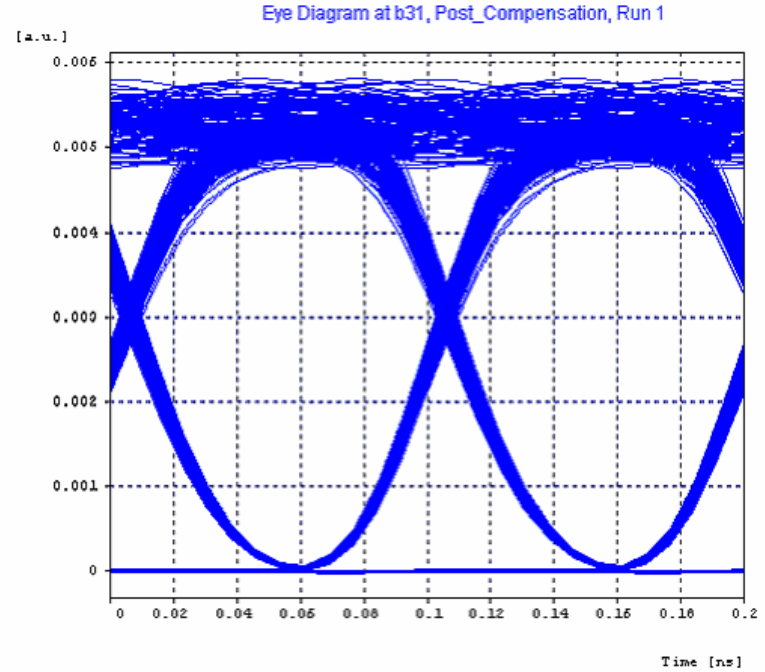

Figure 4.48 Eye diagram

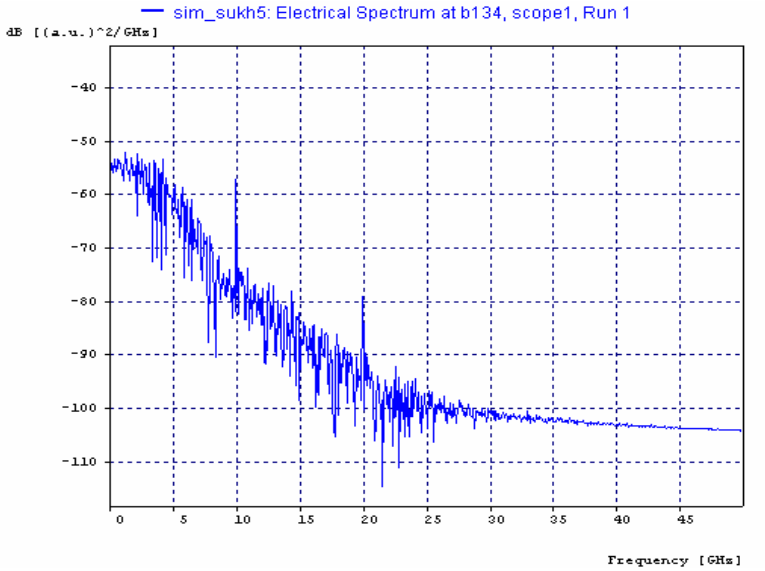

Figure 4.49 Electrical spectrum

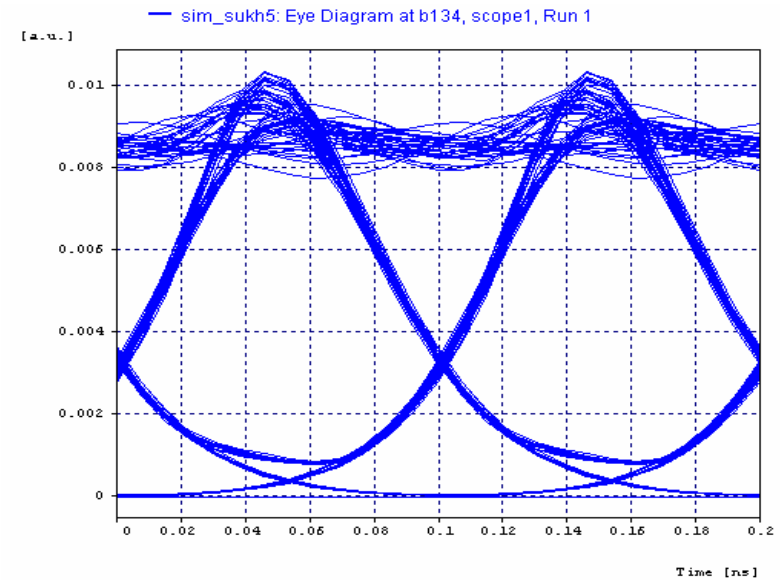

Figure 4.50 Eye diagram at 10 km length

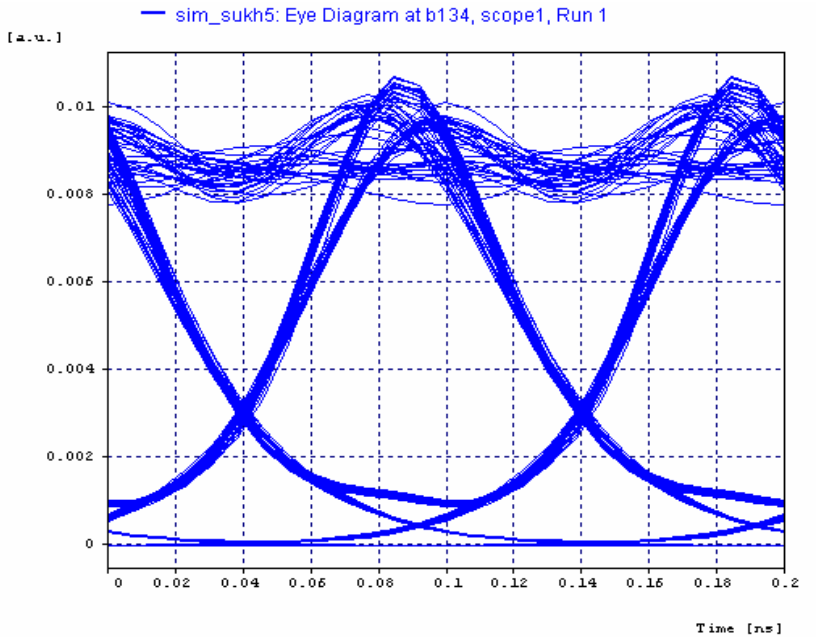

Figure 4.51 Eye diagram at 20 km length

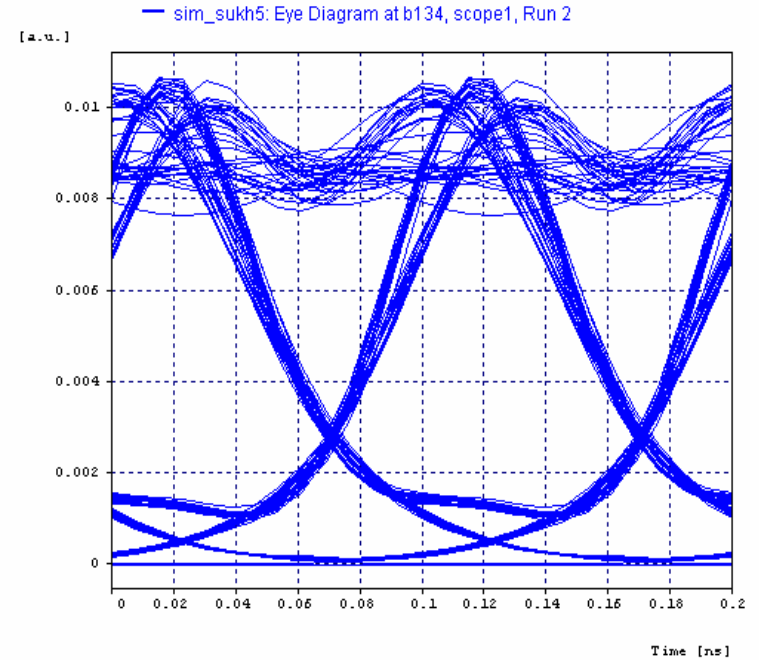

Figure 4.52 Eye diagram at 30 km length

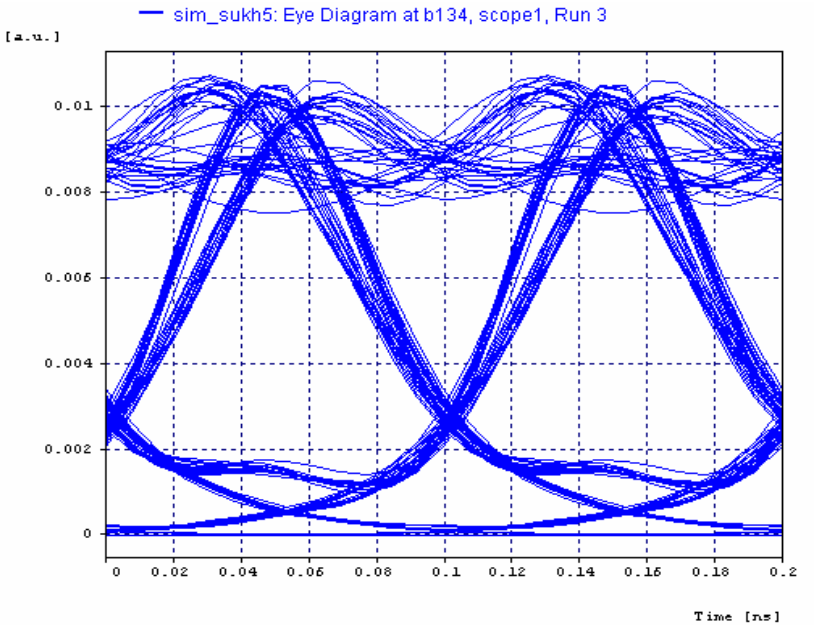

Figure 4.53 Eye diagram at 40 km length

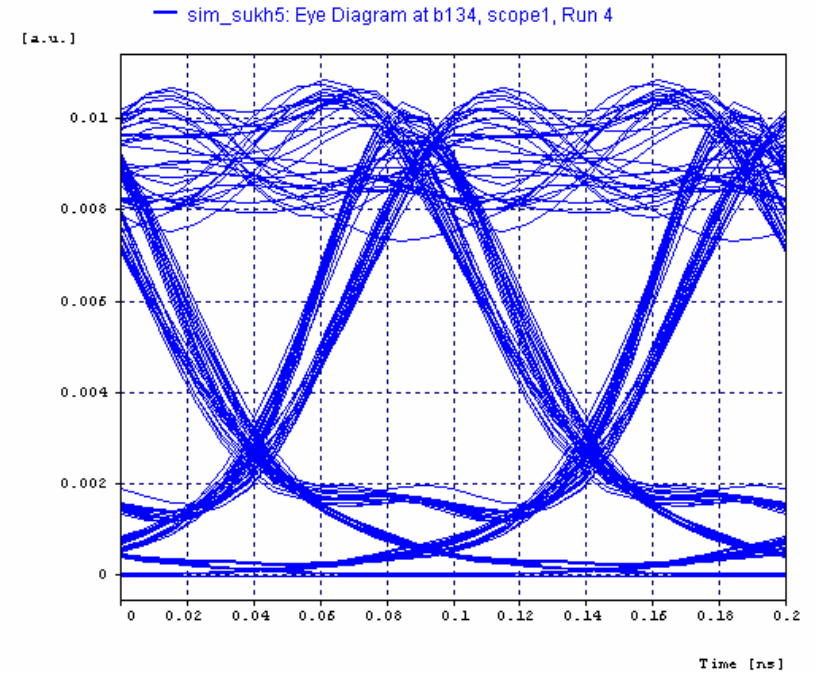

Figure 4.54 Eye diagram at 50 km length

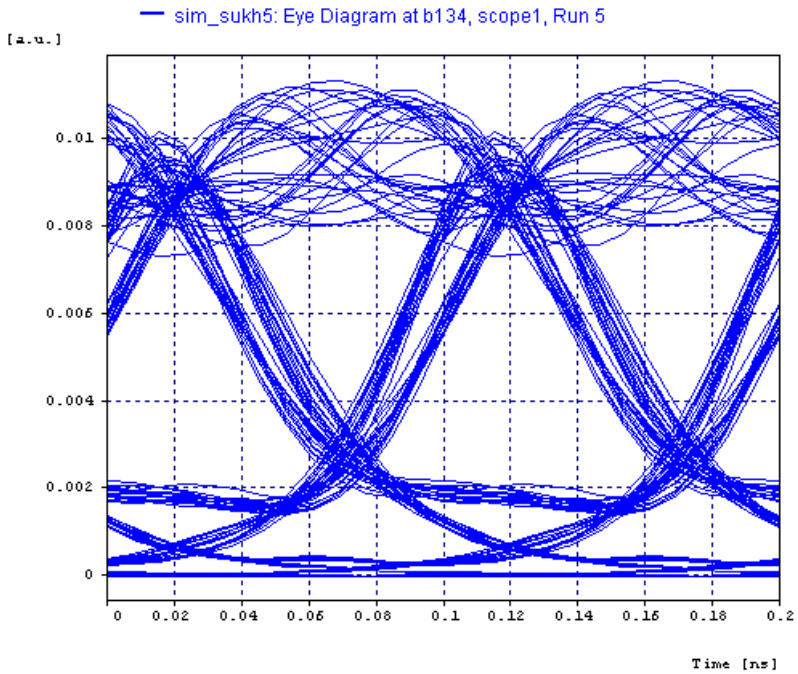

Figure 4.55 Eye diagram at 60 km length

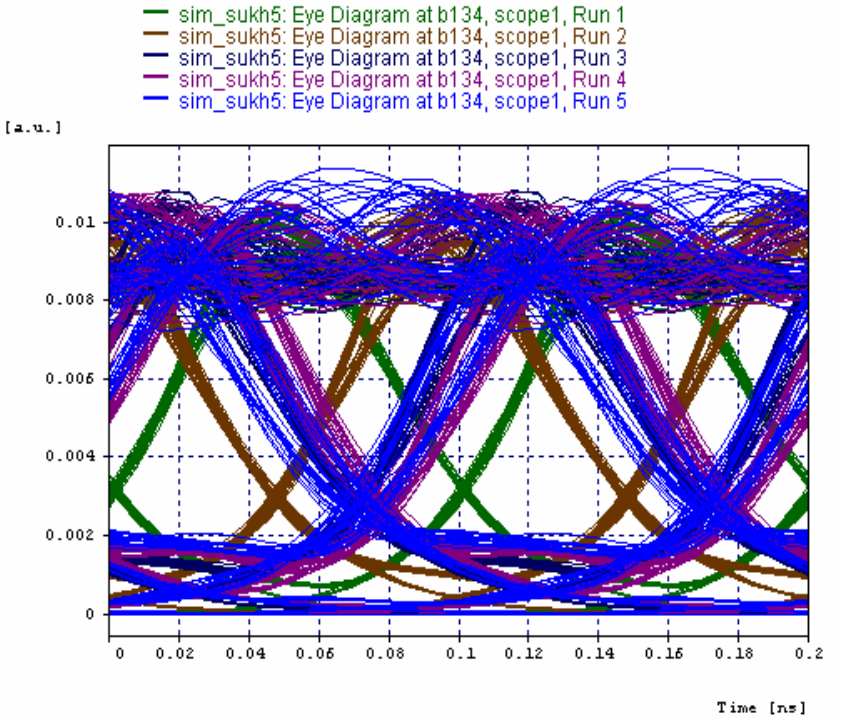

Figure 4.56 Eye diagram at 10, 20, 30, 40, 50 km length

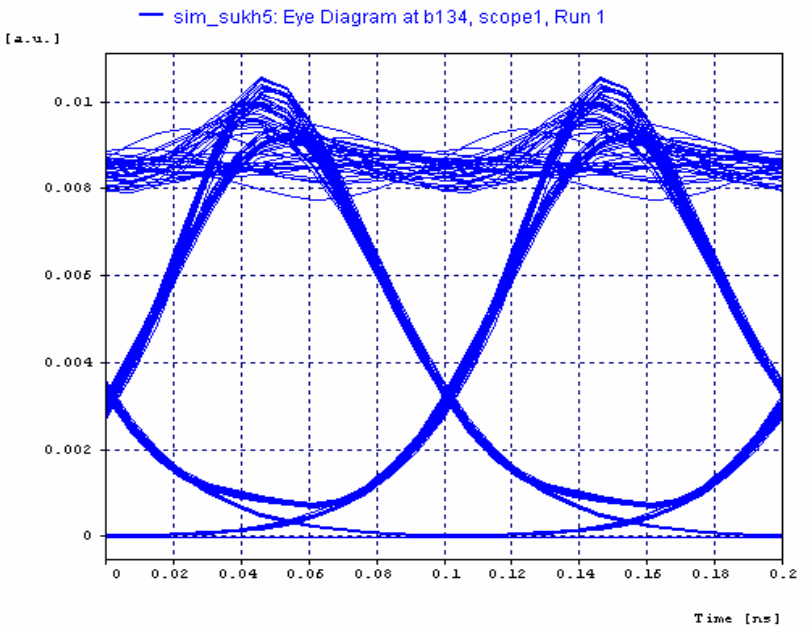

Figure 4.57 Eye diagram at dispersion 8 ps/nm/km

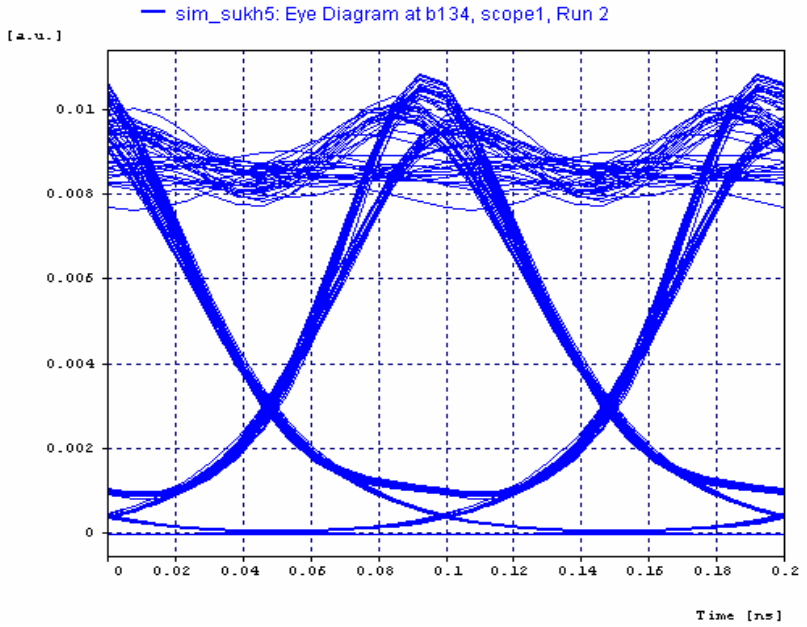

Figure 4.58 Eye diagram at dispersion 10 ps/nm/km

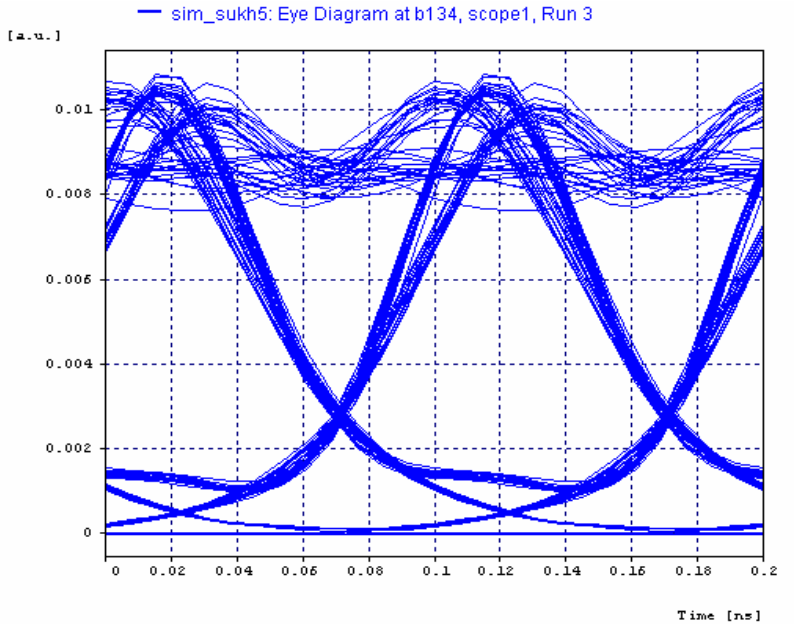

Figure 4.59 Eye diagram at dispersion 12 ps/nm/km

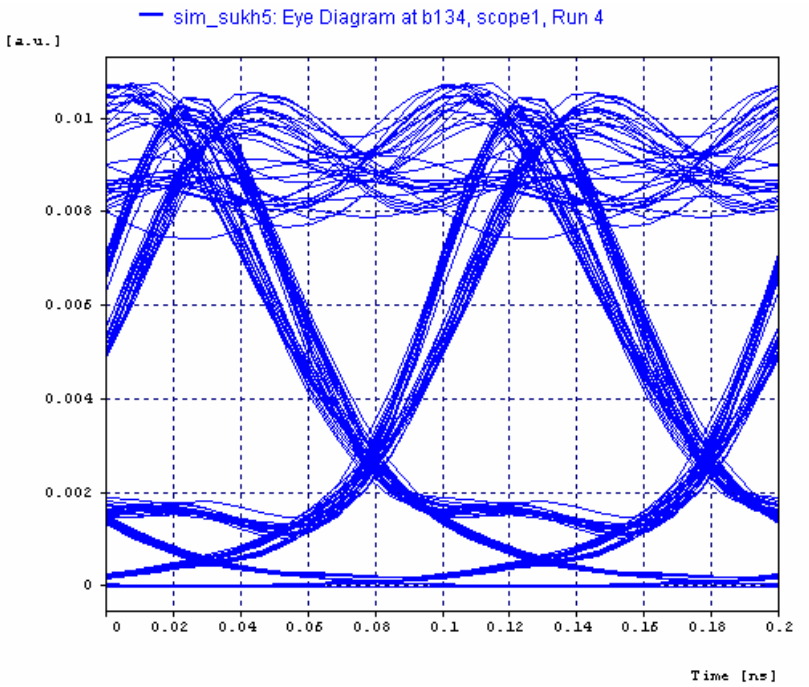

Figure 4.60 Eye diagram at dispersion 14 ps/nm/km

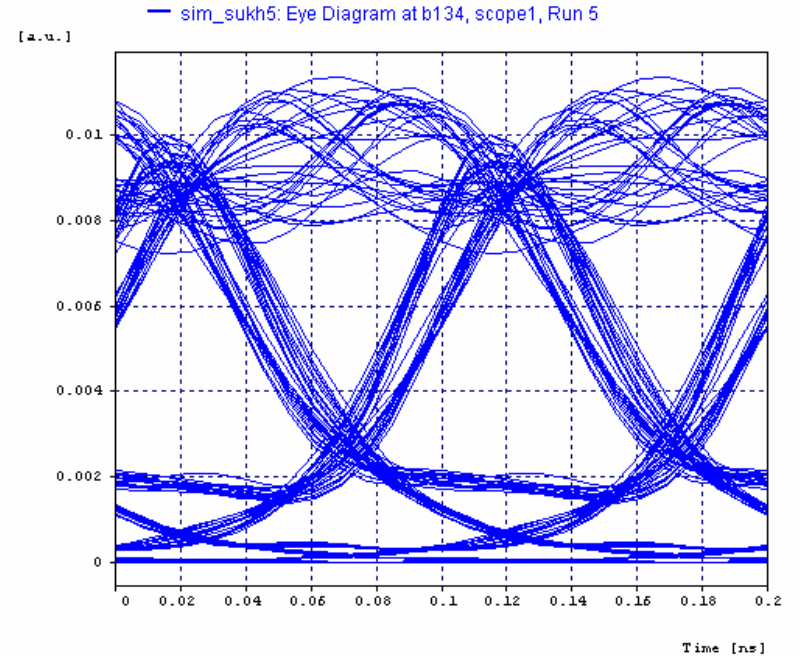

Figure 4.61 Eye diagram at dispersion 16 ps/nm/km

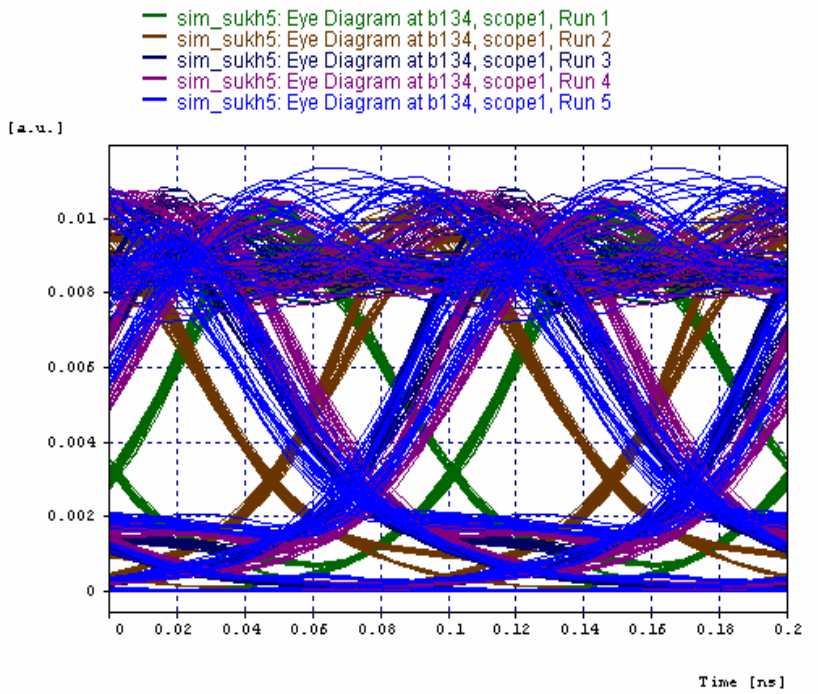

Figure 4.62 Eye diagram at dispersion 8, 10, 12, 14, 16 ps/nm/km

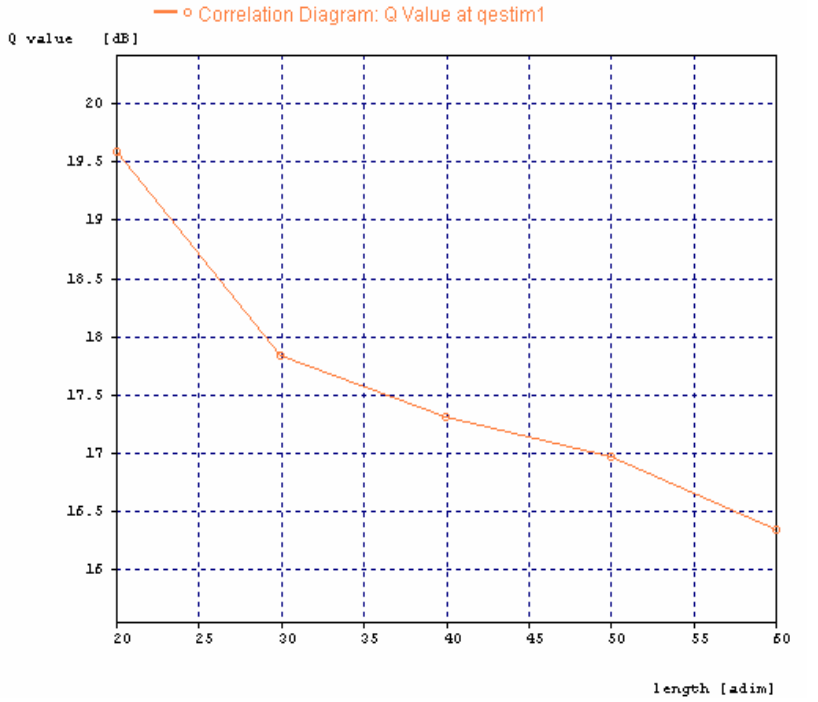

Figure 4.63 Q value

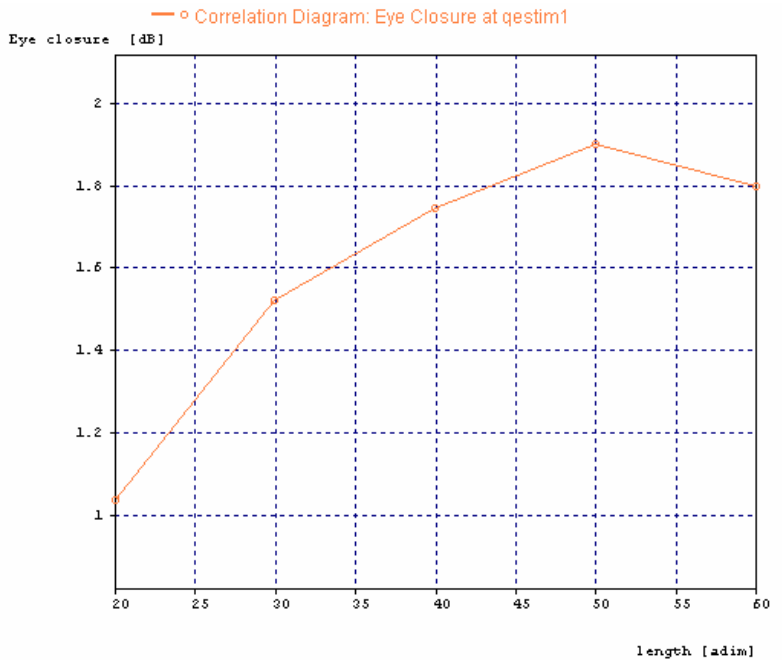

Figure 4.64 Eye closure

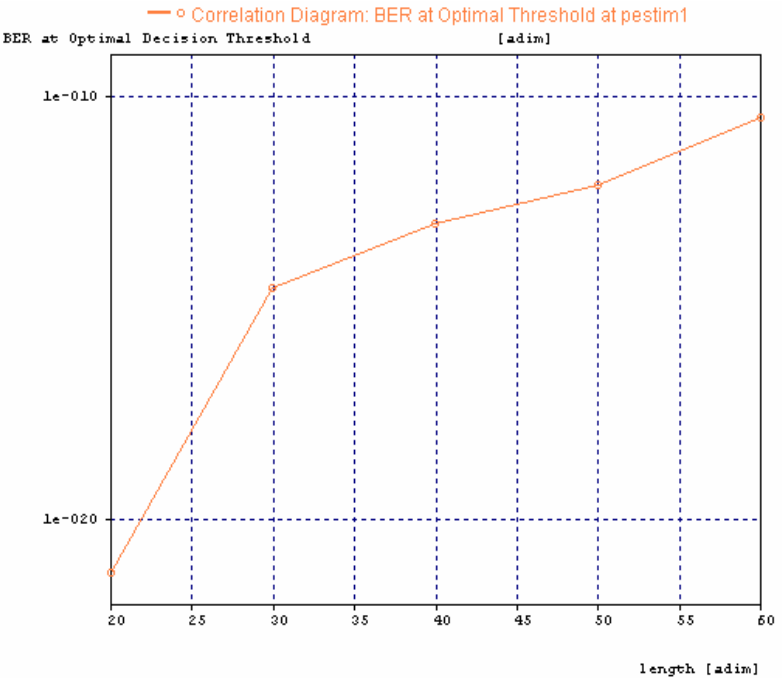

Figure 4.65 BER at optimal threshold

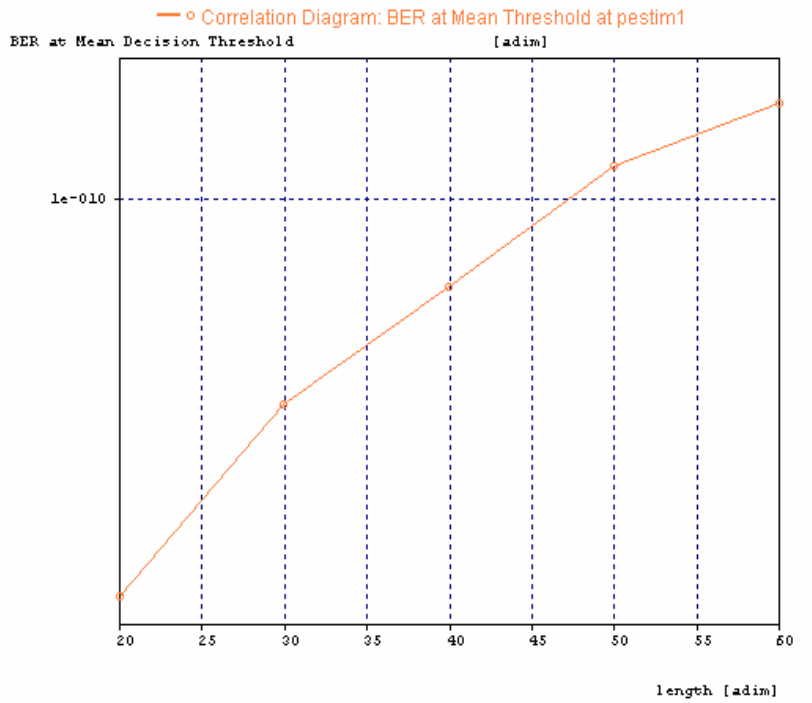

Figure 4.66 BER at mean threshold

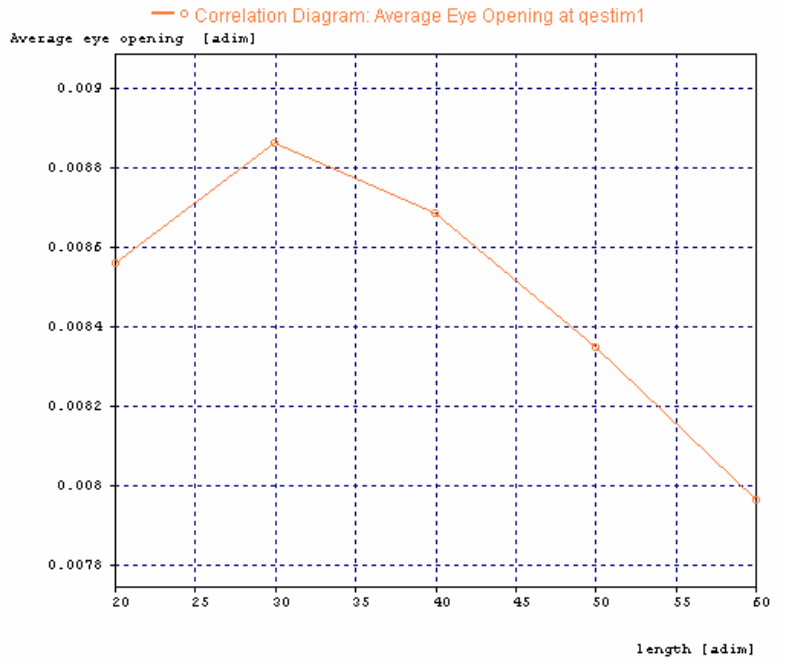

Figure 4.67 Average eye opening

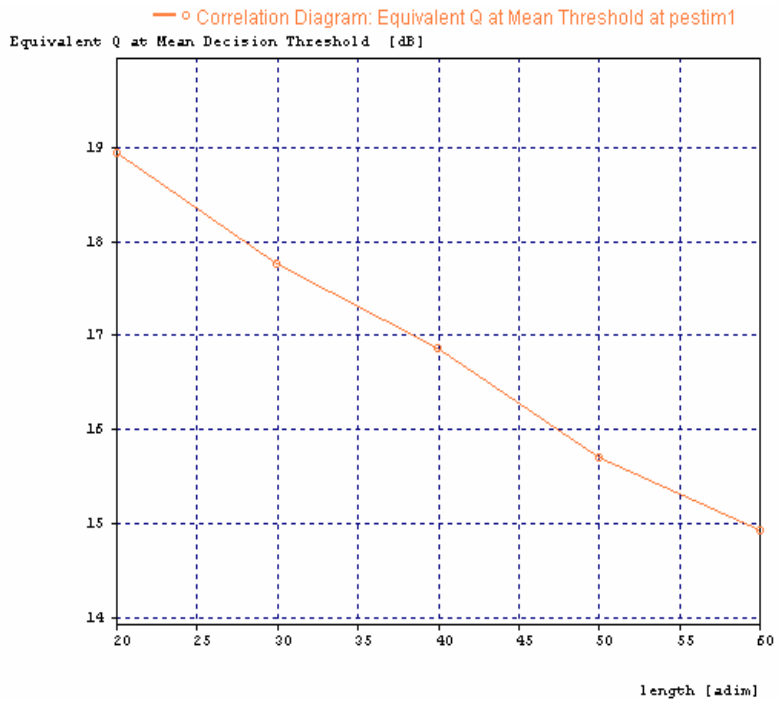

Figure 4.68 Equivalent Q at mean threshold

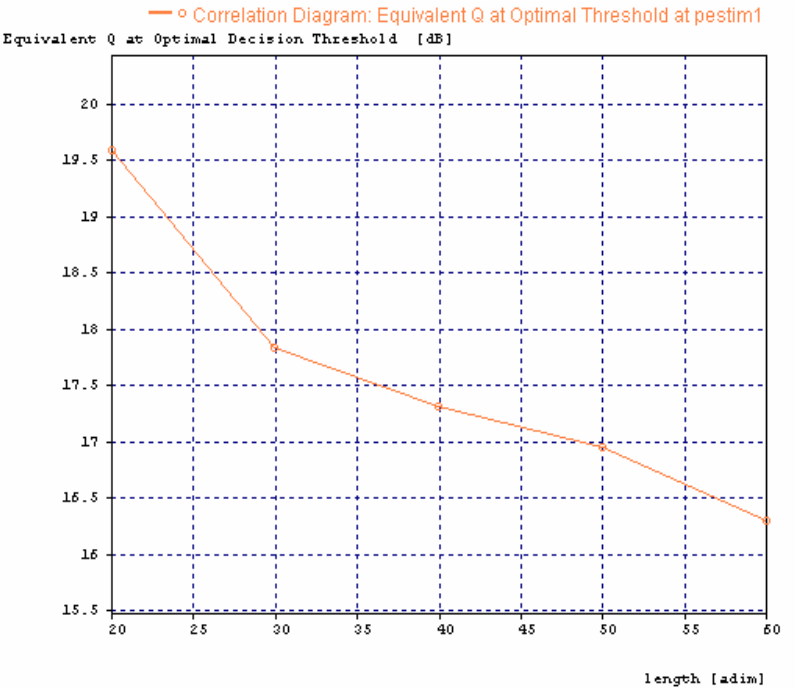

Figure 4.69 Equivalent Q at optimal threshold

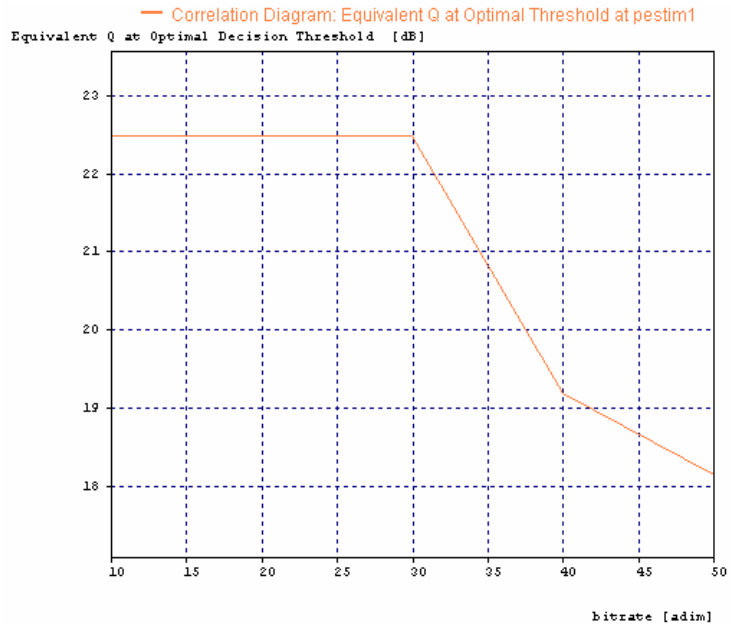

Figure 4.70 BER at optimal threshold

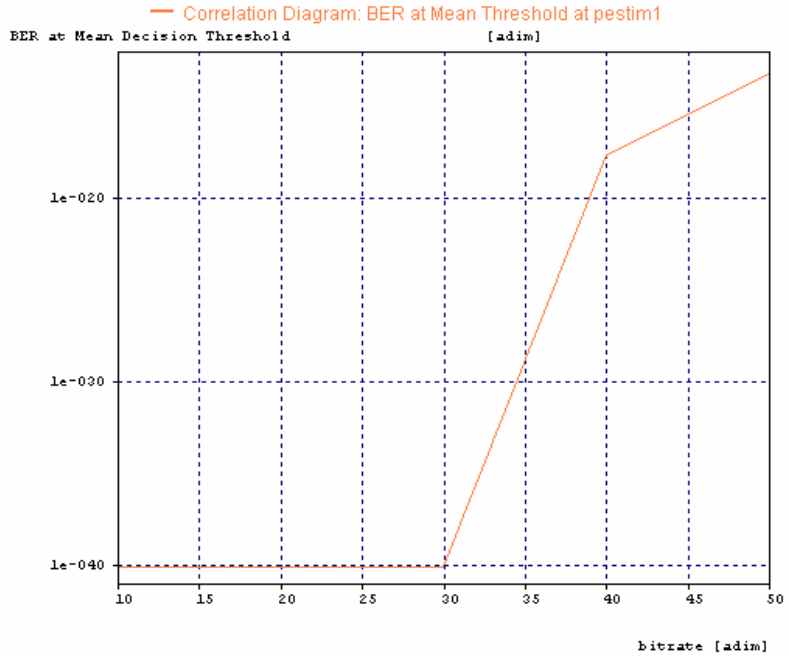

Figure 4.71 BER at mean optimal threshold

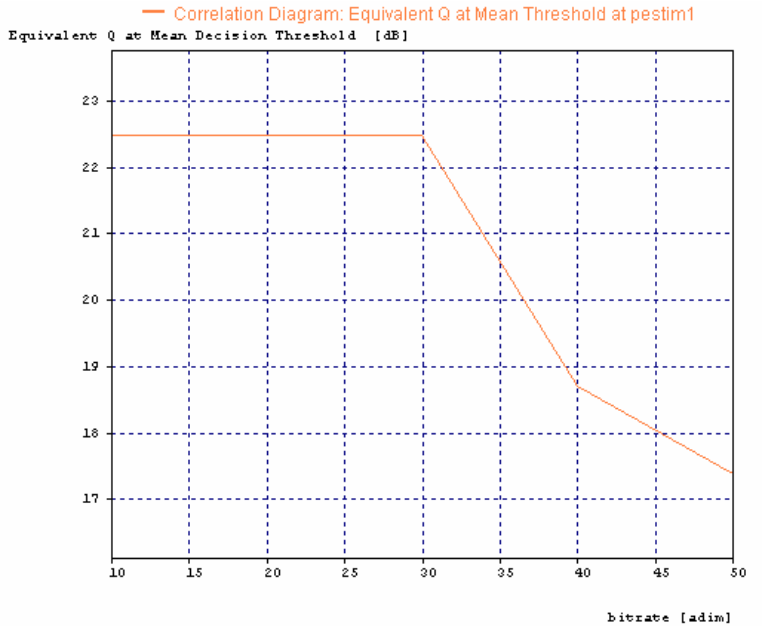

Figure 4.72 Equivalent Q at mean threshold

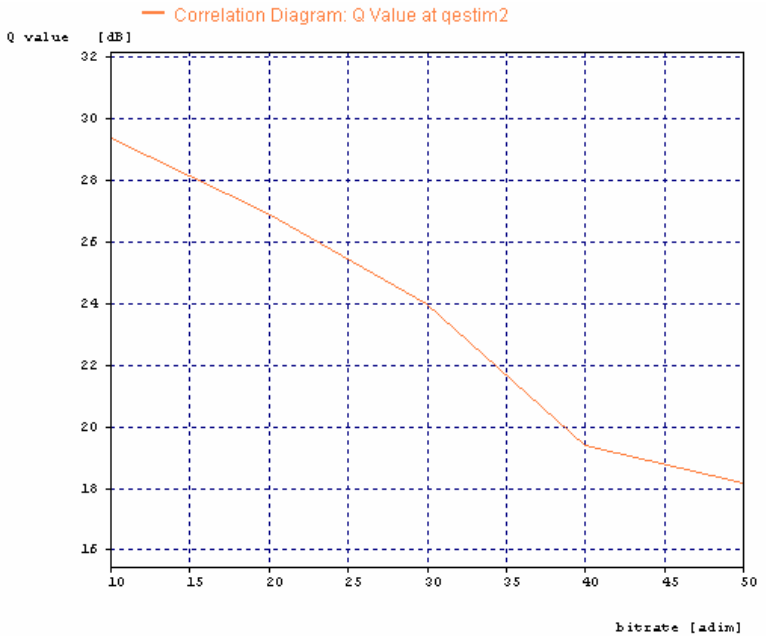

Figure 4.73 Q value

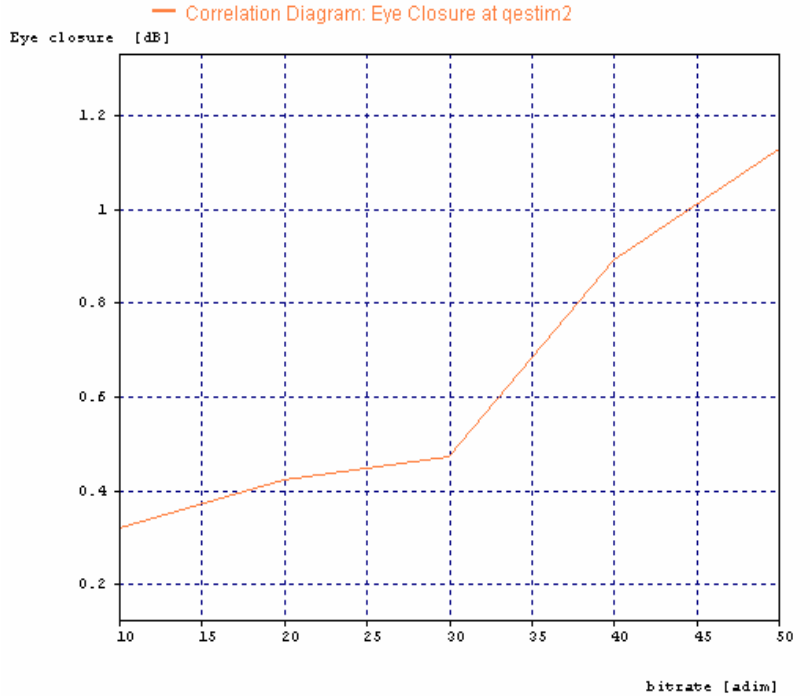

Figure 4.74 Eye closure

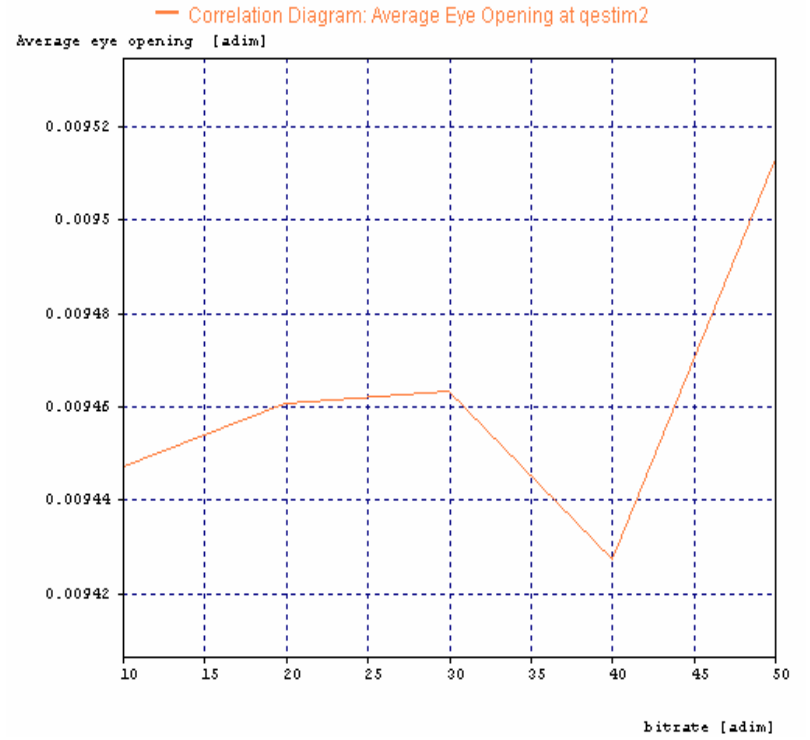

Figure 4.75 Average Eye opening

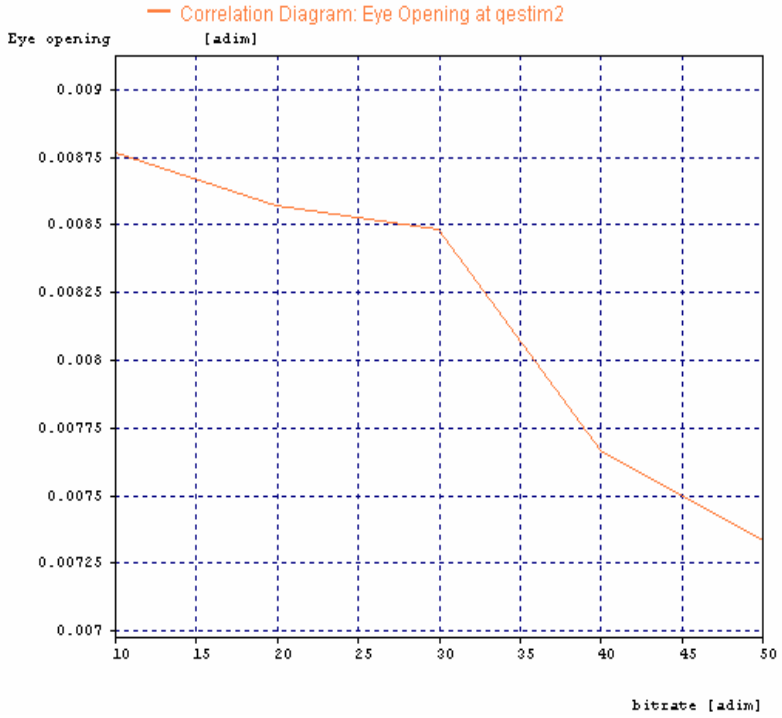

Figure 4.76 Eye opening

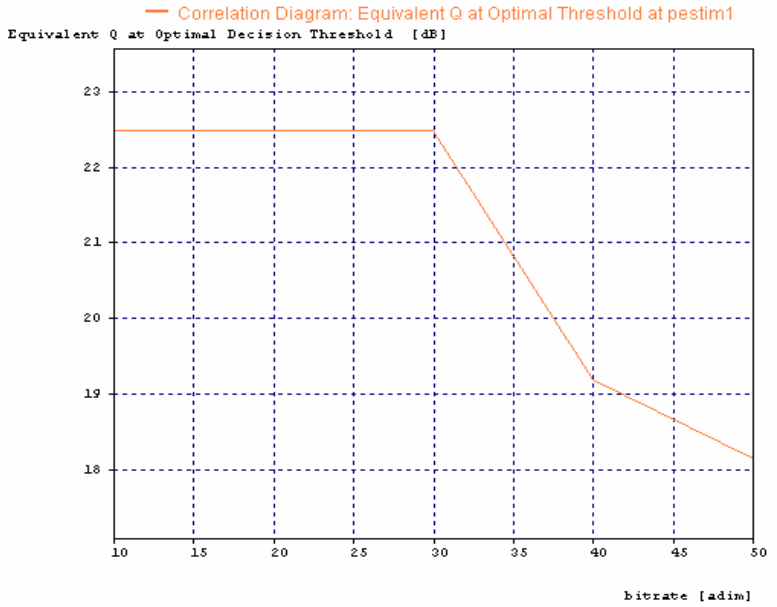

Figure 4.77 Equivalent Q at optimal threshold

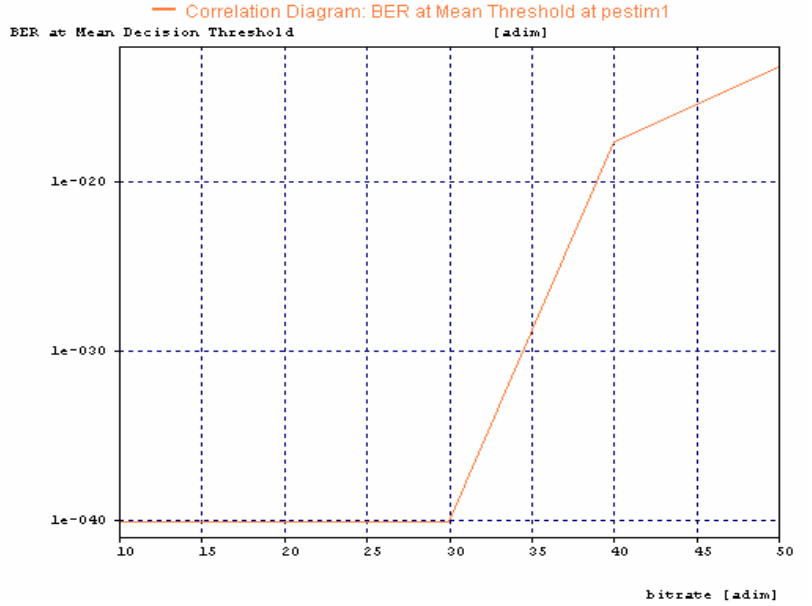

Figure 4.78 BER at mean threshold

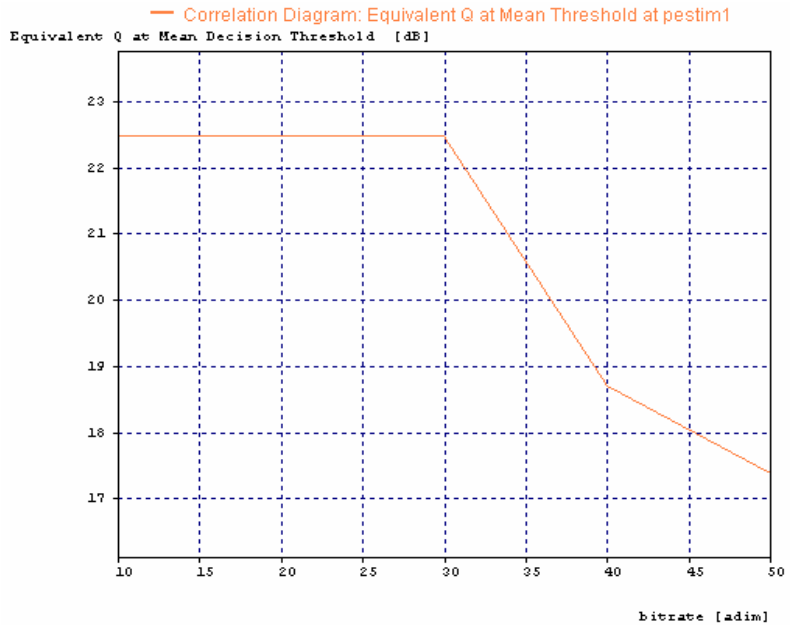

Figure 4.79 Equivalent Q at mean threshold

CHAPTER 5

DEPENDENCE OF SELF PHASE MODULATION IMPAIRMENTS ON RESIDUAL DISPERSION IN 10 Gb/s BASED TERRESTRIAL TRANSMISSION USING STANDARD FIBER WITH SEMICONDUCTOR OPTICAL AMPLIFIER (SOA)

5.1 Introduction of Semiconductor optical amplifier (SOA)

Semiconductor optical amplifiers are amplifiers which use a semiconductor to provide the gain medium. Recent designs include anti-reflective coatings and tilted waveguide and window regions which can reduce end face reflection to less than 0.001%. Since this creates a loss of power from the cavity which is greater than the gain it prevents the amplifier from acting as a laser. Such amplifiers are often used in telecommunication systems in the form of fiber-pigtailed components, operating at signal wavelengths between 0.85 µm and 1.6 µm and generating gains of up to 30 dB. The semiconductor optical amplifier is of small size and electrically pumped. It can be potentially less expensive than the EDFA and can be integrated with semiconductor lasers, modulators, etc. However, the performance is still not comparable with the EDFA. The SOA has higher noise, lower gain, moderate polarization dependence and high nonlinearity with fast transient time. This originates from the short nanosecond or less upper state lifetime, so that the gain reacts rapidly to changes of pump or signal power and the changes of gain also because phase changes which can distort the signals. This nonlinearity presents the most severe problem for optical communication applications. However it provides the possibility for gain in different wavelength regions form the EDFA. "Linear optical amplifiers" using gain clamping techniques have been developed [47].

5.2 Simulation setups

The various simulation setups under consideration is shown in figure 5.1 Pre compensation with SOA. The description of pre compensation with SOA is reported I section 5.2.1 and results of simulations are reported in section 5.2.2.

5.2.1 Simulation of pre compensation with SOA

In order to illustrate how pre compensation can be studied, the system is simulated with block diagram shown in figure 5.1. In this case, the transmitter section consists of data source, electrical driver (NRZ), laser source (CW_ Lorentzian) and amplitude modulator ($\sin^2$_MZ) is connected with optical spectrum analyzer which is used to observe the optical spectrum. Three SOA and two SSMF are connected in alternate to each other such that the output of SOA is fed to the next SSMF connected to it. The output of last SOA is given to optical raised cosine filter which is connected to receiver section. In receiver section PIN is connected to an electrical Bessel filter and the final result is shown through electrical scope, Q estimator and bit error rate estimator.

5.2.2 Results and discussion regarding simulation of pre compensation based on SOA

The simulation results from different simulation systems are predicted. The results of simulation setup in figures 5.2 to 5.7 shows the electrical spectrum on 10 Gb/s bitrate on different length of 10, 20, 30, 40, 50, 60 km and dispersion values 8, 10, 12, 14, 15, 16 ps/nm/km.

Eye diagrams for different lengths

The results of eye diagrams are shown in figures 5.8 to 5.13 for different length. Eye opening decreases and eye closure increases with increase the length of SSMF i.e. eye opening penalty increases as the length of single mode fiber increases. The best result is observed with 10 km length of single mode fiber.

Optical spectrums

The results of optical spectrum at frequency range [193.362, 193.467 THz] are shown in Figure 5.14 to 5.19.

Result based on Q and bit error rate estimator for different lengths

Figure 5.20 shows the result of Q value on 20, 30, 40, 50, 60 km length of fiber which is 6.02 dB at all values of length.

Figure 5.21 shows the result of equivalent Q at optimal threshold on 20, 30, 40, 50, 60 km length of fiber which is 6.02 dB at all values of length.

Figure 5.22 shows the result of equivalent Q at mean threshold on 20, 30, 40, 50, 60 km length of fiber which is 6.02 dB at all values of length.

Figure 5.23 shows the result of average eye opening on 20, 30, 40, 50, 60 km length of fiber which is 0.010 at 20 Km, 0.05 at 40 Km and 0.0142 at 60 Km.

Figure 5.24 shows the result of BER at mean threshold on 20, 30, 40, 50, 60 km length of fiber which is 0.024 at all values of length.

Figure 5.25 shows the result of BER at optimal threshold on 20, 30, 40, 50, 60 km length of fiber which is 0.024 at all values of length.

Result based on Q and bit error rate estimator for different dispersion

Figure 5.26 shows the result of Q value at 7, 9, 11, 13, 15 ps/nm/km dispersion of fiber which is 7.1 dB at 7 ps/nm/km and 6.01 dB for 9 to15 ps/nm/km.

Figure 5.27 shows the result of BER at mean threshold on 7, 9, 11, 13, 15 ps/nm/km dispersion of fiber which is 0.25 at all values.

Figure 5.28 shows the result of BER at optimal threshold on 7, 9, 11, 13, 15 ps/nm/km dispersion of fiber which is 0.01 at 7 ps/nm/km and 0.025 at 9 to 15 ps/nm/km.

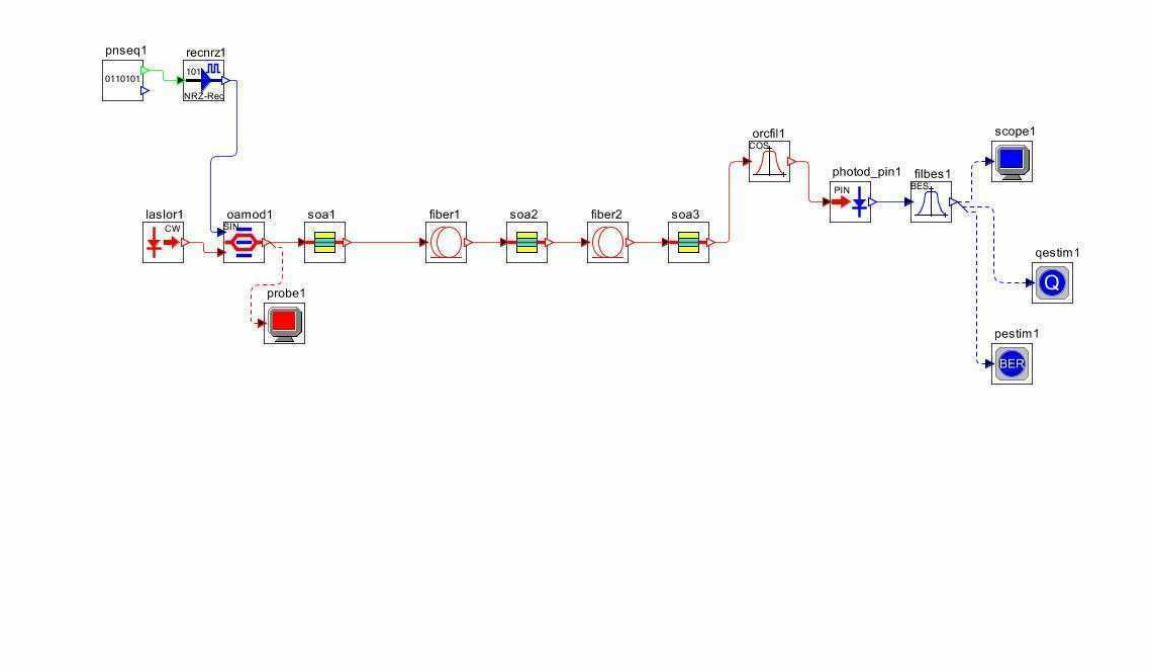

Figure5.1 Pre compensation with SOA

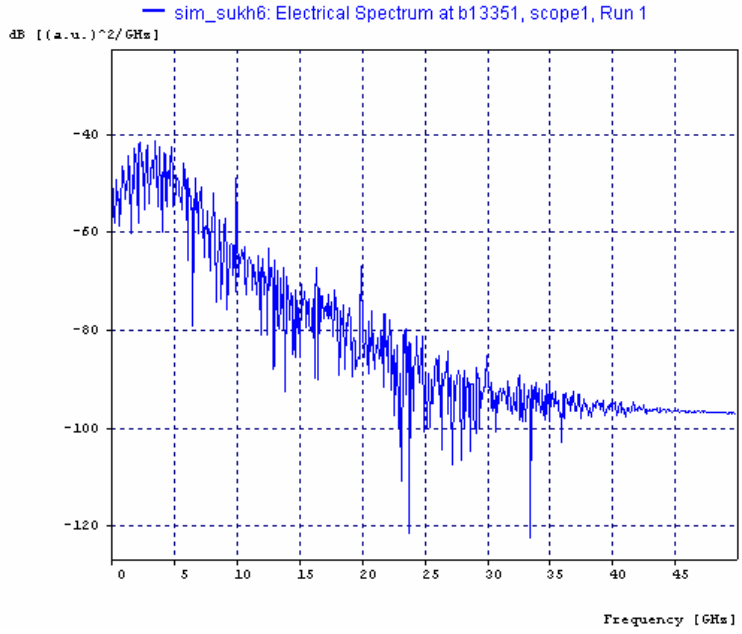

Figure 5.2 Electrical spectrum

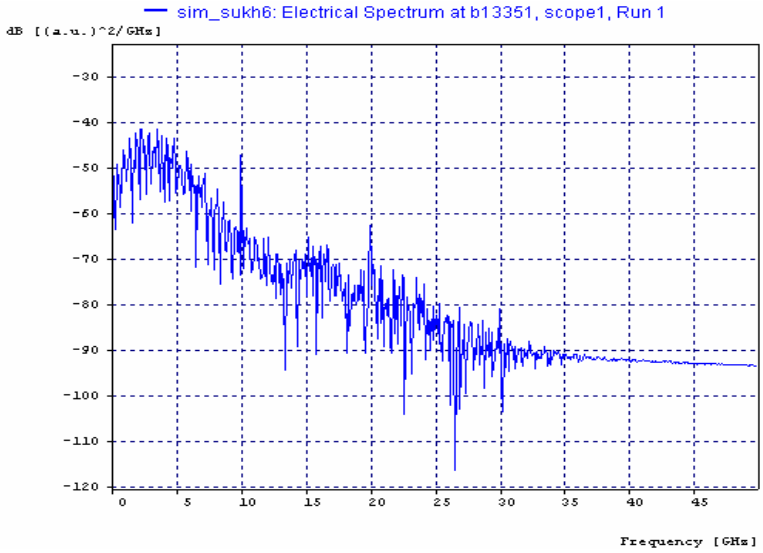

Figure 5.3 Electrical spectrum

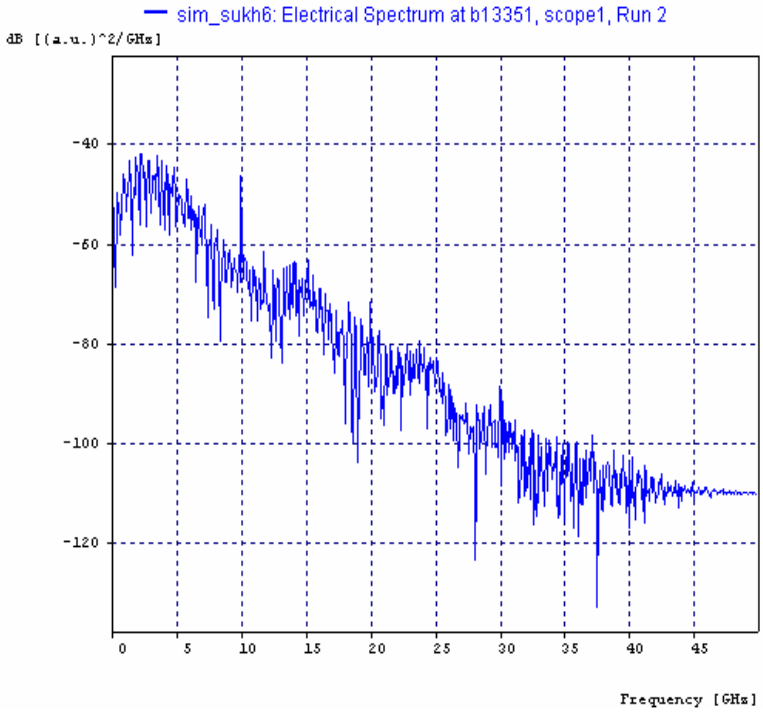

Figure 5.4 Electrical spectrum

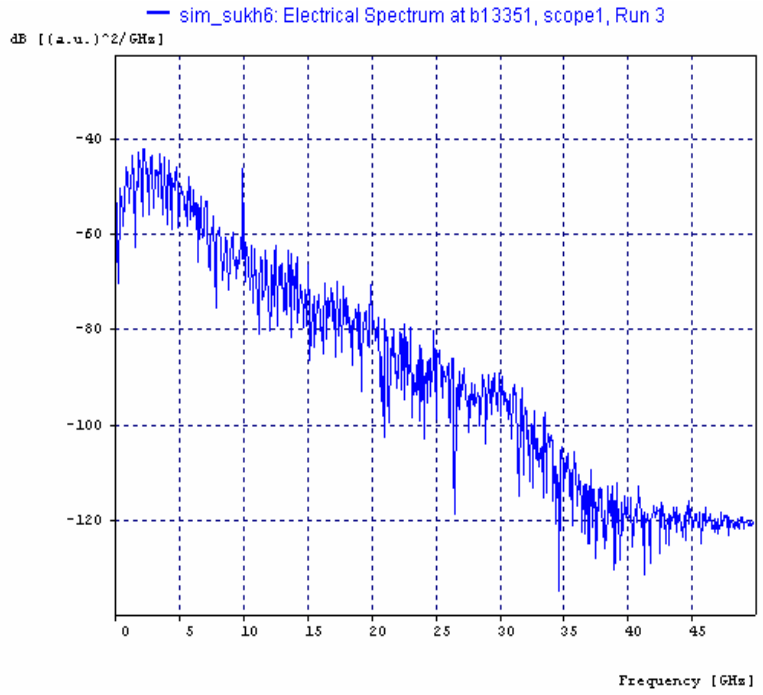

Figure 5.5 Electrical spectrum

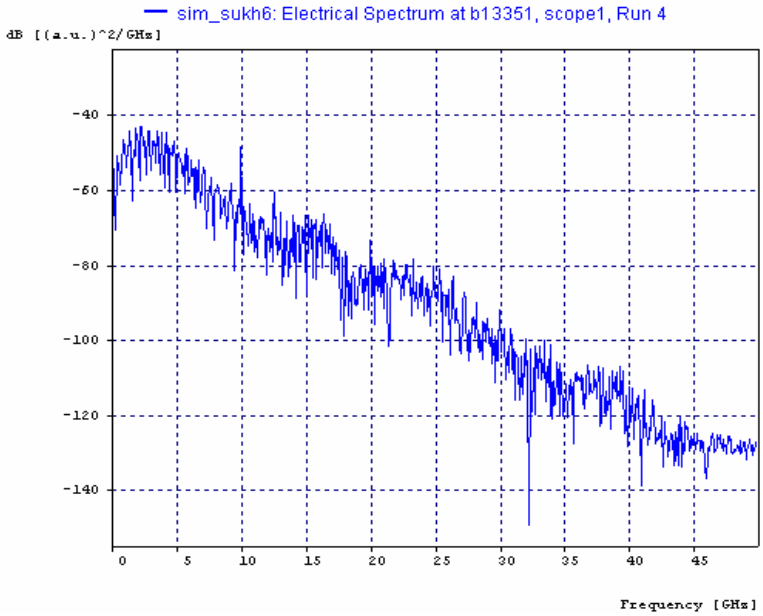

Figure 5.6 Electrical spectrum

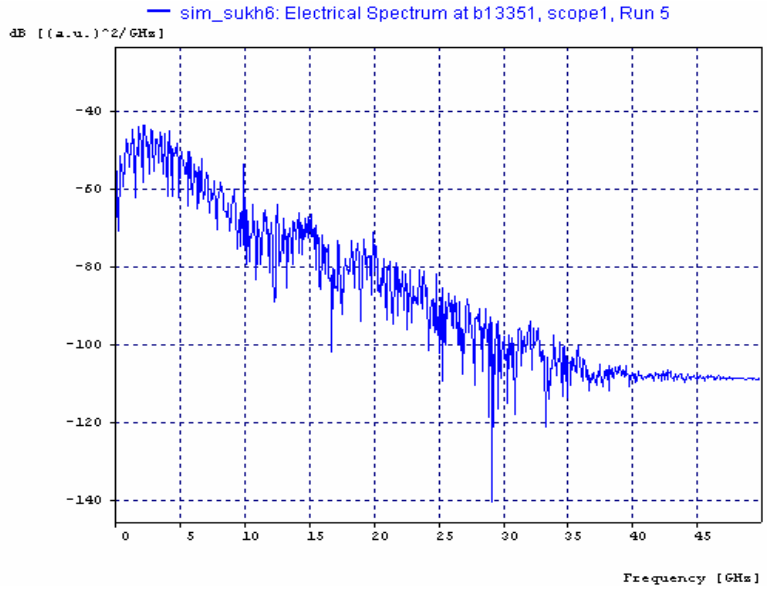

Figure 5.7 Electrical spectrum

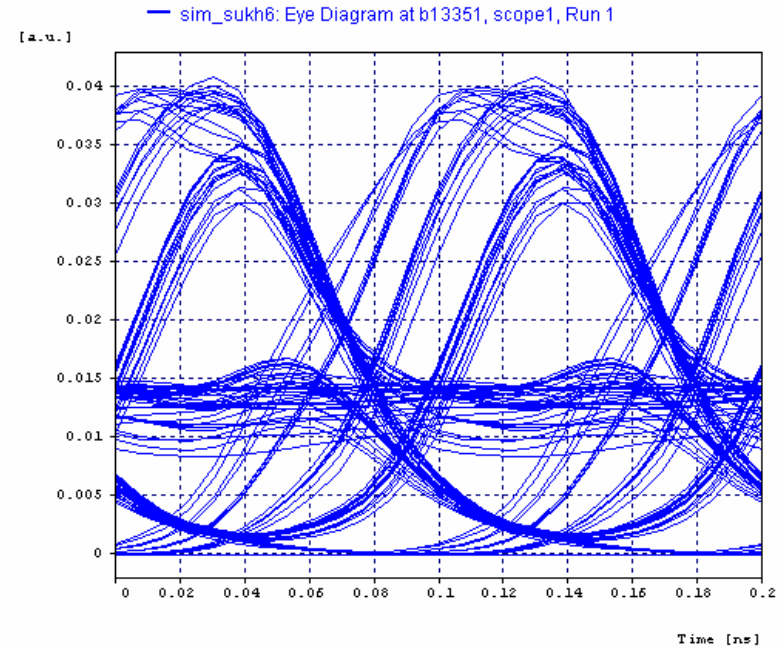

Figure 5.8 Eye diagram at 10 km length

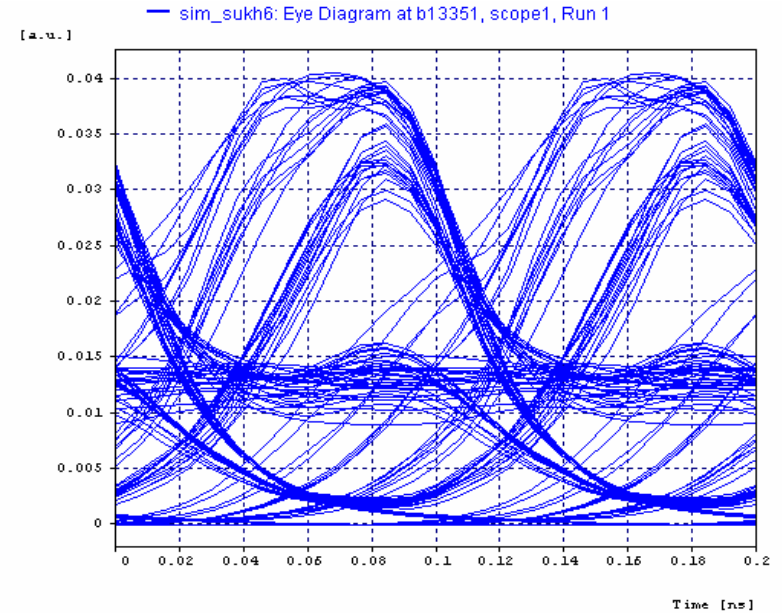

Figure 5.9 Eye diagram at 20 km length

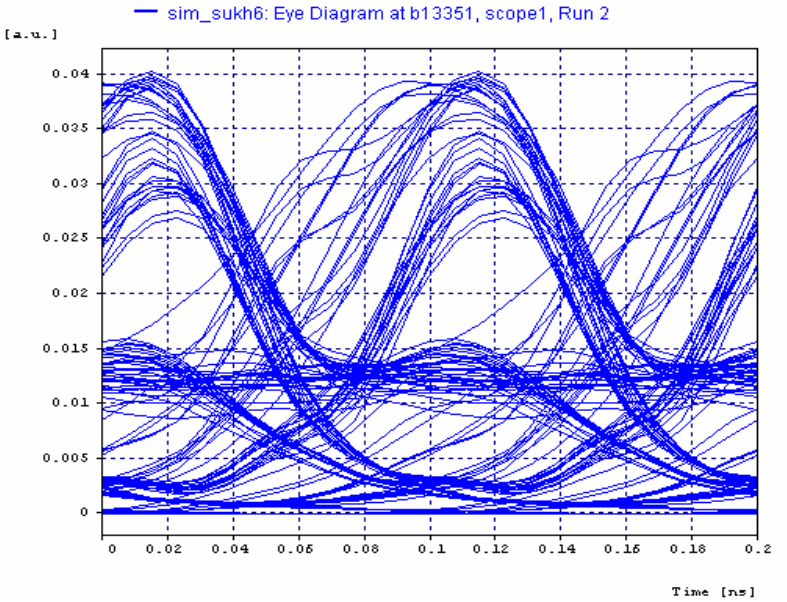

Figure 5.10 Eye diagram at 30 km length

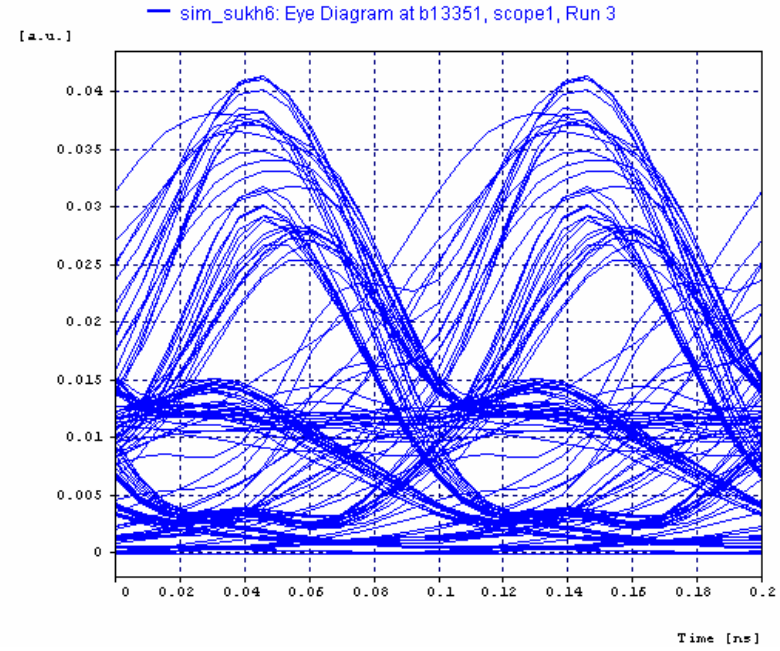

Figure 5.11 Eye diagram at 40 km length

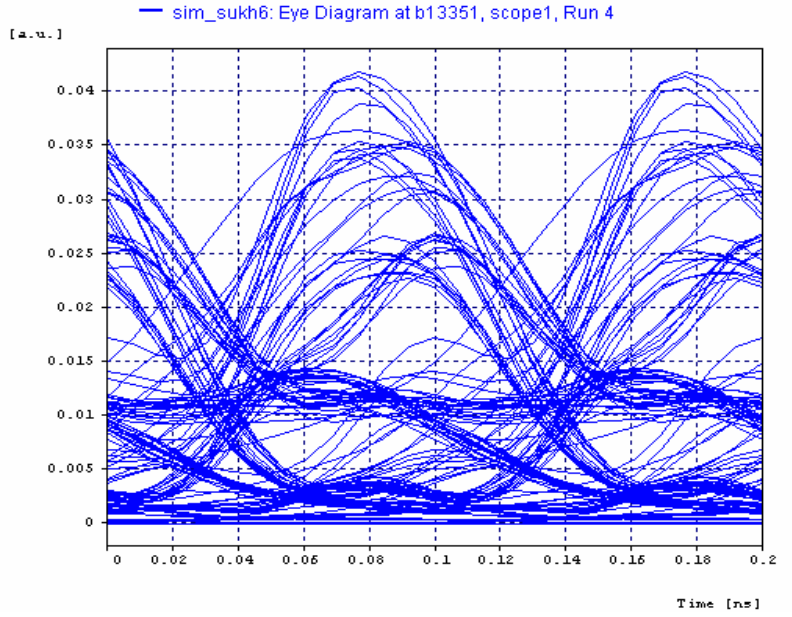

Figure 5.12 Eye diagram at 50 km length

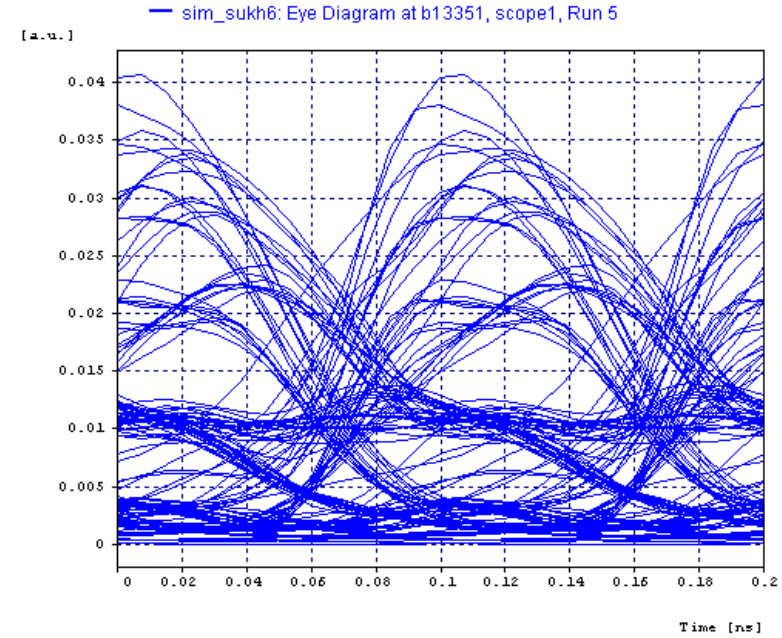

Figure 5.13 Eye diagram at 60 km length

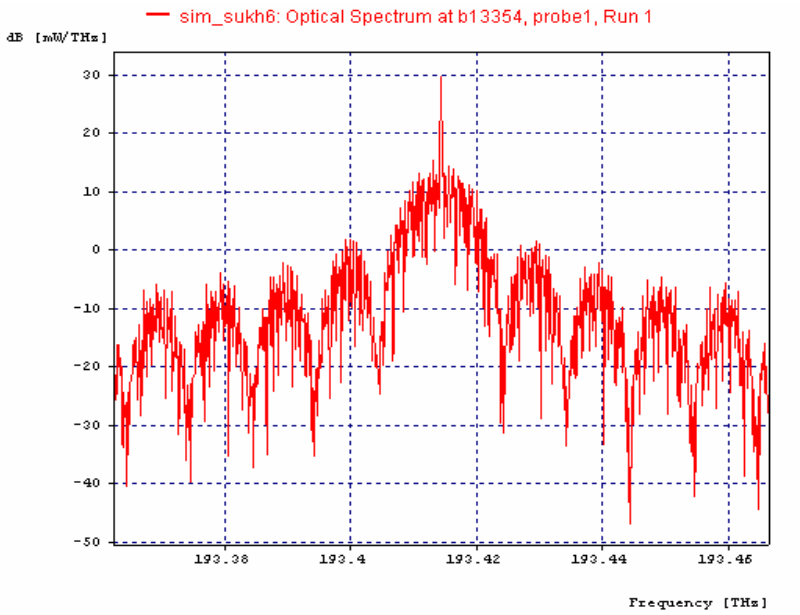

Figure 5.14 Optical spectrum

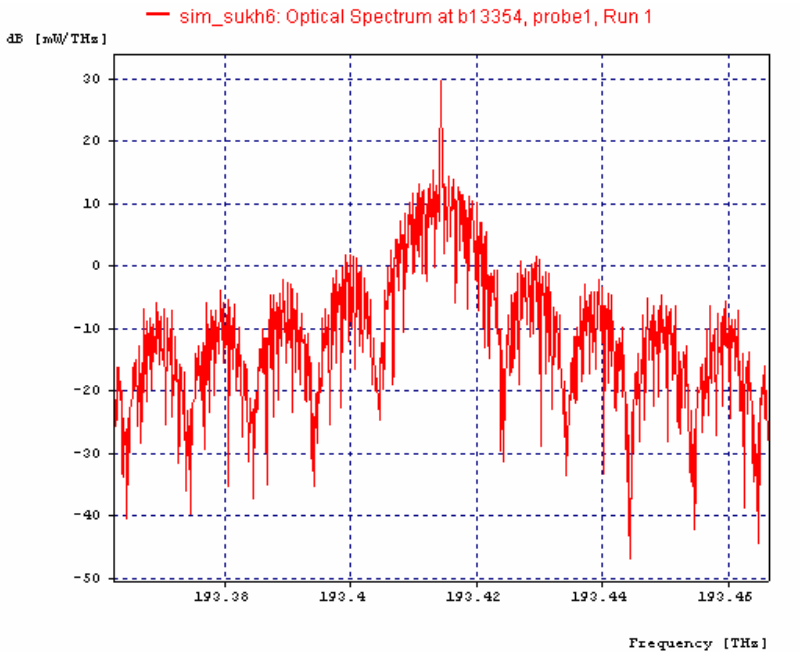

Figure 5.15 Optical spectrum

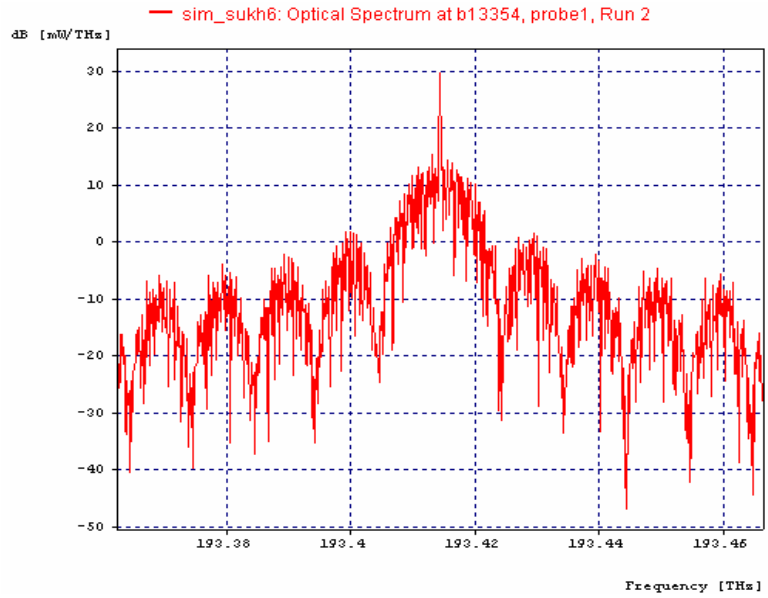

Figure 5.16 Optical spectrum

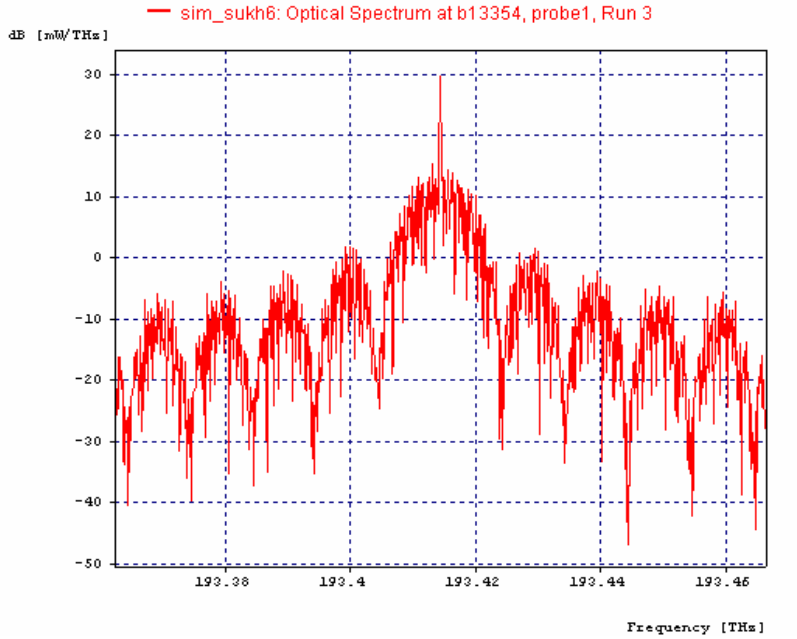

Figure 5.17 Optical spectrum

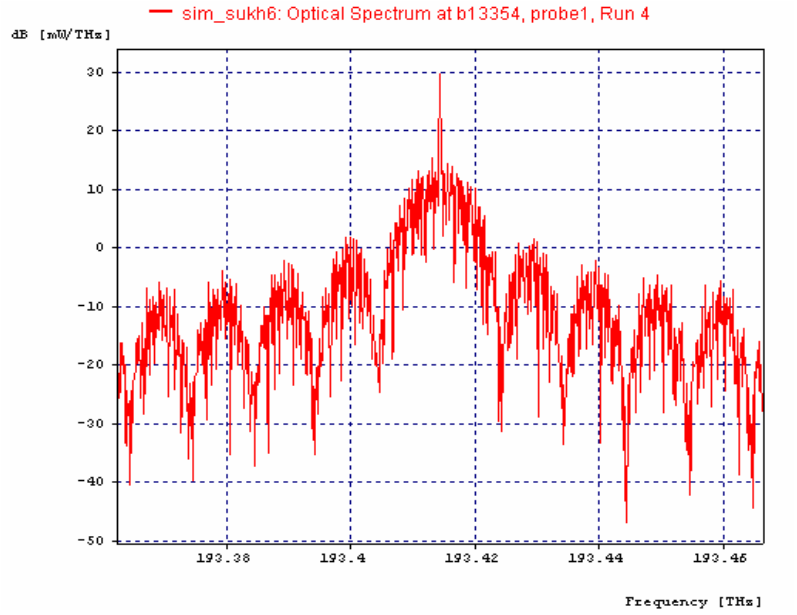

Figure 5.18 Optical spectrum

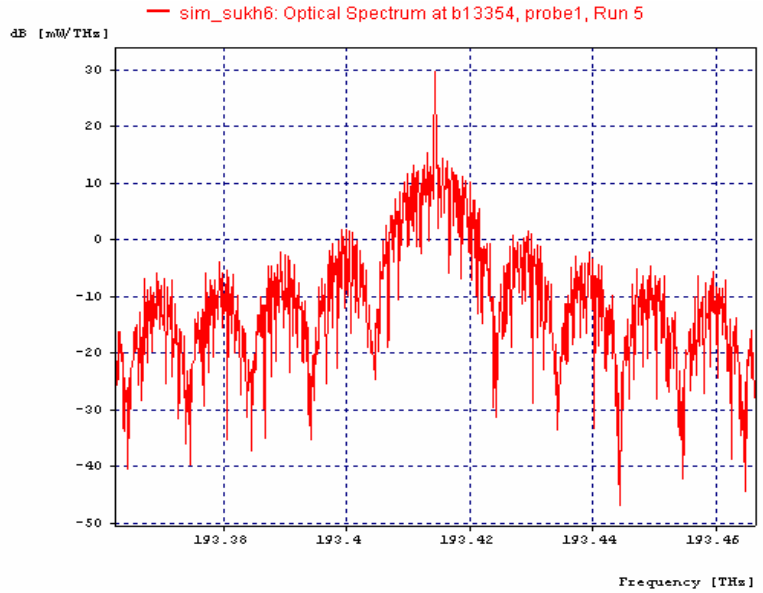

Figure 5.19 Optical spectrum

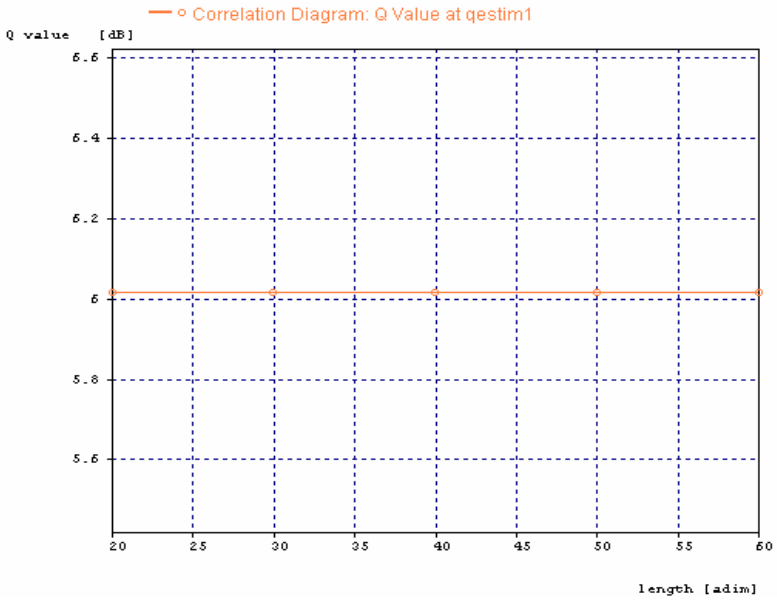

Figure 5.20 Q value at length

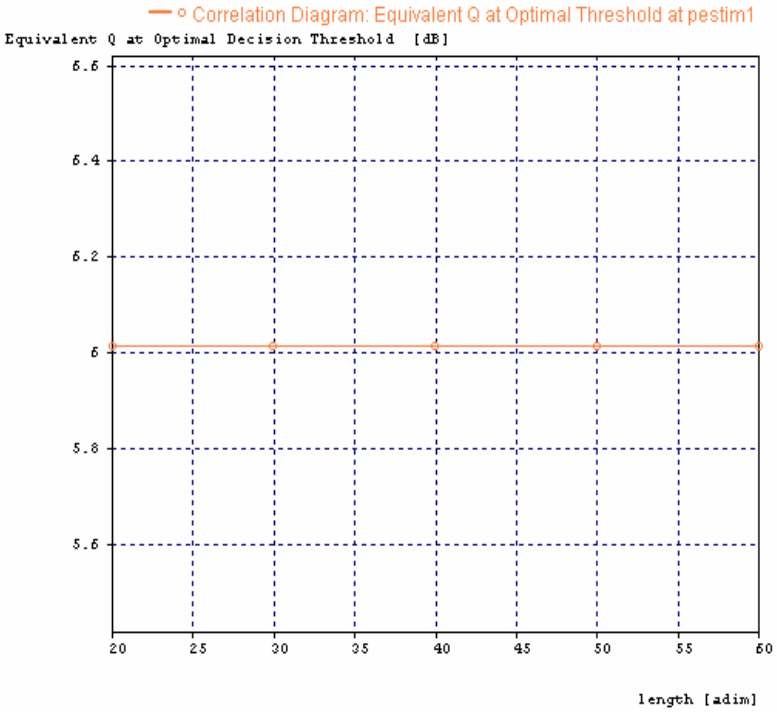

Figure 5.21 Equivalent Q at optimal threshold at length

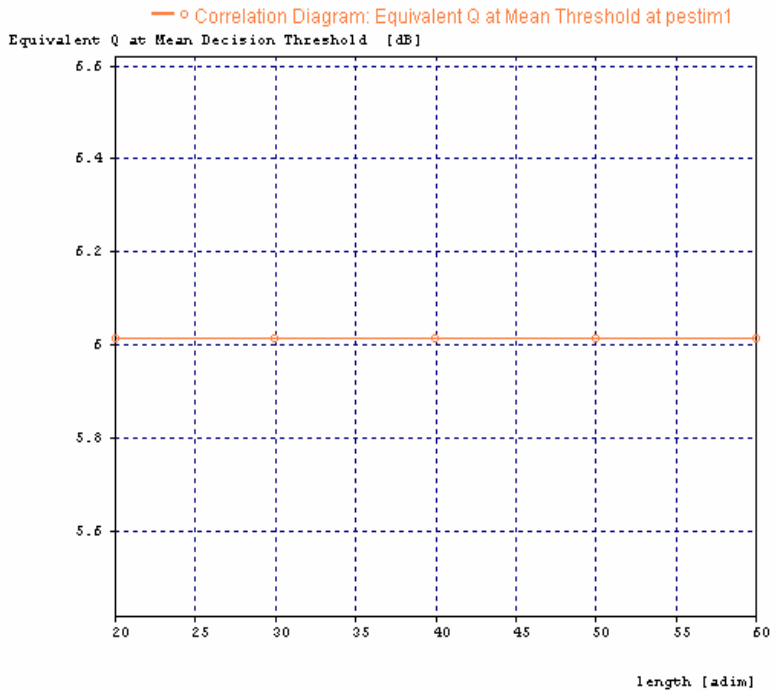

Figure 5.22 Equivalent Q at mean threshold at length

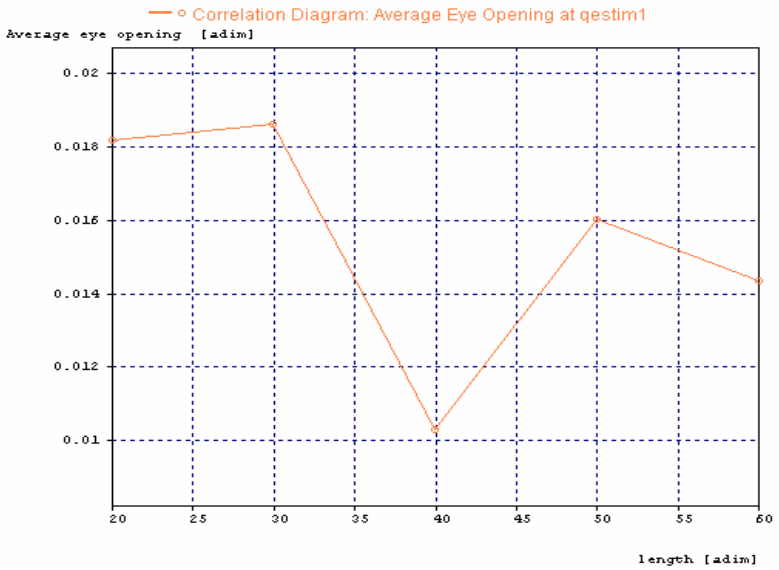

Figure 5.23 Average eye opening at length

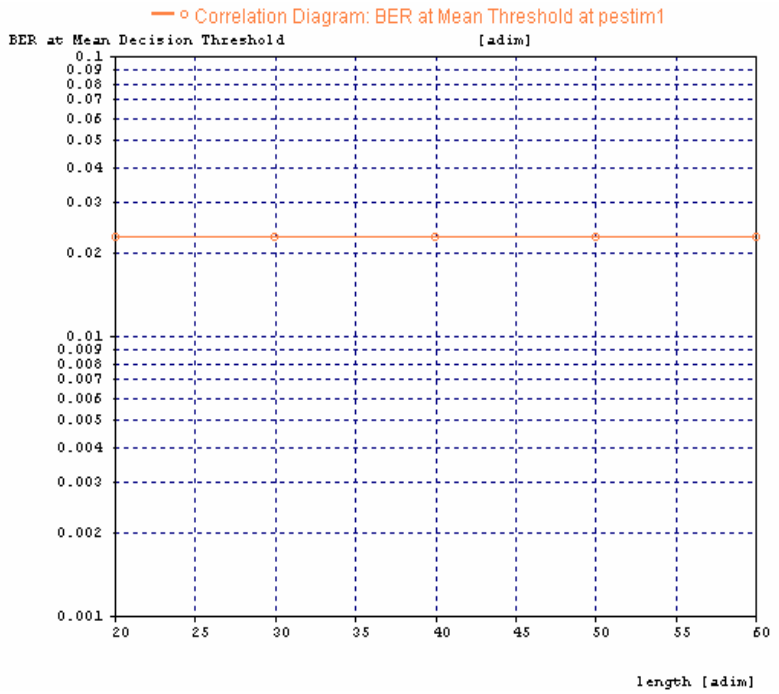

Figure 5.24 BER at mean threshold

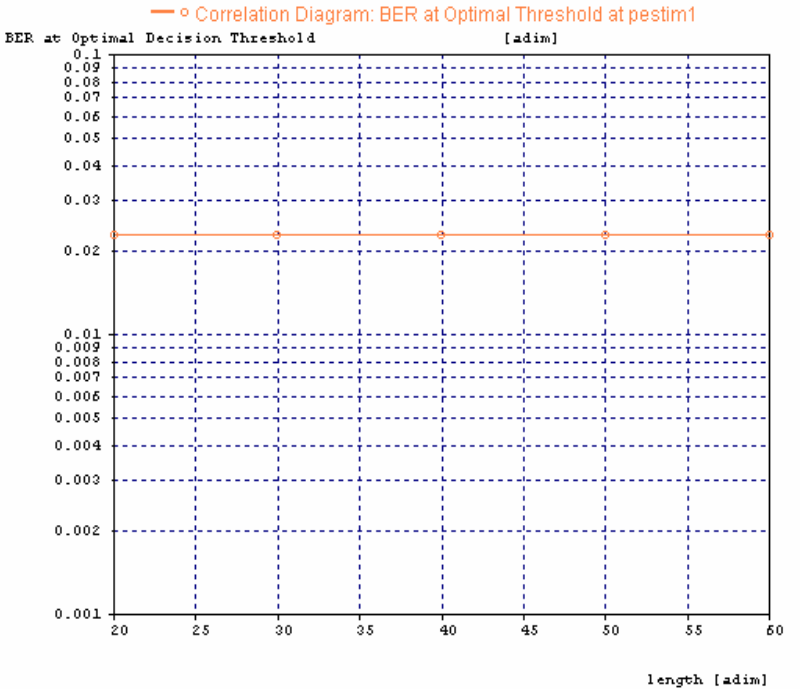

Figure 5.25 BER at optimal threshold at length

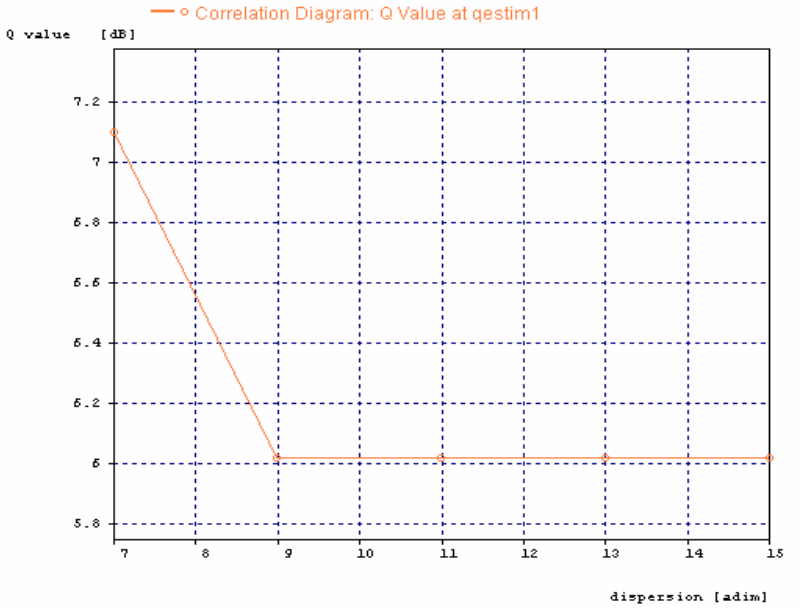

Figure 5.26 Q value at dispersion

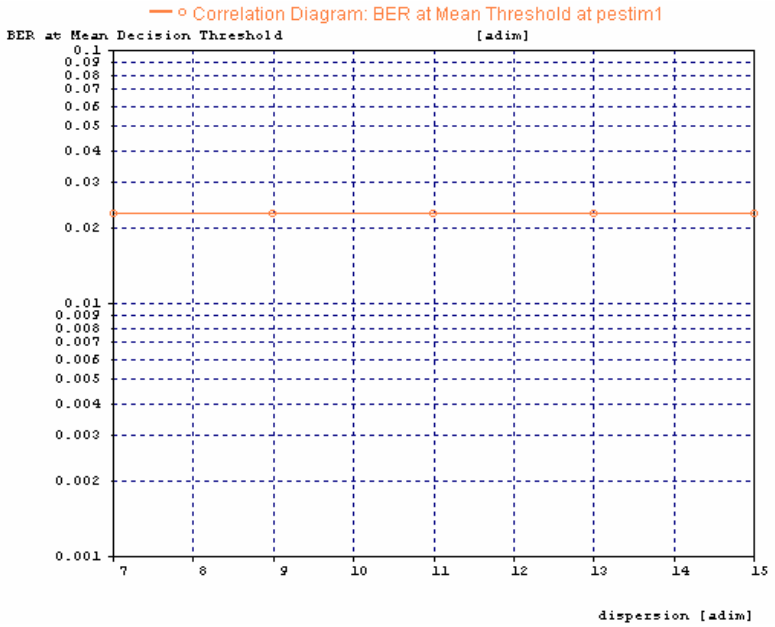

Figure 5.27 BER at mean threshold at dispersion

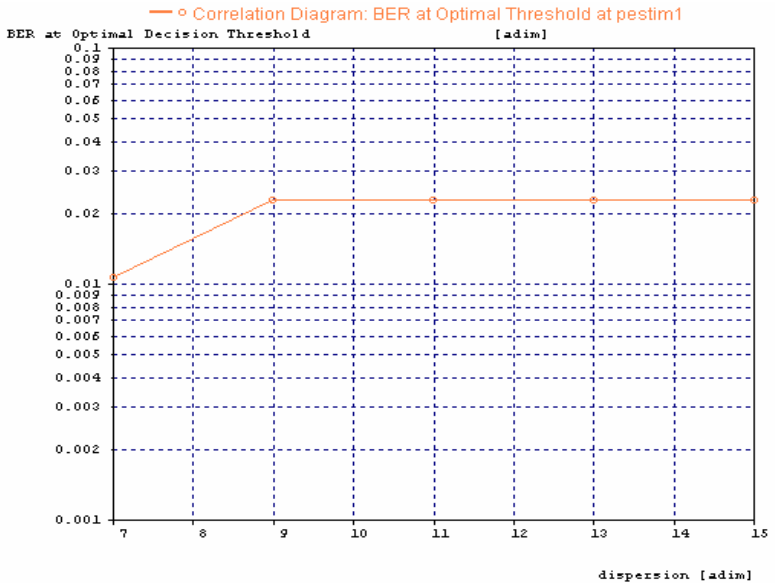

Figure 5.28 BER at optimal threshold at dispersion

5.3 Results and discussion regarding comparison of pre compensation

on the bases of EDFA and SOA

Result based on Q and bit error rate estimator for different dispersion

Figure 5.29 shows the result of Q value at 7, 9, 11, 13, 15 ps/nm/km dispersion of fiber which is 29 dB at 7 ps/nm/km and 18 dB at 15 ps/nm/km for EDFA and 3 dB at 7 ps/nm/km and 1 dB for 9 to15 ps/nm/km for SOA.

Figure 5.30 shows the result of eye closure on 7, 9, 11, 13, 15 ps/nm/km dispersion of fiber which is 7 dB at 7 ps/nm/km and 23 dB at 15 ps/nm/km for EDFA and 0.3 dB at 7 ps/nm/km and 1.1 dB at15 ps/nm/km for SOA.

Figure 5.31 shows the result of average eye opening on 7, 9, 11, 13, 15 ps/nm/km dispersion of fiber which is 0.08 at 7 ps/nm/km and 0.089 at 15 ps/nm/km for EDFA and 0.017 at 7 ps/nm/km and 0.11 at15 ps/nm/km for SOA.

Figure 5.32 shows the result of eye opening on 7, 9, 11, 13, 15 ps/nm/km dispersion of fiber which is 0.088 at 7 ps/nm/km and 0.072 at 15 ps/nm/km for EDFA and 0.001 at 7 ps/nm/km and 0.0003 for 9 and 0.0006 at 15 ps/nm/km for SOA.

Figure 5.33 shows the result of BER at optimal threshold on 7, 9, 11, 13, 15 ps/nm/km dispersion of fiber which is 1e-040 at 7 to 11 ps/nm/km, 1e-020 at 13 ps/nm/km and 1e-013 at 15 ps/nm/km for EDFA and 1e-001at 7 ps/nm/km and 1e-0008 at 15 ps/nm/km for SOA.

Figure 5.34 shows the result of equivalent Q at optimal threshold on 7, 9, 11, 13, 15 ps/nm/km dispersion of fiber which is 22.5 dB at 7 to 11 ps/nm/km and 10 dB at 15 ps/nm/ for EDFA and 7 dB at 7 ps/nm/km and 6 dB at 15 ps/nm/km for SOA.

Figure 5.35 shows the result of BER at mean threshold on 7, 9, 11, 13, 15 ps/nm/km dispersion of fiber which is 1e-040 at 7 to 11 ps/nm/km, 1e-018 at 13 ps/nm/km and 1e-014 at 15 ps/nm/km for EDFA and 1e-001 at all values for SOA.

Figure 5.36 shows the result of equivalent Q at mean threshold on 7, 9, 11, 13, 15 ps/nm/km dispersion of fiber which is 22.5 dB at 7 to 11 ps/nm/km and 17 dB at 15 ps/nm/ for EDFA and 6 dB at all values for SOA.

Figure 5.37 shows the result of Q value at 10, 20, 30, 40, 50 Gb/s bit rate which is 29 dB at 10 Gb/s bit rate and 17 dB at 50 Gb/s bit rate for EDFA and 3 dB at 10 Gb/s bit rate and 1 dB for 50 Gb/s bit rate for SOA.

Figure 5.38 shows the result of eye closure on 10, 20, 30, 40, 50 Gb/s bit rate which is 7 dB at 10 Gb/s bit rate and 23 dB at 50 Gb/s bit rate for EDFA and 0.2 dB at 10 Gb/s bit rate and 2 dB for 50 Gb/s bit rate for SOA.

Figure 5.39 shows the result of average eye opening on 10, 20, 30, 40, 50 Gb/s bit rate which is 0.08 at 10 Gb/s bit rate and 0.08 at 50 Gb/s bit rate for EDFA and 0.0162 at 10 Gb/s bit rate and 0.007 for 50 Gb/s bit rate for SOA.

Figure 5.40 shows the result of eye opening on 10, 20, 30, 40, 50 Gb/s bit rate which is 0.0087 at 10 Gb/s bit rate and 0.0074 at 50 Gb/s bit rate for EDFA and 0.003 at 10 Gb/s bit rate and 0.000 for 50 Gb/s bit rate for SOA.

Figure 5.41 shows the result of BER at optimal threshold 10, 20, 30, 40, 50 Gb/s bit rate which is 1e-040 at 10 Gb/s bit rate and 1e-014 at 50 Gb/s bit rate for EDFA and 1e-002 at 10 Gb/s bit rate and 1e-0018 for 50 Gb/s bit rate for SOA.

Figure 5.42 shows the result of equivalent Q at optimal threshold 10, 20, 30, 40, 50 Gb/s bitrate which is 22.5 dB at 10 Gb/s bit rate and 10 dB at 50 Gb/s bit rate for EDFA and 7 dB at 10 Gb/s bit rate and 6 dB for 50 Gb/s bit rate for SOA.

Figure 5.43 shows the result of BER at mean threshold on 10, 20, 30, 40, 50 Gb/s bit rate which is 1e-040 at 10 Gb/s bit rate and 1e-014 at 50 Gb/s bit rate for EDFA and 1e-002 at 10 Gb/s bit rate and 1e-002 for 50 Gb/s bit rate for SOA.

Figure 5.44 shows the result of equivalent Q at mean threshold 10, 20, 30, 40, 50 Gb/s bit rate which is 22.5 dB at 10 Gb/s bit rate and 17 dB at 50 Gb/s bit rate for EDFA and 6 dB at 10 Gb/s bit rate and 6 dB for 50 Gb/s bit rate for SOA.

The results observed in pre compensation with EDFA and SOA are compared on the basis of dispersion and bit rate in which the best results are found with EDFA.

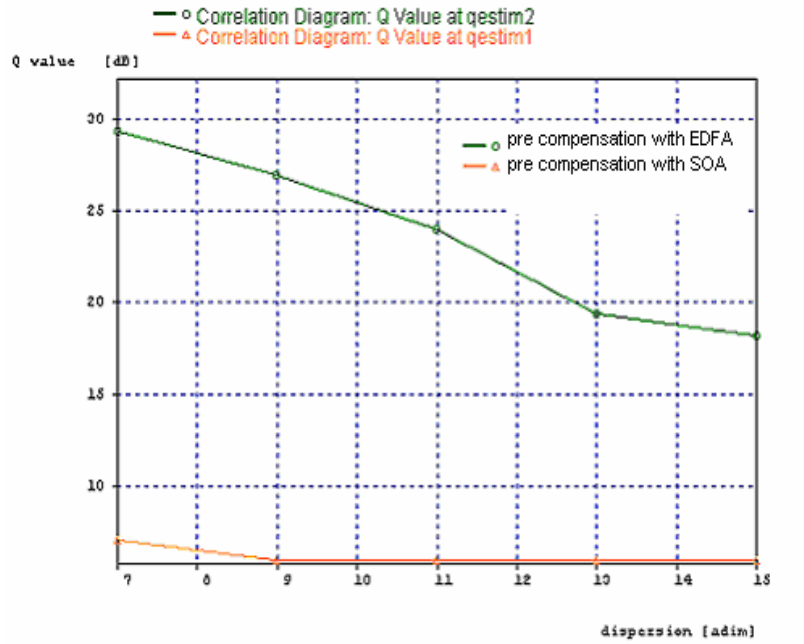

Figure 5.29 Q value

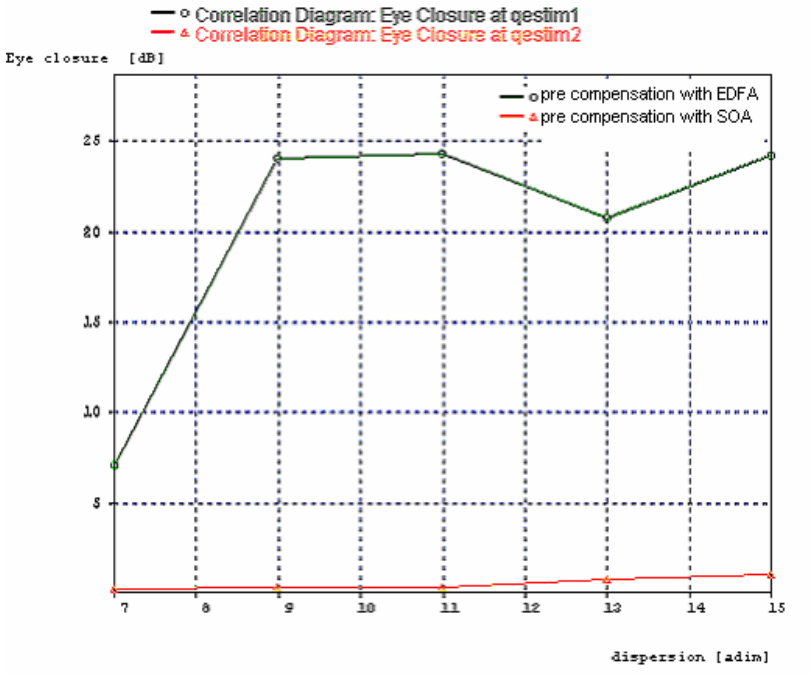

Figure 5.30 Eye closure

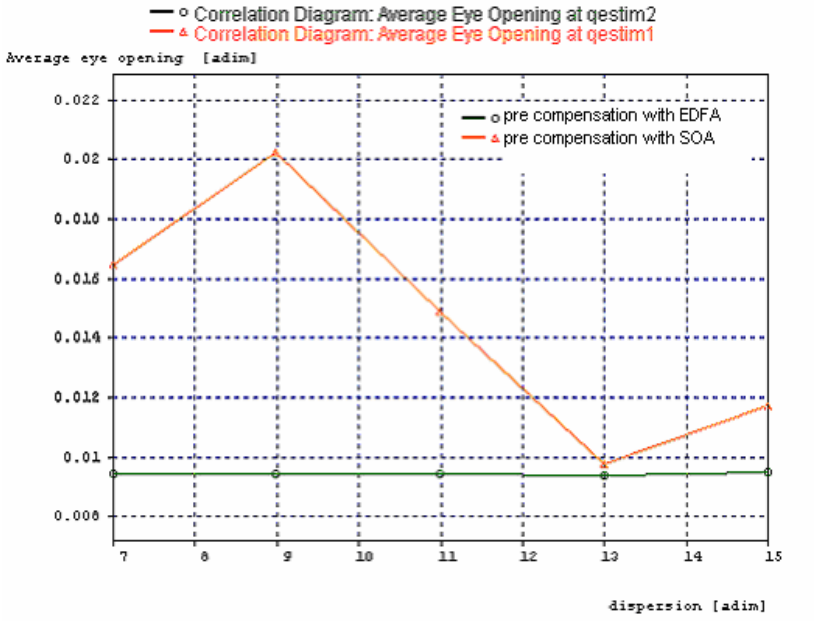

Figure 5.31 Average eye opening

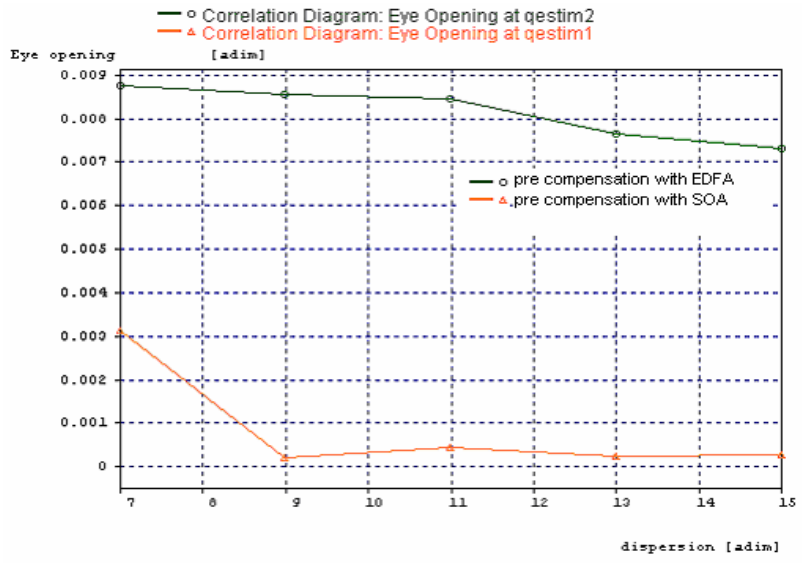

Figure 5.32 Eye opening

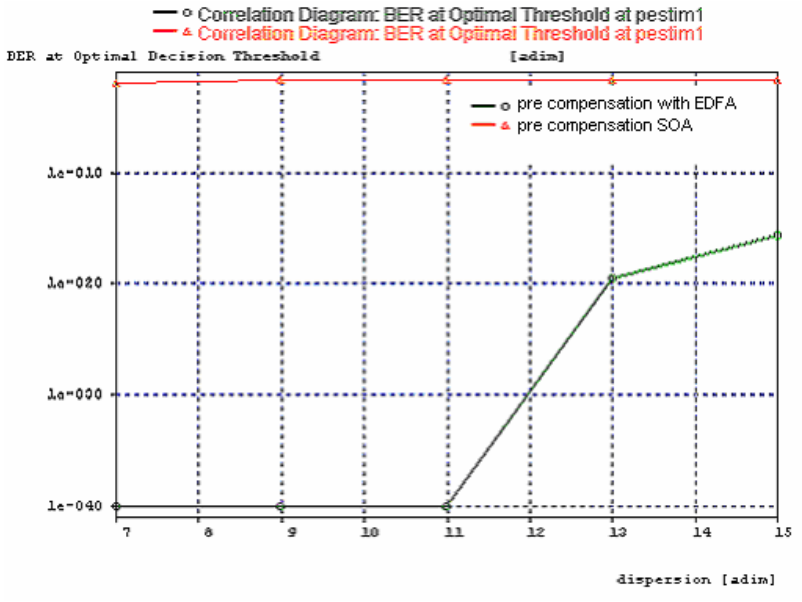

Figure 5.33 BER at optimal threshold

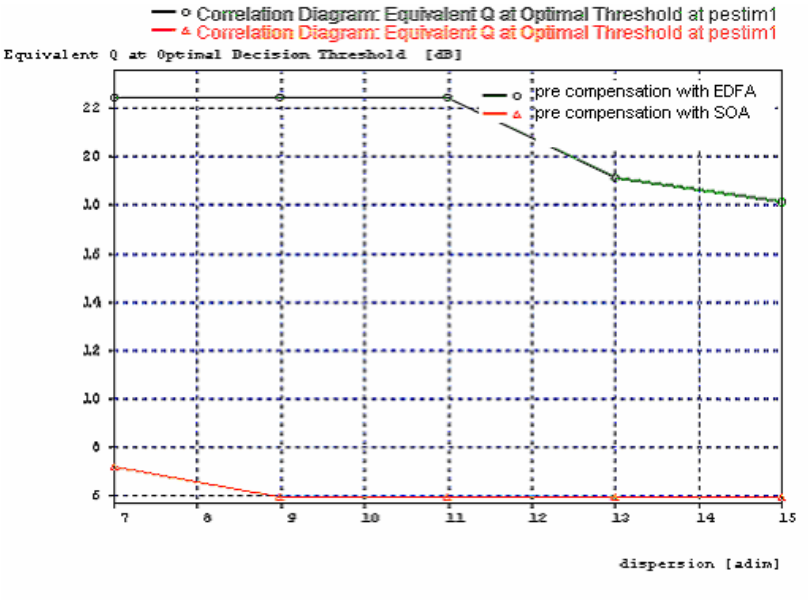

Figure 5.34 Equivalent Q at optimal threshold

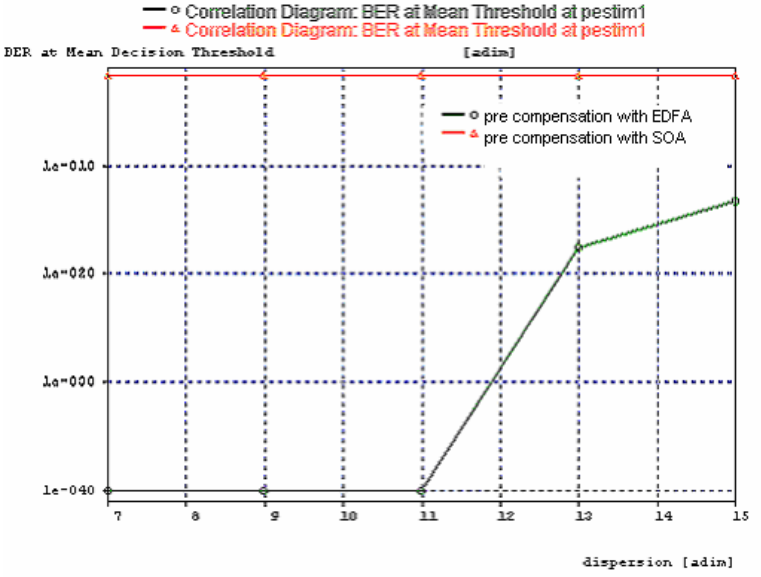

Figure 5.35 BER at mean threshold

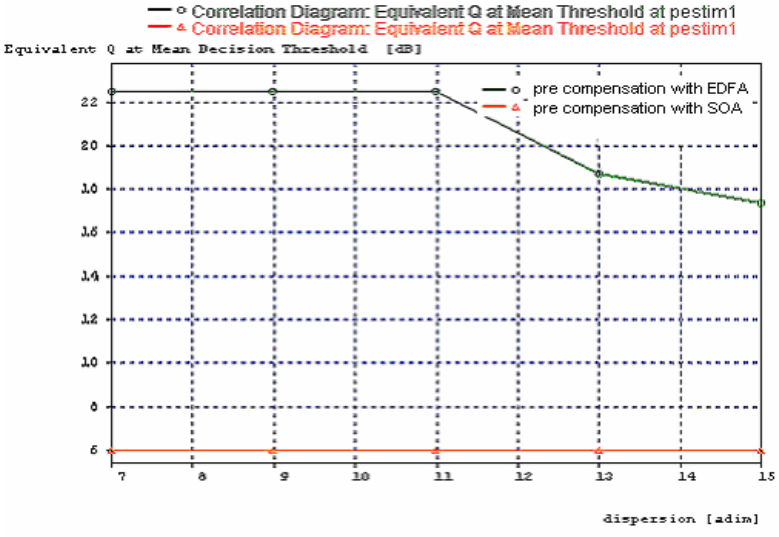

Figure 5.36 Equivalent Q at mean threshold

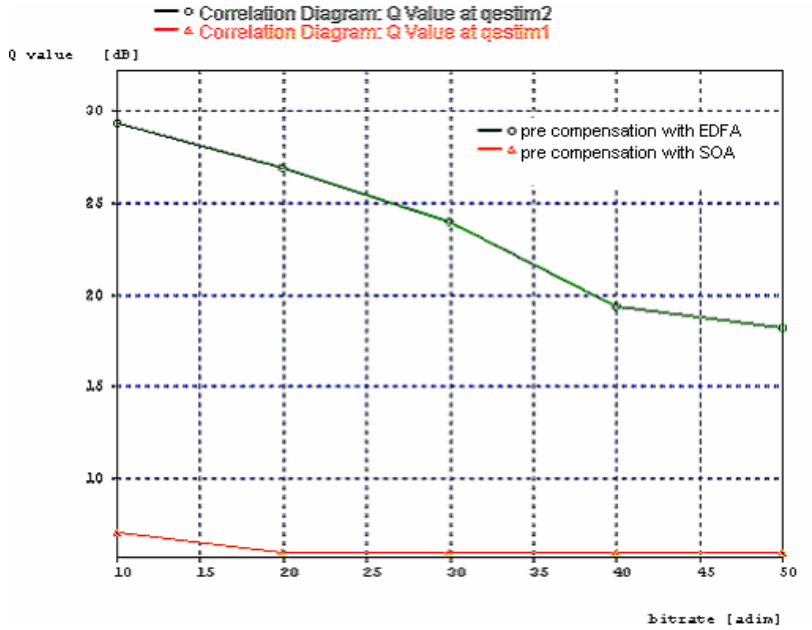

Figure 5.37 Q value

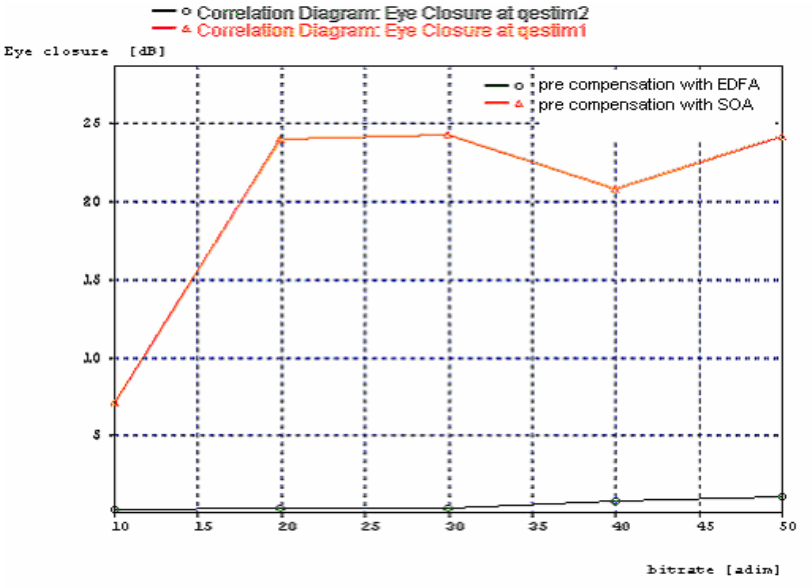

Figure 5.38 Eye closure

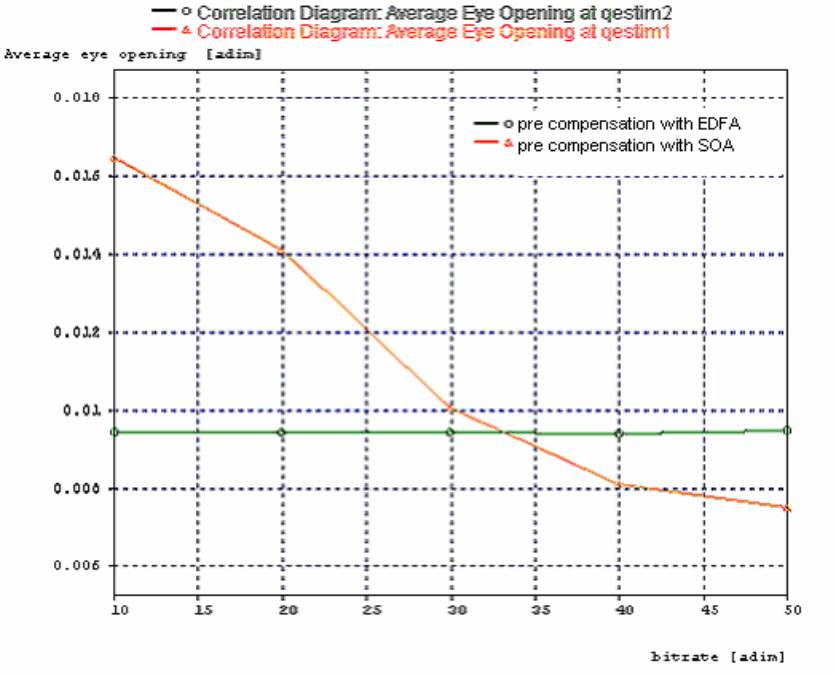

Figure 5.39 Average eye opening

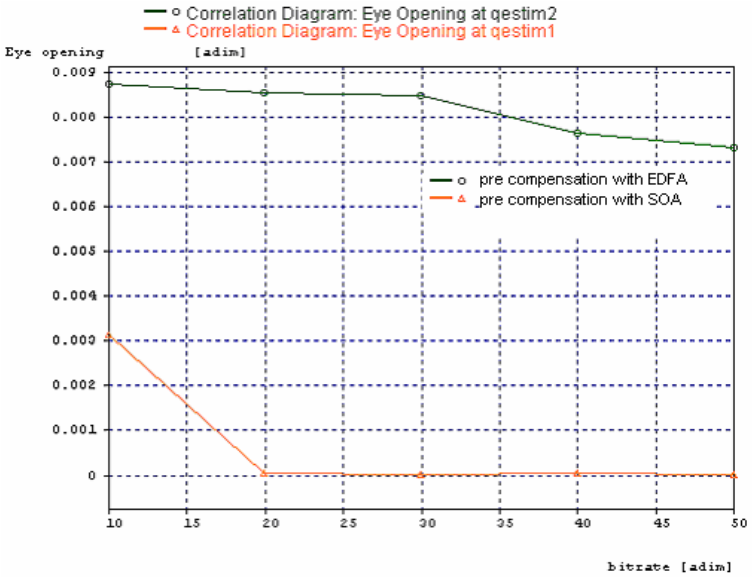

Figure 5.40 Eye opening

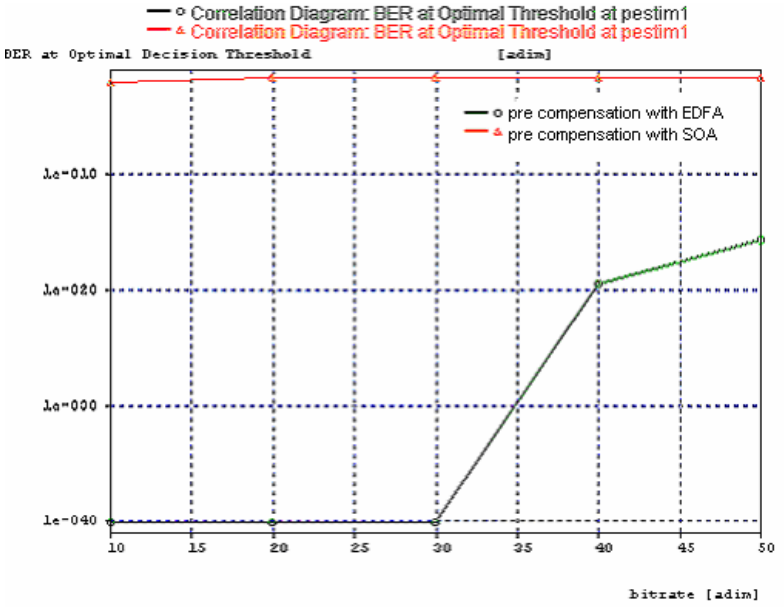

Figure 5.41 BER at optimal threshold

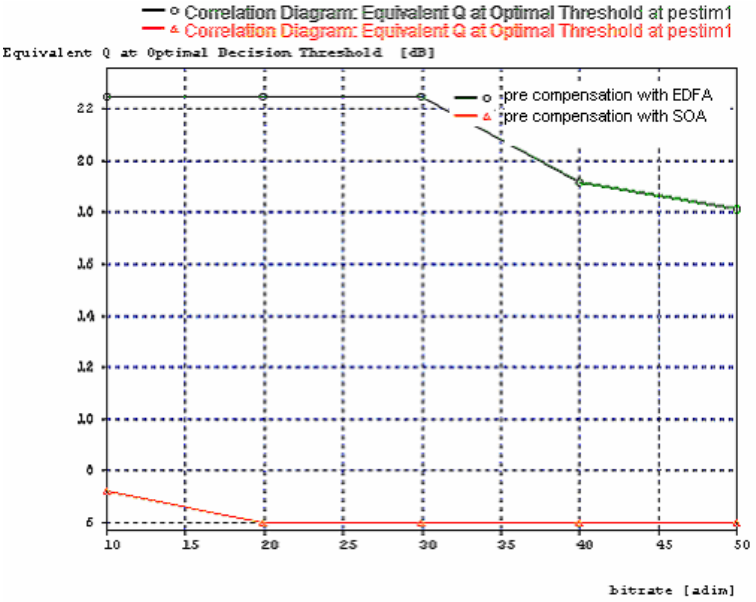

Figure 5.42 Equivalent at Q at optimal threshold

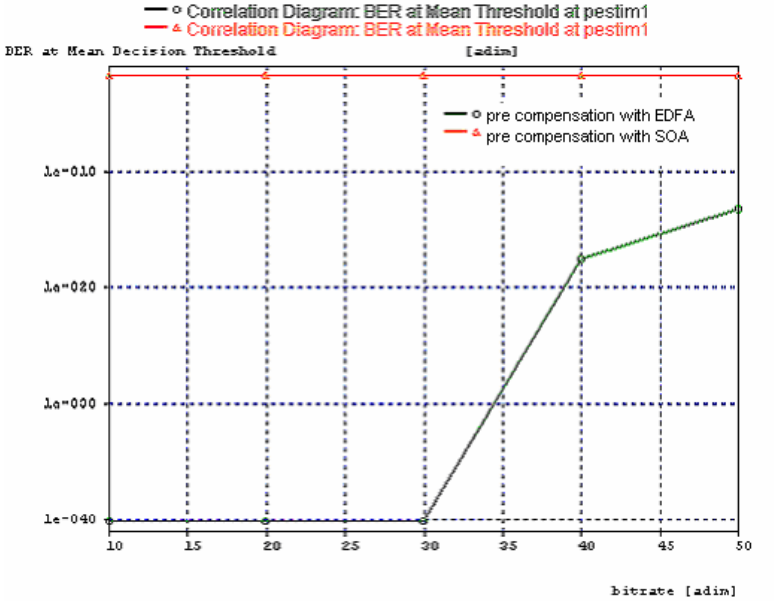

Figure 5.43 BER at mean threshold at pestim

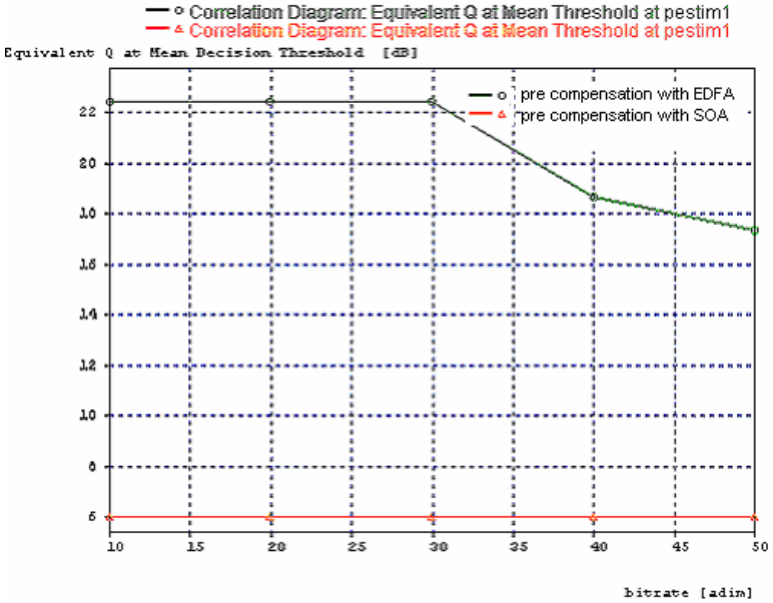

Figure 5.44 Equivalent Q at mean threshold

CHAPTER 6

CONCLUSION AND FUTURE SCOPE OF WORK

6.1 Conclusion

The main purpose of this research work is to investigate the limitations of broadband optical communication system with dispersion and self phase modulation to make efficient fiber optical communication system. We have been discussed the performance of the self phase modulation compensated transmissions based on pre compensation techniques by varying the length of single mode fiber and dispersion at 10 Gb/s. From the eye diagrams, bit error rate (BER) and the Q-factor characteristics, it is clear that as we changing the length of single mode fiber at 10 Gb/s the performance of self phase modulation compensated transmissions based on pre compensation techniques on the length of 10 km is the best. We have also discussed the bit error rate (BER) and the Q-factor characteristics at 10 Gb/s to 40 Gb/s.

We have been also compared the pre compensation technique with EDFA and SOA. It is analyzed that the output taken from EDFA is better than SOA.

6.2 Future scope of work

In this thesis, the work is reported on self phase modulation (SPM) system. The nonlinear effects such as four wave mixing (FWM) and cross phase modulation (XPM) are not included in this work. In future can be included four wave mixing and cross phase modulation. Further, the crosstalk due to other fiber nonlinearities like stimulated Brillouin scattering and stimulated Raman scattering can be studied.

In this research work, the polarization effects have been ignored. These effects along with dispersion and the fiber nonlinearities may be treated in analytical forms and result can be compared with present analytical method. The other types of impairments like thermal noise quantum noise can also be added to study the combined impact for broadband optical communication systems with dispersion and fiber nonlinearities.

REFERENCES

[1] Agrawal G.P., "Fiber Optic Communication Systems," John Wiley and Sons, New York, 1997.

[2] J.M. Senior, "Optical Fiber Communications," Prentice Hall, New Delhi.

[3] G.Keiser, "Coherent Optical Fiber Communications," Optical Fiber Communications, McGraw- Hill, New York, 1991.

[4] Agrawal G.P., "Nonlinear Fiber Optics," Second Ed., Academic Press, San Diego, 1995.

[5] H. Sugahara, Kodama, "Optimal dispersion management for wave length division multiplexed RZ optical pulse transmission," Elect .Lett. No.34, pp. 902, 1998.

[6] Caponi R., Calvani R., Grazioli E, "Fem to second Transform- limited pulse generation by compensating for linear chirp of SPM spectra in Dispersion Shifted Fibers," Journal of Fiber and integrated Optics 17 pp. 41-50, 1998.

[7] Pinault S.C. and Potasek M. J., "Frequency broadening by self-phase modulation in optical fibers," Journal of Optical Society of America, B, vol.2, no.8, pp. 1318-1319, August, 1985.

[8] Chiang T. K. et. al., "Cross-phase modulation in Dispersive fibers: Theoretical and experimental investigation of the impact of modulation frequency," IEEE Photonics Technology Letters, vol.6, no.6, pp. 733-736, June, 1994.

[9] Inoue K. et. al., "Four wave mixing in an optical fiber in the zero-Dispersion wave length region," Journal of Light wave Technology, vol.10 no.11,pp 1553-1560, 1992.

[10] Becker P.C, Olsson N.A.and Simpson J.R., "Erbium-Doped Fiber Amplifiers: Fundamentals and Technology," Academic Press, 1999.

[11] K.C. Kao and G.A. Hockham, "Dielectric fiber surfaces waveguides for optical frequencies," Proceedings of IEEE, vol. 133, pp. 1151-1158, July, 1996.

[12] Pinault S.C. and Potasek M.J., "Frequency broadening by self-phase modulation in optical fibers," Journal of Optical Society of America, B, vol.2, no.8, pp. 1318-1319, August, 1985.

[13] Cartaxo A.V.T. et al., “Rigorous Assessment of Small Signal Analysis for Linear and Dispersive Optical Communication Systems Operating Near Zero Dispersion Wavelength, ”Journal of Light wave Technology,vol.17,No.1, pp. 86-94, January, 1999.

[14] Cartledge J.C., “Combining SPM and Optimum Conditions to Improve the Performance of 10 Gb/s. Transmission Systems Using M Q W Mach-Zehnder Modulators,”Journal of Light wave Technology, vol.18, No.5, pp. 647-655, May, 2000.

[15] Tang J. et al., “The Multispan Effects of Kerr Nonlinearity and Amplifier Noise son Shannon Channel Capacity of a Dispersion Free Nonlinear Optical Fiber,” Journal of Light wave Technology, vol.19, No.8, pp. 1110-1115, August, 2001.

[16] Frank Yang S. Marhic M.E and Kazovsky L.G., “Nonlinear Crosstalk and Two Counter measures in SCM-WDM Optical Communication Systems, ”Journal of Light wave Technology, vol.18, No.4, pp. 512-520, April, 2000.

[17] Sono A., Miyamoto Y., Kuwahara S. and TobaH.,“A40Gb/sWDM Transmission with SPM/XPM suppression Through Pre chirping and Dispersion Management,” Journal of Light wave Technology, vol.18, No.11, pp. 1519-1527, November, 2000.

[18] Yu J., Jeppesen P., "Simultaneous All Optical Demultiplexing and Regeneration Based on Self Phase and Cross Phase Modulation in Dispersion Shifted Fibers,” Journal of Light wave Technology, vol.19,No.7, pp. 941-949, July, 2001.

[19] Numai T. Kubota Q., “Analysis of Repeated Unequally Spaced Channels for FDM Light wave Systems, ”Journal of Light wave Technology, vol.18, No.5, pp. 656-664, May, 2000.

[20] Radic S., Pen dock G., Srivastava A., Wyockhi P. and Chraply ivy A.V., “Four Wave Mixing in Optical Links Using Quasi I Distributed Optical Amplifiers, ”Journal of Light wave Technology, vol.19, No.5, pp. 636-645, May, 2001.

[21] Kikuchi K. and Lorattanasane C., “Compensation for Pulse Waveform Distortion in Ultra-long Distance Optical Communication Systems by Using Nonlinear Optical Phase Conjugation, "in Proc OAA'93, Japan, 1993.

[22] Chernikov V.S., Kashyap R. and Taylor J.R., "Dispersion Compensation of 100-Gbit/s Optical Fiber Transmission by using a Chirped-fiber-grating Transmission Filter,"OFC' 95 Technical Digest, pp. 99-100, 1995.

[23] Djupsjobaka A. and Sahlen O., "Dispersion Compensation by Differential Time Delay, "IEEE, Journal of Light wave Technology, vol.12, No.10 .pp. 1849-1853, October, 1994.

[24] E.A.Golovchenko,"Dispersion managed solution dynamics," Opt. Lett 22, pp 281- 289,1997.

[25] J.H.B. Nijhof, "Energy enhancement of dispersion managed solitons and WDM,"Elect.Lett.34, pp. 481, 1998.

[26] Masaki Anemia, "Pulse Broadening due to Higher Order Dispersion and its Transmission limit,"Journal of Light wave Technology, vol.20, No.4, pp. 591-597, April, 2002.

[27] Bergano N.S. and Davidson C.R., Wavelength division multiplexing in Long-haul Transmission systems," IEEE Journal of Light wave Technology, vol.14, No.6, pp. 1299-1308, June, 1996.

[28] John Crisp, Barry Elliott, "Introduction to Fiber Optics**",** 3rd edition, 2005.

[29] H.Sugahara, Kodama, "Optimal dispersion management for wavelength division multiplexed R Z optical pulse transmission," Elect. Lett. No.34, pp. 902, 1998.

[30] Roeland J. Nuyts, Yong Kwan Park and Philippe Gallium, "Dispersion equalization of a 10 Gb/s bit rate Repeatered Transmission System Using Dispersion compensating Fibers", Journal of Light wave Technology , vol. 15, Issue:. 1, pp, 31-42, January, 1997.

[31] C.M. Weinert, R. Ludwig, W. Pieper, H. G. Weber, D. Breuer, K. Peterman and F.Kuppers " 40 and 440× Gb/s time TDM/WDM standard transmission fiber", Journal of Light wave Technology, vol. 17, No. 11, November, 1999.

[32] E.E.basch, "Optical Fiber Transmission" Ist ed. 1986.

[33] John Crisp, Barry Elliott, "Introduction to Fiber Optics**",** 3rd edition, 2005.

[34] Kawanishi, "Ultra High-Speed Optical Time-Division-Multiplexed Transmission Technology Based on Optical Signal Processing", IEEE Journal of Quantum Electronics, 34, pp. 2064-2078, 1998.

[35] V. Mikhailov, R. I. Killey, J. Prat and P. Bayvel, " Limitation to WDM Transmission Distance due to Cross-Phase Modulation Induced Spectral Broadening in Dispersion Compensated Standard Fiber Systems" IEEE Photonics Technology Letters, vol. 11, No. 8, August, 1999

[36] Giovanni Bellotti, Matteo Varani, Cristian Francia, **"**Intensity Distortion Induce by Cross Phase Modulation and Chromatic Dispersion in Optical-Fiber with Dispersion Compensation' IEEE Photonics Technology Letters, vol. 10, No. 12, December, 1998.

[37] Shuai Shen, Cheng-Chun Chang, Harshad P. Sardesai, Vikrant Binjrajka and Andrew M. Weiner "Effects of Self Phase Modulation on Sub-500 fs Pulse Transmission over Dispersion Compensated Fiber Links" Journal of light wave technology. vol. 17, No. 3, March, 1999

[38] Bengt-Erik Olsson and Daniel J. Blumenthal, "Pulse Restoration by Self-Phase Modulation Broadened Optical Spectrum" Journal of light wave Technology, vol. 20, No. 7, July, 2002

[39] N. Bloembergen, "Recent Progress in Four-Wave Mixing Spectroscopy," in Laser Spectroscopy IV, edited by H. Walther and K. W. Rothe, (Springer, Berlin, 1979)

[40] L.H. Spiekman et al., "Transmission of 8 DWDM Channels at 20Gbit/s over 160 km of Standard Fiber Using a Cascade of Semiconductor Optical Amplifiers", IEEE Photonics Technology Letters, vol. 12, pp. 717-719, 2000.

[41] Ilya Lyubomirsky,, Tiequn Qui, Jose Romanahir Nayfeh, Michael Y. Frankel, Michael G. Taylor, "Interplay of Fiber Nonlinearity and Optical Filtering Ultra dense WDM" IEEE Photonics Technology Letters, vol. 15, No. 1, January, 2003.

[42] Vivek Alwayn, "Optical Network Design and Implementation" published by C Edition 2004.

[43] J.Wang and K.Petermann, "Small signal analysis for dispersive optical communication systems," J. Light wave Techno. vol. 10, pp. 96–100, January, 1992.

[44] G. Bellotti, M.Varani, C. Francia and A. Bononi, "Intensity distortion induced by cross-phase modulation and chromatic dispersion in optical-fiber transmissions

with dispersion compensation, ” IEEE Photon. Techno. Lett., vol. 10, pp. 1745–1747, December, 1998.

[45] D. Breuer, C. Kurtzke and K. Petermann, “Optimum dispersion management for nonlinear optical single-channel systems,” in Proc. OFC’95,Feb. 1995, pp. 196 - 197.

[46] B. Schmaus, M. Berger, M. Rasztovits-Wiech, A. Schinabeck and D. Werner, “Modular dispersion compensation scheme for high bitrate single channel and WDM transmission with varying channel power,” in Proc. ECOC’97, September, 1997, pp. 239–242.

[47] Björlin E. Staffan and Bowers John E., "Noise Figure of Vertical-Cavity Semiconductor Optical Amplifiers," IEEE Journal of Quantum Electronics, vol. 38, No. 1, January, 2002, pp. 61-66.

APPENDIX

Figure 4.6 Electrical spectrum in which peak frequency 2.88889[GHz] peak power -51.078544

Figure 4.7 Electrical spectrum in which peak frequency 2.88889[GHz] peak power 4.14962e-005[au] -43.8199[10^x log10 [au] in range 0, 49.97[GHz]

Figure 4.8 Electrical spectrum in which peak frequency 2.88889[GHz] peak power 4.13743e-005[au] -43.8327[10^x log10 [au] in range 0,49.97[GHz]

Figure 4.9 Electrical spectrum in which peak frequency 2.88889[GHz] peak power 4.15788e-005[au] -43.8113[10^x log10 [au] in range 0,49.97[GHz]

Figure 4.10 Electrical spectrum in which peak frequency 2.88889[GHz] peak power 4.14072e-005[au] -43.8292[10^x log10 [au] in range 0,49.97[GHz]

Figure 4.12 Eye diagram in which sampling time [opt] 0.0230769 [ns] decision threshold[opt] 0.00278222[au] Q value 24.0106 [line] Q value 27.608077 [dB] Bit error rate 1e-040 opening 0.00847335 [au] average opening 0.0092433 [au] closure 0.377718 dB Jitter 0.0171988 [ns]

Figure 4.13 Eye diagram in which sampling time [opt] 0.0307692 [ns] decision threshold[opt] 0.00284302[au] Q value 29.445 [line] Q value 29.380245 [dB] Bit error rate 1e-040opening 0.00876657 [au] average opening 0.00944746 [au] closure 0.324851 dB Jitter 0.0167555 [ns]

Figure 4.14 Eye diagram in which sampling time [opt] 0.0769231 [ns] decision threshold [opt] 0.00357192[au] Q value 22.2241 [line] Q value 26.936493 [dB] Bit error rate 1e-040 opening 0.00857739 [au] average opening 0.00946109 [au] closure 0.425861 dB Jitter 0.0166266 [ns]

Figure 4.15 Eye diagram in which sampling time [opt] 0.00769231 [ns] decision threshold [opt] 0.00449261[au] Q value 15.8743 [line] Q value 24.013899 [dB] Bit error rate 1e-040 opening 0.00848629 [au] average opening 0.00946343 [au] closure 0.473311 dB Jitter 0.0126448 [ns]

Figure 4.17 Eye diagram in which sampling time [opt] 0.0230769 [ns] decision threshold [opt] 0.00424432[au] Q value 9.34047 [line] Q value 19.407374 [dB] Bit error rate 3.76812e-020 opening 0.00767139 [au] average opening 0.0094277 [au] closure 0.895319 dB Jitter 0.47514 [ns]

Figure 4.18 Eye diagram in which sampling time [opt] 0.00769231 [ns] decision threshold [opt] 0.00539212[au] Q value 8.14916 [line] Q value 18.222261 [dB] Bit error rate 2.90963e-016 opening 0.00733359 [au] average opening 0.00951333 [au] closure 1.730163 dB Jitter 0.0158271 [ns]

Figure 4.19 Eye diagram in which sampling time [opt] 0.0307692 [ns] decision threshold [opt] 0.00284302[au] Q value 29.445 [line] Q value 29.380245 [dB] Bit error rate 1e-040 opening 0.00876657 [au] average opening 0.00944746 [au] closure 0.324851 dB Jitter 0.0167555 [ns]

Figure 4.20 Eye diagram in which sampling time [opt] 0.00769231 [ns] decision threshold [opt] 0.00449261[au] Q value 15.8743 [line] Q value 24.013899 [dB] Bit error rate 1e-040 opening 0.00848629 [au] average opening 0.00946343 [au] closure 0.473311 dB Jitter 0.0126448 [ns]

Figure 4.21 Eye diagram in which sampling time [opt] 0.00769231 [ns] decision threshold [opt] 0.00449261[au] Q value 15.8743 [line] Q value 24.013899 [dB] Bit error rate 1e-040 opening 0.00848629 [au] average opening 0.00946343 [au] closure 0.473311 dB Jitter 0.0126448 [ns]

Figure 4.22 Eye diagram in which sampling time [opt] 0.0230769 [ns] decision threshold [opt] 0.00424432[au] Q value 9.34047 [line] Q value 19.407374 [dB] Bit error rate 3.76812e-020 opening 0.00767139 [au] average opening 0.0094277 [au] closure 0.895319 dB Jitter 0.47514 [ns]

Figure 4.23 Eye diagram in which sampling time [opt] 0.00769231 [ns] decision threshold [opt] 0.00539212[au] Q value 8.14916 [line] Q value 18.222261 [dB] Bit error rate 2.90963e-016 opening 0.00733359 [au] average opening 0.00951333 [au] closure 1.730163 dB Jitter 0.0158271 [ns]

Figure 4.25 Optical spectrum in which power 0.230169 [mw],-6.37953 [dBm] in range [193.362;193.467] [THZ]

Figure 4.31 Q value in which mean value 23.5398 standard deviation 3.66889 variance 13.4608

Figure 4.32 Eye opening in which mean value 0.630499 standard deviation 0.258509 variance 0.0668269

Figure 4.51 Eye diagram in which sampling time [opt] 0.0615385 [ns] decision threshold [opt] 0.00414603[au] Q value 13.4137 [line] Q value 22.550980 [dB] Bit error rate 1.50007e-039 opening 0.00698474 [au] average opening 0.00854013 [au] closure 0.873118 dB Jitter 0.0132452 [ns]

Figure 4.52 Eye diagram in which sampling time [opt] 0 [ns] decision threshold [opt] 0.00582619 [au] Q value 3.08731 [line] Q value 9.791614 [dB] Bit error rate 0.00115183 opening 0.000599 [au] average opening 0.00736197 [au] closure 10.895674 dB Jitter 0.0139087 [ns]

Figure 4.53 Eye diagram in which sampling time [opt] 0.0153846 [ns] decision threshold [opt] 0.00551259 [au] Q value 2.97925 [line] Q value 9.482150 [dB] Bit error rate 0.00143351 opening 0.000242205 [au] average opening 0.00742118 [au] closure 14.862890 dB Jitter 0.00748216 [ns]

Figure 4.54 Eye diagram in which sampling time [opt] 0.00761231 [ns] decision threshold [opt] 0.0051587[au] Q value 2.8161 [line] Q value 8.992969 [dB] Bit error rate 0.00251129 opening 0.000160304 [au] average opening 0.00736591 [au] closure 16.622808 dB Jitter 0.00726075 [ns]

Figure 4.55 Eye diagram in which sampling time [opt] 0.0153846 [ns] decision threshold [opt] 0.0047953[au] Q value 2.58734 [line] Q value 8.257063 [dB] Bit error rate 0.00484611 opening 6.54007e-005 [au] average opening 0.00720122 [au] closure 20.418236 dB Jitter 0.00748429 [ns]

Figure 4.57 Eye diagram in which sampling time [opt] 0.0615385 [ns] decision threshold [opt] 0.00414603[au] Q value 13.4137 [line] Q value 22.550980 [dB] Bit error rate 1.50007e-039 opening 0.00698474 [au] average opening 0.00854013 [au] closure 0.873118 dB Jitter 0.0132452 [ns]

Figure 4.58 Eye diagram in which sampling time [opt] 0 [ns] decision threshold [opt] 0.00582619 [au] Q value 3.08731 [line] Q value 9.791614 [dB] Bit error rate 0.00115183 opening 0.000599 [au] average opening 0.00736197 [au] closure 10.895674 dB Jitter 0.0139087 [ns]

Figure 4.59 Eye diagram in which sampling time [opt] 0.0153846 [ns] decision threshold [opt] 0.00551259 [au] Q value 2.97925 [line] Q value 9.482150 [dB] Bit error rate

0.00143351 opening 0.000242205 [au] average opening 0.00742118 [au] closure 14.862890 dB Jitter 0.00748216 [ns]

Figure 4.60 Eye diagram in which sampling time [opt] 0.00761231 [ns] decision threshold [opt] 0.0051587[au] Q value 2.8161 [line] Q value 8.992969 [dB] Bit error rate 0.00251129 opening 0.000160304 [au] average opening 0.00736591 [au] closure 16.622808 dB Jitter 0.00726075 [ns]

Figure 4.61 Eye diagram in which sampling time [opt] 0.0153846 [ns] decision threshold [opt] 0.0047953[au] Q value 2.58734 [line] Q value 8.257063 [dB] Bit error rate 0.00484611 opening 6.54007e-005 [au] average opening 0.00720122 [au] closure 20.418236 dB Jitter 0.00748429 [ns]

Figure 4.63 Q value in which mean value 18.4964 standard deviation 1.79612 variance 3.22605

Figure 4.64 Eye closure in which mean value 1.46101 standard deviation 0.344987 variance 0.119016

Figure 4.65 BER at optimal threshold in which maximum value 9.16045e-012 minimum value 0 peak value 0

Figure 4.66 BER at mean threshold in which maximum value 18.3074 minimum value 1.78269 peak value 3.178

Figure 4.67 Average eye opening in which mean value 0.00857892 standard deviation 0.000222074 variance 4.93167

Figure 4.68 Equivalent Q at mean threshold in which maximum value 17.8191minimam value 1.91957 peak value 3.68473

Figure 4.69 Equivalent Q at optimal threshold in which maximum value 1.6661e-009minimam value 3.45079e-009 peak value 1.1908e-017

Figure 4.70 BER at optimal threshold in which maximum value 19.3074 minimum value 2.78269 peak value 3.378

Figure 4.71 BER at mean threshold in which mean value 9.16045e-012 standard deviation 0 variance 0

Figure 4.72 Equivalent Q at optimal threshold in which maximum value 17.8191 minimum value 1.91957 peak value 3.68473

Figure 4.73 Q value in which mean value 16.4964 standard deviation 1.59612 variance 2.22605

Figure 4.74 in which mean value 1.46101 standard deviation 0.344987 variance 0.119016

Figure 4.75 Average eye opening in which mean value 0.00837892 standard deviation 0.000222074 variance 4.93167e-008

Figure 4.76 Eye opening in which mean value 0.00615282 standard deviation 0.000548609 variance 13.4608

Figure 4.77 Equivalent Q at optimal threshold in which maximum value 21.123 minimum value 1.6384 peak value 2.68437

Figure 4.78 BER at mean threshold in which maximum value 8.50949e-015minimam value 0 peak value 0

Figure 4.79 Equivalent Q at mean threshold in which maximum value 20.9072 minimum value 1.90575 peak value 3.63187

Figure 5.2 Electrical spectrum in which power 0.00024625 -36.4747.10^x log10[au] in range 0.49.97

Figure 5.8 Eye diagram in which sampling time [opt] 0.0692308 [ns] decision threshold [opt] 0.00660361[au] Q value 2.26618 [line] Q value 7.105869 [dB] Bit error rate 0.010803 opening 0.00315979 [au] average opening 0.0164836 [au] closure 7.173926 dB Jitter 0.0240449 [ns]

Figure 5.9 Eye diagram in which sampling time [opt] 0 [ns] decision threshold [opt] 0.00787996 [au] Q value 2 [line] Q value 6.020600 [dB] Bit error rate 0.0227501 opening 5.58635e-005 [au] average opening 0.0142155 [au] closure 24.056350 dB Jitter 0.0133169 [ns]

Figure 5.10 Eye diagram in which sampling time [opt] 0 [ns] decision threshold [opt] 0.00883409 [au] Q value 2 [line] Q value 6.020600 [dB] Bit error rate 0.0227501 opening 3.71402e-005 [au] average opening 0.0100984 [au] closure 24.344069 dB Jitter 0.00711114 [ns]

Figure 5.11 Eye diagram in which sampling time [opt] 0 [ns] decision threshold [opt] 0.00873409 [au] Q value 2 [line] Q value 6.020600 [dB] Bit error rate 0.0227501 opening 5.69146e-005 [au] average opening 0.00812256 [au] closure 22.841723 dB Jitter 0.00705578 [ns]

Figure 5.12 Eye diagram in which sampling time [opt] 0 [ns] decision threshold [opt] 0.00827377 [au] Q value 2 [line] Q value 6.020600 [dB] Bit error rate 0.0227501 opening 6.69146e-005 [au] average opening 0.00812256 [au] closure 20.841723 dB Jitter 0.00706588 [ns]

Figure 5.13 Eye diagram in which sampling time [opt] 0 [ns] decision threshold [opt] 0.00785478 [au] Q value 2 [line] Q value 6.020600 [dB] Bit error rate 0.0227501 opening 2.83681e-005 [au] average opening 0.00751119 [au] closure 24.228789 dB Jitter 0.00718841 [ns]

Figure 5.14 Optical spectrum in which power 0.230169 [mw],-6.37953 [dBm] in range [193.362;193.467] [THZ]

Figure 5.20 Q value in which mean value 6.15626 standard deviation 0.282396 variance 0.0797476

Figure 5.21 Equivalent Q at optimal threshold in which mean value 0.02275 standard deviation 0 variance 0.

Figure 5.22 Equivalent Q at mean threshold in which mean value 6.01801 standard deviation 0 variance 0

Figure 5.23 Average eye opening in which mean value 0.011095 standard deviation 0.00299225 variance 8.95354e-006

Figure 5.24 BER at mean threshold in which mean value 0.0212566 standard deviation 0.00310871 variance 9.66407e-006

Figure 5.25 BER at optimal threshold in which mean value 6.16832 standard deviation 0.3129 variance 0.0979067

Figure 5.26 Q value in which mean value 6.15626 standard deviation 0.282396 variance 0.0797476

Figure 5.27 BER at mean threshold in which mean value 0.0212566 standard deviation 0.00310871 variance 9.66407e-006

Figure 5.28 BER at optimal threshold in which mean value 6.16832 standard deviation 0.3129 variance 0.0979067